BIM FOR ENERGY MODELLING OF GREEN BUILDINGS

by

Haidar E. Al-Haidary

A Thesis Presented to the Faculty of the
American University of Sharjah
College of Engineering
In Partial Fulfillment
of the Requirements
for the Degree of

Master of Science in
Civil Engineering

Sharjah, United Arab Emirates

November 2018

Approval Signatures

We, the undersigned, approve the Master's Thesis of Haidar E. Al-Haidary

Thesis Title: BIM For Energy Modelling of Green Buildings

Signature	**Date of Signature** (dd/mm/yyyy)
_____	_____
Dr. Adil K. Tamimi Professor, Department of Civil Engineering Thesis Advisor	
_____	_____
Mr. Hisham AlWakil Architect, Diar Consultancy Thesis Committee Member	
_____	_____
Dr. Mohammad AlHamaydeh Associate Professor, Department of Civil Engineering Thesis Committee Member	
_____	_____
Dr. Abdulrahman Al-Ali Professor, Department of Electrical Engineering Thesis Committee Member	
_____	_____
Dr. Irtishad Ahmad Head, Department of Civil Engineering	
_____	_____
Dr. Ghaleb Husseini Associate Dean for Graduate Affairs and Research College of Engineering	
_____	_____
Dr. Richard Schoephoerster Dean, College of Engineering	
_____	_____
Dr. Mohamed El-Tarhuni Vice Provost for Graduate Studies	

Acknowledgement

I would like to take this opportunity to thank my family for their indispensable support throughout my academic journey. I would also like to thank my thesis advisor Professor Al-Tamimi for his continuous guidance and for the wisdom he has imparted on me. His office door was always open whenever I required encouragement or direction and his enthusiasm towards research was very inspiring. Furthermore, I would also like to show my gratitude to Mr. Hashim Alwakil who without his insights this work would not have been possible. His cheerful attitude, vision, and perpetual willingness to help made the most difficult times memorable.

I would also like to acknowledge the support of Mr. Hayder Awni, Mr. Georgios Chamilothoris and the entire team at the Campus Services Centre (CSC Building). I would also like to thank Professor Katsos from the American University of Sharjah's Office of Sustainability and Dr. Basim Abbas from Middle East Insulation for their support.

I would also like to thank my friends and colleagues for tolerating, supporting, and encouraging my work and finally, I would like to thank the professors of the Civil Engineering department who taught me the master level courses and the American University of Sharjah for supporting my master's degree with the generous Graduate Assistantship program.

Abstract

Energy conservation has become a priority for many governments and sustainable building standards such as LEEDS and Estidama. This is largely due to the high energy demand of buildings and the rising concerns over the impact fossil-fuel-generated electricity has on the environment. With buildings consuming up to 40% of global energy, the demand for energy-efficient buildings has steadily increased. This study employs the Building Information Modelling (BIM) technology namely Autodesk Revit and the energy modelling software, IES-VE, to analyze the effectiveness of passive design measures such as the building's orientation and external envelope on its energy consumption. The analysis was performed on a case-study office building and both thermal imaging and the experimental measurement of the building envelope's U-value were conducted to assist the investigation. The study proves that with just basic knowledge about the HVAC system, the building can be modelled to within 3% of the actual consumption when comparing the colder months. The case-study building was also found to have an EUI of 357.8 kWh/m^2/yr according to the model's consumption, this is relatively lower than the actual EUI of the building of 411.2 kWh/m^2/yr obtained using the building's total estimated consumption. Furthermore, the total savings achieved by increasing the insulation levels of the external wall, adding 100 mm of insulation to the slab on grade, fitting high performance windows, and optimizing the orientation of the building, was 2.77%. The maximum savings achieved from any one efficiency measure, however, was about 1.6%, achieved when using high-performance glazing. It was also shown that although the case-study building had no thermal bridges, all thermal bridges detected on other buildings were about 2˚C different from the insulated elements. The study also showed that the U-value calculated by the IES VE software was 0.2354 W/m^2K, differing by 31% when compared to the 0.339 W/m^2K as measured in-situ. The study finally concludes that a modern office building gains little benefit from retrofit measures that minimize heat gain, however, the framework of BIM, IR camera, and in-situ U-value measurement proved effective.

Keywords: ***Energy Modelling, IES-VE, Building Information Modelling, Green Buildings, Building Envelope, Passive Design, Thermal Imaging, Heat flux Sensors, In-situ U-value, Thermal Bridges, Model Calibration***

Table of Contents

List of Figures

List of Tables

List of Abbreviations

AEC	Architecture, Engineering, and Construction
AHU	Air Handling Unit
BIM	Building Information Modelling
CDD	Cooling Degree Day
CHW	Chilled Water
EPS	Expanded Polystyrene
EUI	Energy Utilization Index or Energy Use Intensity
FCU	Fan Coil Unit
GFP	Gas Filled Panel
GHG	Green House Gases
HVAC	Heating, Ventilation, and Air Conditioning
IR	Infra-Red
IFOV	Instantaneous Field of View
MEP	Mechanical, Electrical, and Plumbing
PCM	Phase Change Materials
PUR	Polyurethane
VIP	Vacuum Insulation Panel
XPS	Extruded Polystyrene

Chapter 1. Introduction

In this chapter, an overview introducing energy conservation in buildings is presented along with an organisation of the work presented in this thesis. This is followed by the background and motivation for this study, the research significance, and finally the thesis objectives.

1.1. Overview

Due to the high energy demand of buildings and the rising concerns over the impact electricity from fossil fuels has on the environment, energy conservation has become a priority of many governments and sustainable building standards such as LEEDS and Estidama. However, the methods employed in achieving this efficiency are yet to be fully explored. Energy efficiency measures are generally categorized as either applied through active factors such as the HVAC and lighting systems or through passive factors such as the building's orientation and envelope. This study shall focus on the use of energy modelling software, namely IES-VE, to determine the effect of some passive measures, such as the building envelope, on the building's energy consumption. Chapter 1 of this research introduces green buildings and the objectives of the thesis. Chapter 2 provides a literature review of relevant work in this field followed by the methodology used to achieve the objectives in chapter 3. Chapter 4 provides an analysis of the climate in the UAE and how it affects design decisions. Chapter 5 introduces the case study building for this study and provides an analysis of its energy consumption. Chapter 6 then presents the modelling of the building geometrically in Revit and the different design options considered in IES VE. Chapter 7 investigates the availability of any thermal bridges in the case study building while chapter 8 compares the actual U-value of the case study building's envelope as measured experimentally to the value calculated theoretically. Finally, chapter 9 summarizes the main conclusions of this study and suggests directions for future research work.

1.2. Background and Motivation

With urbanization spawning in every major city across the globe, and an ever-increasing population, prospects of reducing the environmental hazards of human construction looked grim. Urban environments consume between 25% and 40% of

global energy, and generate 30% to 40% of both solid waste and greenhouse gas emissions worldwide [1], [2]. While the manufacturing of building materials further accounts for about 10% of global energy consumption [2]. Around the world, these figures are reinforced by local statistics. In the U.S, about 40% of the total energy consumption, 72% of electricity consumption, and 38% of CO_2 emissions is due to buildings [3], [4]. In Great Britain, about 27% of emissions is due to buildings [4]. In Iran, about 40% of the total energy consumption is attributed to buildings [5]. In Canada, residential and commercial buildings account for about 33% of energy consumption and about 35% of greenhouse gas emissions [6].

On these grounds the architecture, engineering, and construction (AEC) industries have engaged in the production of green and high-performance buildings to allow for the continued growth of sustainable cities. Although often used interchangeably, green buildings are typically defined as life-cycle oriented, environmentally-responsible, and resource-efficient structures while high performance buildings are all that along with other high performance parameters such as safety, durability, cost-benefit and so on [2]. Whichever is to be designed, the real-estate market has force-shifted to accommodate them gracefully. Therefore, the field for work is clearly vast. In the U.S for instance, the American Housing Survey by the US Census Bureau estimates over 60% of houses are over 30 years old and energy inefficient [3].

In 2008, a McGraw Hill Construction report found green buildings operating at 14% lower costs than traditional buildings and consequently had an 11% increase in value [2], signalling the onset of new financial considerations in design. The benefits of green and high-performance buildings however extend beyond the altruistic and financial. They have become a symbol of prestige and sophistication, much like size with the Great Pyramid of Giza. For one, the United Arab Emirates (UAE), under the vision of its leaders, have displayed an unequivocal interest in transforming the country into a hub for sustainability.

The UAE Energy Strategy 2050 was announced in 2015 and included goals of increasing consumption efficiency by 40% and reducing the power-generation carbon footprint by 70% [7]. Also, the Environment Vision 2030 was announced by Abu Dhabi acknowledging the high electricity consumption of households in the emirate (10x world average) and outlining mitigation of climate change impacts as one of its five

priority areas [8]. The Estidama Pearl Rating System, yet another step towards the vision, was mandated on April 2010, serving as a framework for the design, construction, and operation of buildings in Abu Dhabi. Dubai has assured its involvement as well, with various bodies and organizations, such as the Dubai Supreme Council of Energy, set up to administer the transformation. The government-owned Etihad Energy Services Company, set a quick pace by saving 54 GWh of energy through the retrofit of 2,178 buildings in 2016 [9]. Furthermore, the Dubai Integrated Energy Strategy, Dubai Clean Energy Strategy 2050, and the Dubai Carbon Abatement Strategy, were emplaced to lead to, respectively, a 30% reduction in energy consumption in the Emirate by 2030, an increase to 75% of energy production from clean resources by 2050, and a 16% reduction in carbon emissions by 2021. Finally, the Dubai Municipality has played a major role in transforming much of the vision and initiatives to a reality by imposing green building regulations in 2011 on all government buildings and after completing 44 such projects by 2014, mandated the regulations for all buildings in Dubai [10], [11].

The AEC industry in the Emirates has raced ever since to conform to current and upcoming green building regulations and innovate to outpace competition. This research aims to form a tool that links industry practice with academic investigation. The result being an exploratory document scouting effective methods in the design of energy efficient buildings.

1.3. Research Significance

The research literature had previously investigated the effect of certain building envelope factors such as insulation and windows on the energy consumption of the building. However, these studies were conducted on smaller and older buildings that naturally gave high energy savings. Furthermore, previous orientation studies have been conducted on regular shaped and smaller buildings, and may not conclude energy saving results that are indicative of more complex structures.

The significance of this study is to therefore expand the literature base by investigating the effect of insulation, orientation, and other building envelope parameters on an already insulated, modern, office building with an irregular shape. Furthermore, this study also investigates the use of thermal imaging and in-situ U-value measurements as an integral part of the energy model creation process.

1.4. Thesis Objectives

This study shall focus on modelling the energy consumption of buildings and evaluating their energy efficiency, especially through:

- Evaluating various techniques of analysing and enhancing the building envelope.
- Reviewing methods of detecting thermal bridges on the envelope and providing technical solutions.
- Determining the U-value of building walls experimentally using specialized equipment and relevant standards.
- Applying the aforementioned objectives through a case study building on campus, using BIM technology such as Revit and IES-VE.

Chapter 2. Background and Literature Review

In this chapter, a comprehensive literature review of relevant work is presented. First, the definition of green buildings is revised according to literature findings followed by an overview of the factors that affect energy consumption in buildings. The concepts of embodied energy and life cycle analysis form a theoretical framework for decision-making in green building design and have hence been included in the following section. Then the process of Building Information Modelling and building energy modelling software are summarized. Finally, relevant work using energy modelling, thermal imaging, and in-situ U-value measurements to analyse building envelopes is discussed before presenting research findings of traditional and new insulation materials.

2.1. Truly Green Buildings

Although earlier in this document green buildings have been defined as life-cycle oriented and environmentally responsible buildings, this definition, in fact, remains a very general one. Practically, the definition of green buildings is rather elusive, and the green building "tag" has been furnished on various buildings that are considerably different from each other in terms of their sustainability goals. The definition however continues to evolve, with various aspects of enhanced design and construction, added to it as the concepts of sustainability are further studied. In reality, green buildings have encompassed anything from the reduction of materials and embodied energy in materials, the reduction of greenhouse gas emissions during a particular stage or the entire lifecycle of the building, the conservation of water and energy, the reduction of waste from the building, the reduction of the buildings impact on its surrounding ecology, and the design of a high quality indoor environment.

2.1.1. Green building approaches. As a result of this fluid definition, the AEC industry has approached green buildings in many ways. Some have designed traditional buildings that were later enhanced to accommodate some sustainability objectives while others designed a different form of buildings from the very beginning that meet the same objectives but through a sustainable approach [12]. Regardless, the energy aspect has been at the heart of the design; and whether energy is to be generated

via renewable sources or traditional fossil fuels, reducing its consumption remains a vital consideration.

The operational stage of a building which mainly includes heating, cooling, and lighting processes is by far the most energy consuming stage with HVAC systems consuming about 50% of the energy in buildings, 10-20% of final energy use, and generating about a third of the building's carbon emissions [2], [4], [12]–[15]. In the UAE specifically the cooling load accounts for about 70% of the total electricity consumption in residential, commercial and government buildings [16]. These energy consuming processes are greatly influenced by various factors including, the ambient temperature, the building's envelope, orientation, components, size and shape, and its occupant behavior [13].

A broad classification of energy efficiency measures is through the methods employed in improving the building's performance – i.e. active and passive methods – and the techniques involved in optimizing them. Active methods involve the use of power consuming equipment such as HVAC systems and lighting fixtures while passive methods include the building envelope, the building's orientation, natural ventilation, shading, and natural day-lighting [17].

An important contemporary consideration of active measures is the use of IoT devices to control active equipment such as HVAC and lighting or even just simple sensors to collect data about temperature and energy consumption and communicate it wirelessly to a building management system or the house owner for data analysis.

2.1.2. Building orientation. The process of designing green buildings starts from the very beginning, in the planning and preliminary design phase. At this stage the optimum orientation of the building is determined through analyzing solar energy absorption, light penetration, and wind intensity and prevailing direction[4], [18]. For example, a building in the northern hemisphere should face south to take maximum advantage of the sun's heating capacity in the winter. A case study by Abanda and Byers [13], concluded a difference of 17,056 kWh of electricity and 27,988 MJ of gas consumption between the best and worst orientations.

In the UAE, the sunlight penetrates the deepest from the eastern and western facades of the building when the sun is at its lowest positions during sunrise and sunset. Local studies have suggested limiting the window to surface area ratio to about 1:6 and

for only two elevations to gain energy savings of about 55% [18]. The Dubai green building regulation accounts for these and stipulates a northern orientation for at least 50% of the total glazed surface of non-industrial buildings other than villas [19].

2.1.3. Embodied energy and life cycle analysis. The holistic approach to green buildings includes analyzing the energy consumed and the GHG emitted during the entire life cycle of the building from the extraction of raw materials, their processing into building elements, transport to site, installation and assembly, to the operation of the building, refurbishing and maintaining it, to finally deconstruction and disposal of the waste. However, in most cases, only the operational costs of the building are considered. While this may be valid since they form the largest part of the building's energy consumption, the cradle-to-grave viewpoint argues that the use of energy-intensive materials and systems, along with the trend of constructing larger buildings could offset the benefits of energy efficiency measures when a more comprehensive analysis is undertaken [20], [21]. Hence, the importance of considering the embodied energy has been extensively researched. Embodied energy refers to the energy consumed in all the process upstream of and including the assembling of the building. Langston and Langston [20], emphasized that the life cycle approach must be considered even when calculating the embodied energy of materials, hence accounting for the direct and indirect embodied energy in both the initial embodied energy as well as the recurring embodied energy incurred during the repair and refurbishment of the building.

Copiello [21], investigates not only the effect of embodied energy offsetting any gain in operating energy savings but also discusses two other controversial paradoxes that arise when considering the effectiveness of energy efficiency measures. The first also known as the Jevon's paradox considers the effect of increased consumption as general energy efficiency drives the price of energy down, and the second explores the profitability of employing energy efficiency strategies in buildings considering the declining cost of energy. The first of these could have a foreseeable impact, on the micro scale in the UAE, since lower utility bills would increase the spendable income of occupants leading to a more extravagant lifestyle in terms of energy consuming behavior, hence, as Copiello argues, energy efficiency in this regard would not benefit the environment nor the energy demand but rather just contribute to economic growth. However, with the basis of Copiello's argument being the reduction in energy costs due

to a lower demand, on a national level these paradoxes would not have a significant role in the UAE, as the cost of electricity is fixed by the government and heavily subsidized. In Abu Dhabi for instance, electricity is produced at an estimated 0.12 $/kWh while sold at a flat rate of 0.04 $/kWh with UAE nationals entitled to further reductions [16]. Therefore, one may conclude that for considerable and sustainable net gains of energy consumption, energy efficiency strategies must be coupled with educational programs that target the most complex of energy consumption factors, namely occupant behavior.

In Wong's and Zhou's review [2], various tools investigating the impact of the different stages of a building's lifecycle are discussed, indicating the significance of certain commonly neglected aspects. Of these is the emissions from the construction process including construction equipment, which could be of equal importance to energy consumption during the operation phase. Another aspect is estimating and planning for the waste from building demolitions, classifying it, and designing with recycling in mind. As a matter of fact, the authors emphasize the lack of effective tools to accomplish the above and the general concept of Reduce, Reuse, and Recycle in design.

Many researchers have also emphasized considering the building as a complete system and proposed several numerical models to optimize design and decision making parameters [3], [4], [6], [22]. Hence, decisions are made based on the lowest life-cycle cost, whether they are made at the design stage or in accordance with a retrofitting strategy. The complex and intertwined relationships between the variables such as the different costs, energy saving potential, service life, and discount rates need to be analyzed simultaneously to achieve the optimum green option.

2.2. Building Information Modelling and Energy Modelling Software

The concept behind building information modelling (BIM) dates back to the 20th century, and BIM was developed as early as the 1980's, however only recently has its potential come under focus [4]. The essence of building information modelling (BIM) is the collaboration between the various teams involved in a construction project. It provides the capacity for professionals working in different domains (architecture, structure, MEP, facilities management) of a project to funnel their input into a unified project platform, thus streamlining the building project by providing information as

soon as possible and easily identifying clashes in the multi-disciplinary design. Hence, BIM can be thought of as a combination of a process, technology, and people [23]. The technology being the platform or the software which facilitates the 3D modelling of the building and its information management [2]. This makes BIM technology an effective tool for analysing design options, making design related decisions, producing high-quality construction documents, planning the construction phase, predicting building performance, and planning the maintenance phase. The implications of BIM technology is that with all available information, a building could be wholly designed, analysed and constructed virtually without breaking ground on site [13].

It is crucial to note that BIM is not an application but rather a process that enables the storing, manipulating and sharing of information. Software applications achieve this through the creation of objects which store information and can be related to other objects. Hence when data on one object is modified, changes are made on all related objects [24].

Numerous BIM software packages are available in the market and they embody a wide range of applications [23]. Of particular interest here is 3D modelling (e.g. Revit) and energy modelling (e.g. IES-VE), however various other aspects can be considered such as scheduling (with time being the 4^{th} dimension, 4D), cost estimation (5D), sustainability (6D), facilities management (7D), accessibility and so on. In this manner it is possible to include an n^{th} number of dimensions, covering design parameters throughout the building's life cycle [24], [25].

However, with so many software applications, each focusing on a particular domain of a building project, there is a need to facilitate the exchange of data between them. This communication between software is called interoperability and is sometimes the deciding factor on which software is used. The most common form in which data can be exchanged between software applications is through the IFC (Industry Foundation Classes) file format by buildingSMART®, which provides a protocol for saving the building model data using a common language. There are 75 organisations supporting the IFC and about 205 applications claim to be IFC compatible [26]. Another form is through specialised schemas such as specially modified XML (extensible markup language) formats. One such format that is relevant to building energy analysis is the gbXML (green building XML), which has the ability to include

thermal data linked with geometric data. Finally, a third form of software interoperability is via a plug-in that integrates into one of the applications and provides some capabilities of another application. An example of such a plug-in would be the integration of COBie (Construction Operations Building information exchange) in Revit to enable it to generate facilities management data [13], [23], [24].

With regards to energy modelling, there are 417 energy simulation software listed by the US Department of Energy alone [23]. However, many of these are not BIM applications and care has to be taken when choosing the applications that are compatible with each other. The most commonly used energy modelling applications found in the literature were eQUEST, Design Builder, Green Building Studio, Ecotect, and Integrated Environmental Solutions – Virtual Environment (IES-VE).

The analysis of building energy is a very complex process that requires considering multiple dynamic variables and relationships between the building operation, the HVAC system, and the weather, making the role of the software application essential. Though, even with the aid of computer programs, energy modelling of buildings requires a steep learning curve and is often delayed in a project due to the need of a large amount of detailed input data [4].

Finally, although the potential of BIM is well understood and praised in the industry, the lack of a comprehensive do-it-all application and the challenges in interoperability hinder many professionals and organisations from adopting it. Also, the sophistication of the models and the lack of user friendly applications further aggravate the problem [2], [17].

2.3. The Building Envelope

The building envelope is the shell of the building that separates the outdoor from the indoor environment and it consists of elements such as walls, windows, insulation, roof, etc. It encloses the inner part of the building, maintaining its designed thermal and acoustic conditions [17]. The envelope is sometimes distinguished into an outer and inner envelope: the outer defined as the components that are in contact with the external environment and the inner being the components that are in contact with the inner conditioned spaces. On some occasions the outer and inner envelopes are separated by a space while on others they are built into one assembly. Figure 2.1 illustrates the inner and outer envelopes. Also related to the concept of a building's envelope is the thermal

boundary (figure 2.2), defined as the delineation produced by the insulated surfaces [12].

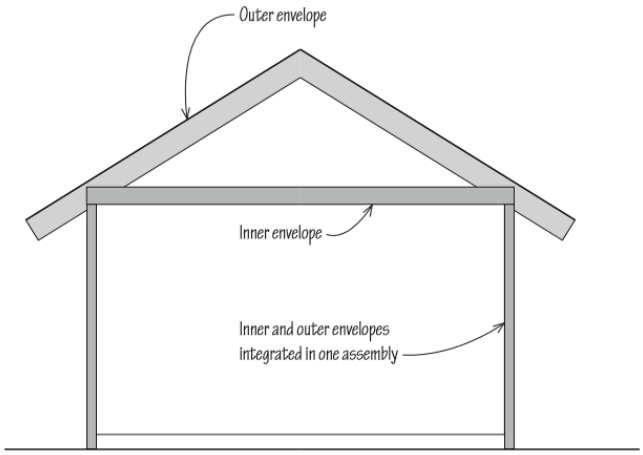

Figure 2.1 - Inner and outer envelope [12]

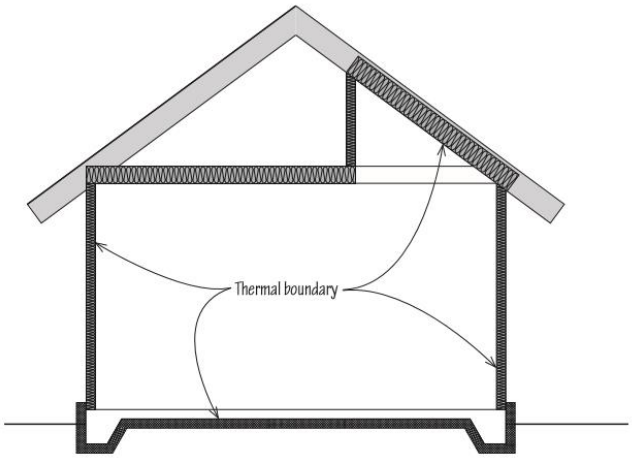

Figure 2.2 - Thermal boundary [12]

One important concept in optimizing the building envelope and maximizing the energy efficiency of a building is that of infiltration. Infiltration is generally the notion of the exchange of air between the interior and exterior of the building. Infiltration needs to be thoroughly addressed and any unplanned for infiltration through the envelope should be ceased. Another concept that needs to be addressed is that of thermal bridges. Thermal bridges are any non-insulating elements that penetrate the thermal boundary causing a thermal leak [12]. The Dubai green building regulations section five mandates the prevention of any air leakage and that all thermal bridges be insulated to prevent any flow of heat from outside the building [19].

2.3.1. The effect of the building envelope on energy consumption. Mostafavi et al. [17] used three energy modelling applications, namely eQUEST, Green building Studio, and an IES-VE plug-in along with Autodesk Revit to evaluate a retrofitted envelope of a dormitories building, at the University of Massachusetts, in terms of energy savings. The original envelope had no insulation and consisted of a single wythe brick veneer in front of a concrete masonry unit (CMU) wall with aluminium-framed, single-glazed windows. The retrofit envelope was to involve replacing the windows on three facades, replacing the veneer brick panels along with the installation of insulation materials between them and the CMU wall, and finally replacing the ribbon windows and storefront glazing on the first floor. Certain aspects of the envelope such as the building orientation and shading of the balconies were also analysed but since it was a retrofit project no further investigation for solutions were conducted.

The retrofit techniques were investigated in two alternative configurations:

- Alternative 1: addition of insulation between the veneer brick and CMU wall.
- Alternative 2: Replacement of the windows as well as addition of insulation.

The model in each of the programs was calibrated using measured energy from building meters before the alternative runs were conducted. Table 2.1 summarizes the calibration accuracy, the U-values of the original envelope and the two alternatives, and the energy savings from each program.

Shoubi et al. [4] investigated the effect on annual energy consumption of changing various materials in the envelope and interior of the building of a double story bungalow in Malaysia. The original building (baseline) was constructed of reinforced concrete and had plastered brick exterior walls, double-glazed, aluminium-framed windows, and hollow core plywood doors. The authors modelled the building in Revit and used Ecotect to perform a separate energy analysis after changing each of the elements listed in table 2.2. Also included in the modifications due to its considerable impact on energy consumption, is the raising of the indoor design temperature by 1 degree.

Table 2.1- Energy analysis result summary [17]

	Baseline	**Alternative 1**	**Alternative 2**
Exterior Walls U-Value (W/m^2K)	1.230	0.540	0.540
Glazing U-Value (W/m^2K)	5.890	5.890	3.120
eQUEST accuracy of electrical use (%)	98	-	-
eQUEST accuracy of gas use (%)	97	-	-
eQUEST potential gas savings (%)	-	16.2	23.8
eQUEST heating load reduction (%)	-	30.2	44.6
GBS accuracy of electrical use (%)	96	-	-
GBS accuracy of gas use (%)	96	-	-
GBS potential gas savings (%)	-	24.9	26.3
GBS heating load reduction (%)	-	29.8	31.4
IES-VE accuracy of gas use (%)	99.8	-	-
IES-VE potential gas savings (%)	-	16.2	23.8

Table 2.2 summarizes the results of the study, however only including the baseline material and the alternative with the highest savings. Where no savings are made the alternative material with the lowest annual consumption is listed. Particularly interesting points made by the study is that, first, no energy savings were detected in the replacement of the hollow core door with a similar polystyrene filled door; and secondly the reduction of windows from 30% to 15% of exterior wall area could reduce about 10-20% of energy losses.

Friess et al. [27] investigated the effect of thermal bridging formed by the un-insulated reinforced concrete (RC) frame on the energy consumption of typical residential villas in Dubai. The study looked at modelled energy consumptions of a case study villa in the as-built condition where an un-insulated RC frame was coupled with insulated-block exterior walls as well as different insulation options applied both as a

retrofit strategy and as a design option. Table 2.3 summarizes the different scenarios modelled.

Table 2.2 - Energy savings of various modifications [4]

Element	Material	Total Energy Consumption (kWh)	Energy Savings (kWh)
Wall	Brick Plaster (basline)	17,600	1000
	Reverse Brick veneer	16,600	
Window	Aluminium framed (baseline)	17,600	800
	Timber framed	16,800	
Floor	Concrete/Tiles (baseline)	17,600	-
	Concrete/Timber	18,500	
Door	Hollow core plywood (baseline)	17,600	100
	Glass sliding door	17,500	
Ceiling	Plaster joists (baseline)	17,600	1500
	Plaster Insulation	16,100	
Indoor Temperature	22 – 26 ˚C	17,600	2350
	23 – 27 ˚C	15,250	
Total	Baseline	17,600	4750
	Best of all modifications	12,850	

The study compared case scenarios A, B, C, and D for the retrofit of the villa's insulation and, as shown in figure 2.3, concluded that the insulation of the RC frame (thermal bridge) had a large impact on the energy consumption of the villa – a 23% reduction – which is almost equal to the gains (24.5% reduction) obtained by covering the entire exterior with a 50 mm EPS layer. Furthermore, case D, which covers the exterior with a 160 mm EPS layer, displayed the highest reduction of almost 30%. Figure 2.4 shows the Energy Utilization Index (EUI) of the different retrofit scenarios.

As for cases E, F, and G, the study shows that case E with no insulation had just a 10% EUI increase over the as built scenario (case A), while the use of un-insulated block with a 50 mm exterior insulation layer showed a 23% reduction in energy consumption. Hence proving that designing a full exterior 50 mm insulation layer with non-insulating block provides just as much energy reduction as with the same insulation layer and insulated blocks. Similarly designing for a full 160 mm insulation layer with un-insulated block provides almost as much energy reduction as the same layer with insulated blocks. Table 2.4 displays this result.

Table 2.3 - The different modelled scenarios [27]

Parameters	Villa
A – as built	20 mm mortar (outer surface) Precast insulated block (200 mm) 15 mm gypsum plastering
B – as built + 50 mm EPS on Thermal bridge only	20 mm mortar (outer surface) 50 mm EPS expanded polystyrene on recessed RC structure only Precast insulated block (200 mm) 15 mm gypsum plastering
C – as built + 50 mm EPS	20 mm mortar (outer surface) 50 mm EPS expanded polystyrene Precast insulated block (200 mm) 15 mm gypsum
D – as built + 160 mm EPS	20 mm mortar (outer surface) 160 mm EPS expanded polystyrene Precast insulated block (200 mm) 15 mm gypsum
E – non-insulated block	20 mm mortar (outer surface) 200 mm concrete block 15 mm gypsum
F – non-insulated block + 50 mm EPS	20 mm mortar (outer surface) 50 mm EPS expanded polystyrene 200 mm concrete block 15 mm gypsum
G – non-insulated block + 160 mm EPS	20 mm mortar (outer surface) 160 mm EPS expanded polystyrene 200 mm concrete block 15 mm gypsum

Finally, the study also investigated the use of high reflectivity triple glazing windows instead of the as-is double glazing ones and recorded a further reduction of 3.7% for case G, and 4.6% for case B. Also, similar to the study by Shoubi et al. this study confirms that adjusting the AC set points by just a few degrees can have a significant impact on the energy consumption of the building.

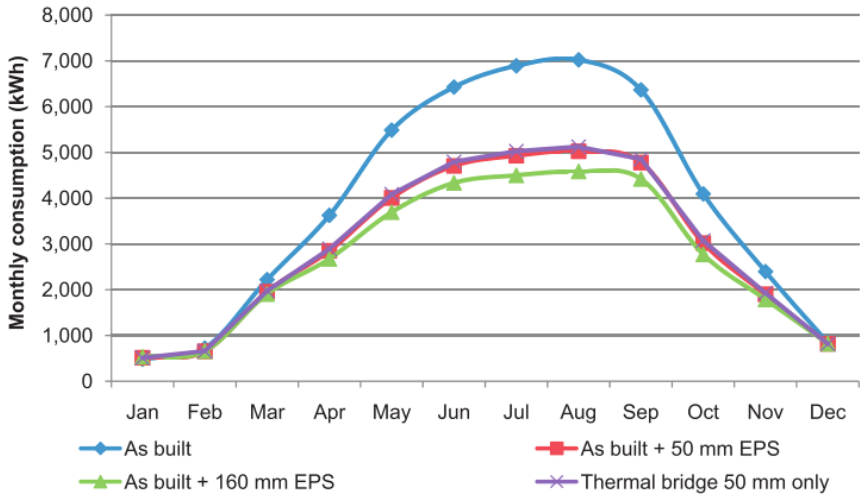

Figure 2.3- Seasonal variation of monthly energy consumption for retrofit alternatives [27]

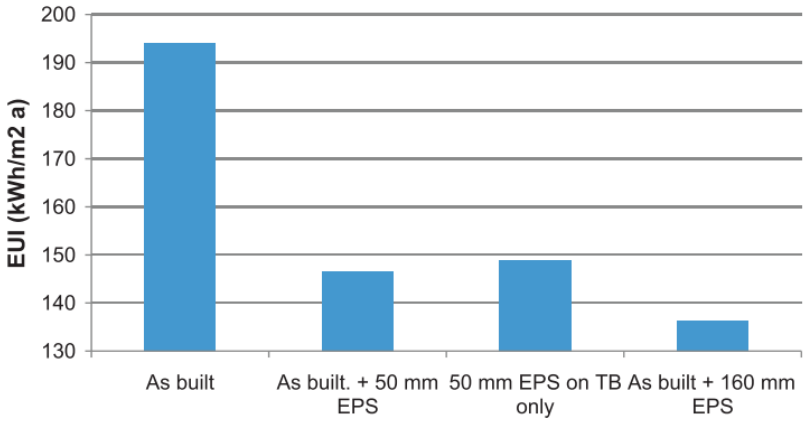

Figure 2.4 - Comparison of EUI for the as-built case vs. three exterior insulation alternatives [27]

Table 2.4 - Energy efficiency impact of insulation alternatives studied [27]

Insulation option	EUI (kWh/m^2 a)	Change with base case (%)
A – as built	205	0
B – as built + 50 mm EPS on TB only	161	–23.3
C – as built + 50 mm EPS full	158	–24.5
D – as built + 160 mm EPS full	148	–29.8
E – non-insulated block	220	+10.6
F – non-insulated block + 50 mm EPS	161	–22.9
G – non-insulated block + 160 mm EPS	149	–29.4

2.3.2. Thermal analysis of the building envelope. Mostafavi et al. [17] used thermal imaging to analyse the thermal mass effect and form a comparison between the brick wall and the glazing through a certain period of the day. Figure 2.5 shows the thermal images of the south-west façade of the building published by the author, at sunset and a few hours later.

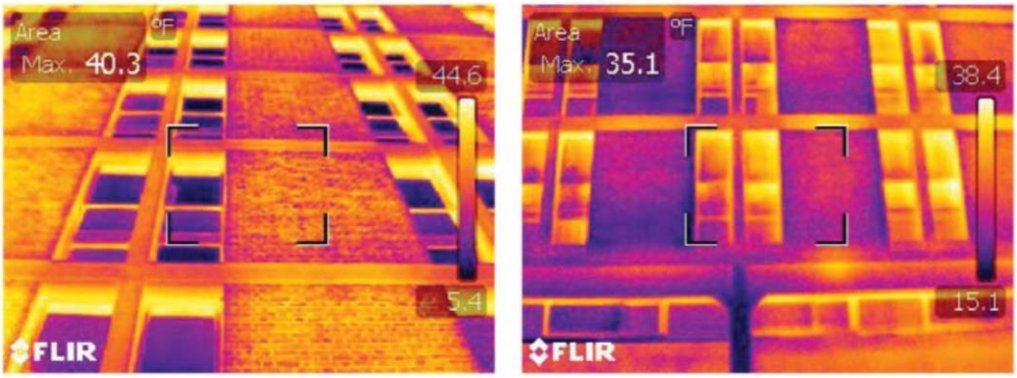

Figure 2.5 - Infrared images at sunset (left) and at 10:00 pm (right)[17].

Furthermore, Balaras and Argiriou [28] introduced thermal imaging in greater detail explaining the effects of emissivity, atmospheric particles, ambient temperature, wind speed, and distance from the target on the accuracy of the thermal measurements. The study then explored some applications of thermal imaging including mechanical, electrical and building envelope inspections. With regards to the building envelope, IR or thermal images can be used to detect missing or damaged insulation, thermal bridges, air leakage, and moisture sources. The study provided some example thermographs of each scenario. Figures 2.6 and 2.7 show thermographs replicated from the study of a missing roof insulation and air leakage from an exterior door.

Another study [29] also showed the effectiveness of thermal images in determining thermal bridges caused by steel studs in a LEED Gold building's envelope. The study emphasized the lack of energy modelling software in accounting for thermal bridges and the need of manual inspections to more accurately size up energy losses through a building's envelope. Figure 2.8 shows the difference in temperature between the insulated envelope and the steel studs.

Figure 2.6 - Thermograph of an interior roof surface with missing insulation [28]

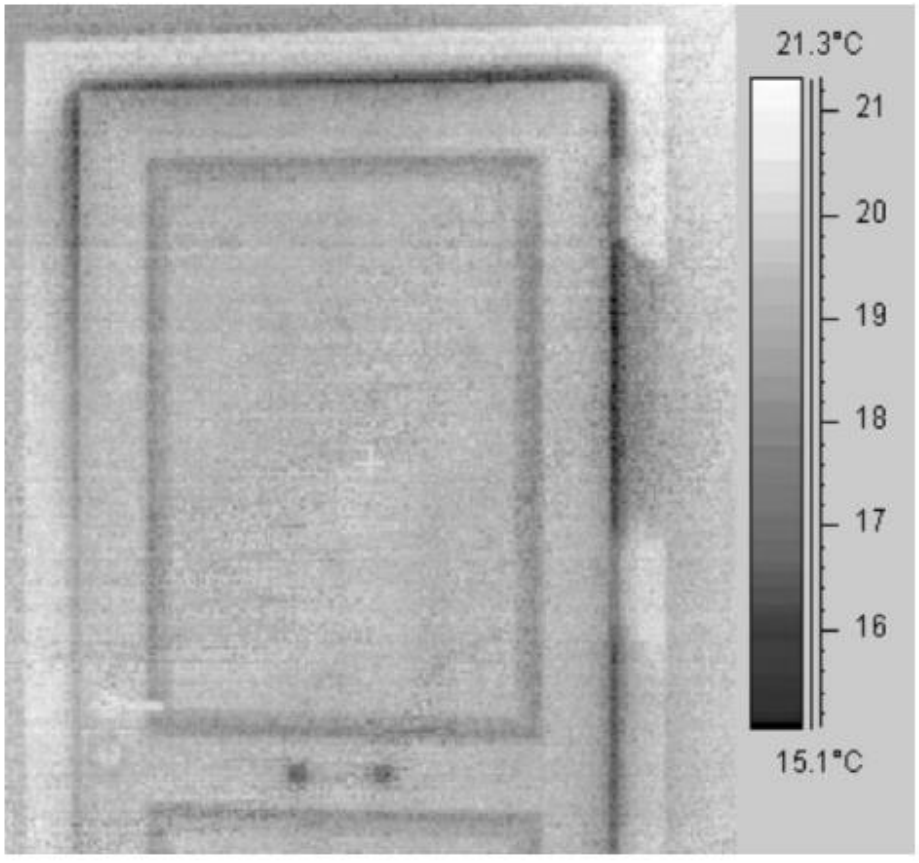

Figure 2.7 - Thermograph of an exterior door viewed from the heated interior space. Cold air infiltration appears in the dark color around the door [28]

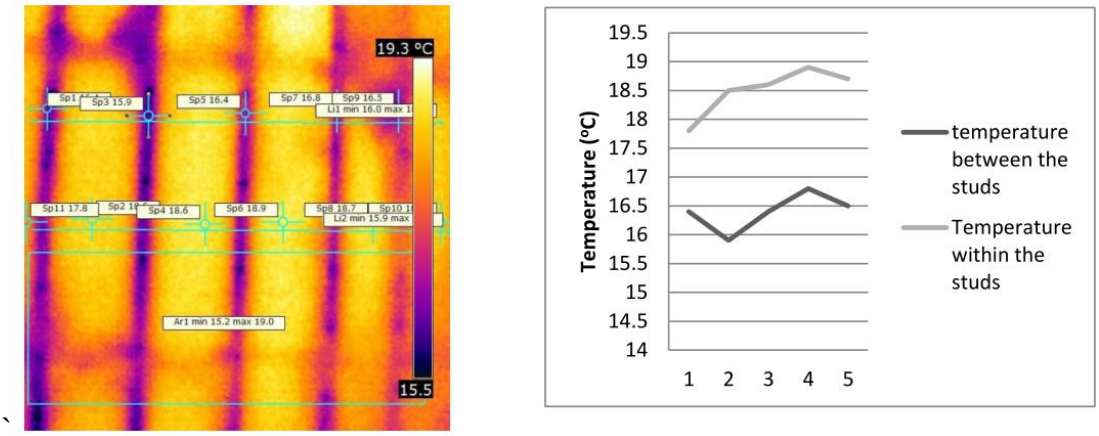

Figure 2.8 - Thermograph showing temperature differences within the steel stud wall (left) and the temperature differences between the steel studs and the area between them (right) [29]

Finally, a study by Fox et al. [30] investigated the difference between thermal imaging inspections conducted by a thorough walk-through method versus a pass-by, external-only imaging method. The study concluded that the walk-through method whereby an inspection is carried out from the exterior and interior of a building is much more effective in detecting envelope defects and thermal leaks as compared to a pass-by method which images only the exterior of the building, however, the former proved much quicker.

2.3.3. In-situ U-value measurement. The literature has well documented research that used the heat flow method as described by ISO 9869 [31] to determine the thermal properties of walls. Asdrubali et al. [32] used the heat flow method to test six green building walls for their experimental U-value and compare them to the theoretical values. The six walls, located in Umbria, Italy, had theoretical U-values that ranged from 0.23 to 0.33 W/m^{2}k, and a 7-day U-value test showed that these theoretical values differed from the actual by 14% at best and up to 43% at worst. Apart from one wall, all walls performed worse than predicted. Another study by Samardzioska and Apostolska [33] tested the U-value of a typical Macedonian façade system (Fragmat NZ-1), on three different buildings. The three tests were also performed using the heat flow method and ranged from 4 to 8 days. The study concluded that the walls, which had actual U-values of 0.227, 0.349, and 0.228 W/m^{2}k indeed coincided with the theoretical U-value of 0.22 W/m^{2}K.

Furthermore, Gaspar et al. [34] also studied the difference between practical and theoretical U-values and besides a literature review that sums up the results of several other works, the authors provide insight into the effect of various test parameters on the accuracy of the results. Most notable of which is the effect of the temperature difference that provides the most accurate results at 19 °C for a test period of 72 h. Lower temperature differences led to more deviations between the actual and theoretical and for more accurate results tests are to be prolonged beyond 72 h.

2.4. Insulation Materials

Jelle [35] reviewed and compared various traditional and state-of-the-art insulation materials for the construction industry. Of particular interest from the traditional materials reviewed, is the mineral wool, expanded polystyrene (EPS), extruded polystyrene (XPS), and polyurethane (PUR).

Mineral wool could be of either glass wool or rock wool and is available in different forms: boards for light application, high-density boards for floor applications, as well as a filler for cavities. Mineral wool typical thermal conductivity values range between 30 to 40 mW/m K, with the value varying with temperature, moisture content and mass density. Mineral wool insulation can be perforated and easily cut to shape on site without loss of thermal resistance.

EPS is mainly produced as boards and has typical thermal conductivity values of 30 to 40 mW/m K, also varying with temperature, mass density and moisture content. It too can be perforated and adjusted on site without any loss of thermal resistance.

XPS is produced in continuous lengths that are cut as required later. It has a closed pore structure and typical thermal conductivity values between 30 to 40 mW/m K as well.

Finally, PUR has closed pore structure filled with an expansion gas of either HFC, CO2, or C6H12. PUR products may come in boards or as an expanding foam to be used on site around fixtures and in cavities. It has typical thermal conductivity values between 20 to 30 mW/m K, which is lower than that for mineral wool and polystyrene products. An important consideration of using PUR is that in case of a fire it emits hydrogen cyanide which is very poisonous.

These findings have also been iterated in a study by Papadopoulos [36] that also compared the traditionally used insulation materials in Europe. Table 2.5 summarizes the comparison.

Finally, Jelle also reviewed some of the latest insulation materials available for the industry to adopt such as vacuum insulation panels (VIP), gas filled panels (GFP), aerogels and phase change materials (PCM). VIPs for example have thermal conductivity values of 3 to 4 mW/m K when new and about 8 mW/m K after 25 years. However, a major drawback is that they can be punctured in the harsh site environment and their thermal conductivity value would rise to about 20 mW/m K. Also, commercially available Aerogels can have thermal conductivity values of 13 to 14 mW/m K but they too have a drawback of a very low tensile strength. Figure 2.9 shows high performance aerogel insulation sheets.

Table 2.5 - Insulation material comparison [36]

Main physical features	Material				
	Glass wool	Stone wool	Extruded polystyrene	Expanded polystyrene	Polyurethane foam
Density (kg/m^3)					
Minimum	13	30	20	18	30
Maximum	100	180	80	50	80
Thermal conductivity factor, λ (W/m K)					
Minimum	0.030	0.033	0.025	0.029	0.020
Maximum	0.045	0.045	0.035	0.041	0.027
Temperature application range (°C)					
Minimum	−100	−100	−60	−80	−50
Maximum	500	750	75	80	120
Resistance to vapour diffusion factor					
Minimum	<1	<1	80	25	50
Maximum	1	1	200	200	>100
Humidity assimilation rate (at 23 °C/80% RH)					
Minimum	<0.1	<0.1	<1[a]	5[a]	5[a]
Maximum	1	1.5			
Reaction to fire class					
Minimum	A1	A1	B1	B1	B1
Maximum	A2	A2	B2	B2	B2
Tensile strength (N/mm^2)					
Minimum	0.005[a]		0.30	0.15	
Maximum			0.35	0.52	
Ultimate tensile strength (N/mm^2)					
Minimum	0.00500	0.00012		0.09000	
Maximum	0.01500	0.00750		0.22000	
Sound absorption degree (at 125 Hz)					
Minimum	0.10	0.05			
Maximum	0.79	0.19			
Sound absorption degree (at 1000 Hz)					
Minimum	0.71	0.92			
Maximum	0.97	0.99			

Figure 2.9 - Aerogel insulation sheets [35]

Chapter 3. Methodology

In this chapter, the research methodology applied to achieve the research objectives is outlined. It mainly constitutes of three layers of tests and observations: development of an energy model for the case study building, using a thermal camera to scan the case-study building's envelope for thermal bridges, and finally testing the case study building's external wall experimentally to determine its U-value.

To focus the scope of this study it is crucial to outline that the main concern is the passive design of buildings such that the energy consumption is reduced inherently. Further, the passive design of buildings is achieved through two main categories of design: optimizing natural ventilation and minimizing heat gain. This study is concerned with minimizing heat gain.

3.1. The Case Study Building

The case study building is to be thoroughly studied by first studying its contextual environment, then studying the building itself by breaking down it's areas, laying out the information available about its construction using the as-built drawings, and finally analyzing its metered consumption in detail. In the analysis of its metered consumption, the building is to be compared to other building types for comparison and the Cooling Degree Days (CDD) analysis tool is to be employed.

3.2. The Energy Model

The case study building is to be BIM-modelled using Autodesk Revit then exported to IES-VE for the energy analysis. Then the energy model is to be calibrated with the utility bills and meters of the case study building to ensure modelled consumption values correspond with the actual performance of the building, and any discrepancies identified. Various parameters regarding the building envelope and building orientation shall be investigated for their effect on the energy consumption.

The choice of using Integrated Environment Solutions – Virtual Environment (IES-VE) as the modelling software stems from the fact that it is the latest in energy modelling software and boasts an upgraded and advanced analysis engine. While Design Builder (with the EnergyPlus engine) has been used for decades, IES-VE is now the preferred choice for the largest consulting companies in the AEC industry.

3.3. Thermal Bridge Investigation

The building envelope is to be thermally analyzed with a thermal camera to search for thermal bridges in accordance with ISO 6781 [37]. The entire building envelope shall be scanned, and certain doubtful locations as determined from the drawings shall be specifically inspected. The detection of any thermal bridges may then lead to an adjustment of the thermal resistance values of the envelope in the energy model according to standards ISO 6946 [38] or ISO 10211, and may perhaps even explain any discrepancies faced in the model calibration. Solutions to the thermal bridges would also be sought out.

3.4. Building Experimental U-Value

The building's external wall shall also be experimentally tested for its U-value, in order to further ensure that the energy model has had the right inputs and to explore reasons for any discrepancies in the model calibration. The test is to be done in accordance with ISO 9869 [31], using a heat flux sensor and a thermocouple. The obtained U-value would then be compared to the one used in the model and calculated based on the materials specified in the drawings.

Chapter 4. The Climate of the UAE and Initial Design Considerations

The United Arab Emirates is located in the northern hemisphere, roughly just north of the Tropic of Cancer (23˚ 5’ N) – more precisely, the Tropic of Cancer passes through the Abu Dhabi desert. Located in the northern hemisphere would mean that the Sun would always reach its maximum altitude (solar noon) in the south.

It is quite useful to understand the movement of the sun in the sky when designing green buildings. It provides the designer with the environmental knowledge necessary to create buildings that are well suited to their location and that utilize their environment as much as possible. To understand the Sun’s movement, it seems apt to start with the equinoxes and solstices. These are the astronomical seasons of the year based on the position of the earth with respect to the sun.

Equinoxes are when the earth is tilted neither towards nor away from the sun and the duration of the day and night are almost equal. This happens twice a year – once around the 21st of March (Vernal Equinox) and once around the 23rd of September (Autumnal Equinox). Likewise, there are two solstices in a year – one around the 21st of June (Summer Solstice) and one around the 21st of December (Winter Solstice).

At the equinoxes the sun shall be level with the equator and will reach the zenith (directly overhead) as seen from the equator. The sun’s level oscillates between the Tropic of Cancer (23.5˚ N) at the Summer Solstice, where the earth is tilted towards the sun, and the Tropic of Capricorn (23.5˚ S) at the December Solstice, where the earth is tilted away from the sun; each time passing the equator at the Equinoxes. These tropical limits at 23.5˚ are nothing but the angle of the earth’s tilt which is also 23.5˚.

The Summer Solstice marks the longest day of the year in the UAE and the onset of shorter days. The sun at solar noon is almost at the zenith (directly overhead) at an altitude of about 88˚ (table 4.1), it rises north of east at an azimuth of about 63˚ and sets north of west at an azimuth of about 297˚. This delineates a northern angle of about 126˚ that will not have direct sunlight at any point of the year – a fact that can be used in the orientation of the building and the design of its glazing to minimize heat gain.

On the other hand, the December Solstice marks the shortest day of the year and the onset of longer days. The sun follows a much lower arch in the sky and has the

lowest altitude at solar noon of about 41˚ (table 4.1), it rises south of east at an azimuth of about 115˚ and sets south of west at an azimuth of about 244˚.

Table 4.1 - Solar data for Sharjah, UAE.

	Daylight Duration			At Noon			Sun Peak	
2018	**h**	**m**	**s**	**Altitude**	**Azimuth**	**Shadow Ratio**	**Culmination**	**Altitude**
20-Jan	10	48	57	44.06	170.51	1.03	12:29:00 PM	44.61
20-Feb	11	26	16	52.99	166.98	0.75	12:31:45 PM	53.81
20-Mar	12	7	16	63.82	165.39	0.49	12:25:33 PM	64.57
20-Apr	12	52	20	75.66	162.97	0.26	12:17:00 PM	76.23
20-May	13	27	51	83.71	147.02	0.11	12:14:33 PM	84.68
20-Jun	13	43	34	85.16	111.88	0.08	12:19:34 PM	88.11
20-Jul	13	30	43	82.7	128.52	0.13	12:24:24 PM	85.33
20-Aug	12	55	49	76.15	157.57	0.25	12:21:27 PM	77.1
20-Sep	12	11	45	65.6	173.01	0.45	12:11:31 PM	65.76
20-Oct	11	28	18	54.33	178.79	0.72	12:02:51 PM	54.34
20-Nov	10	50	38	45	178.8	1	12:03:36 PM	45.01
20-Dec	10	34	25	41.14	175.28	1.14	12:15:30 PM	41.28

Besides the orientation and glazing of the building, the knowledge of the sun's path in the sky around the year would allow for the analysis and design of suitable shading, natural lighting, and solar power strategies.

The difference between the lowest (41˚) and highest altitudes (88˚) is about 47˚ and that is called the solar window. Photovoltaic (PV) panels are designed to always face somewhere in between. For instance, to install a fixed flat PV array, that will not be moved throughout the year, the panels may be tilted an angle of 25.5˚ from the horizontal (collector tilt angle) such that the normal to its' surface would point to an altitude of 64.5˚ – just in between the lowest and highest altitudes of the sun at solar noon. In practice however, the angles used are based on extensive research on maximizing the output and are generally lower – around 18˚ from the horizontal for the Middle East region.

Climate Consultant 6.0 was used to conduct a radiation analysis (Figure 4.1) to determine the average irradiation range throughout the year. For the purpose of flat PV

panel installation, the Global Horizontal Irradiation (GHI) is the metric of interest and it has a maximum hourly record of 1051 Wh/m^2 recorded in May. The highest daily average however was recorded as 7771 Wh/m^2 in June. For the objective of calculating PV panel output the annual hourly mean of 500 Wh/m^2 or the annual daily total mean of 6000 Wh/m^2 may be used. The data from Climate Consultant uses an EPW weather file for the emirate of Abu Dhabi, however the radiation data is sufficiently close to that of the emirate of Sharjah as verified by Muhammed and Sidra [39] and data from the UAE Solar atlas [40] as shown in figure 4.2.

For instance, to calculate the power output of a 50 m^2 flat PV array of 16% efficiency:

$$Power\ Output = Area \times Effieciency \times Radiation$$

$$Power\ Output = 50\ m^2 \times 0.16 \times 6\ kWh/m^2\ =\ 48\ kWh\ per\ day$$

Climate Consultant was also used to determine the global radiation incident on a surface tilted at 25.5˚, and the annual daily total mean jumped to 6500 Wh/m^2, hence increasing the average daily generated solar energy to 52 kWh. This amounts to 18,980 kWh per year.

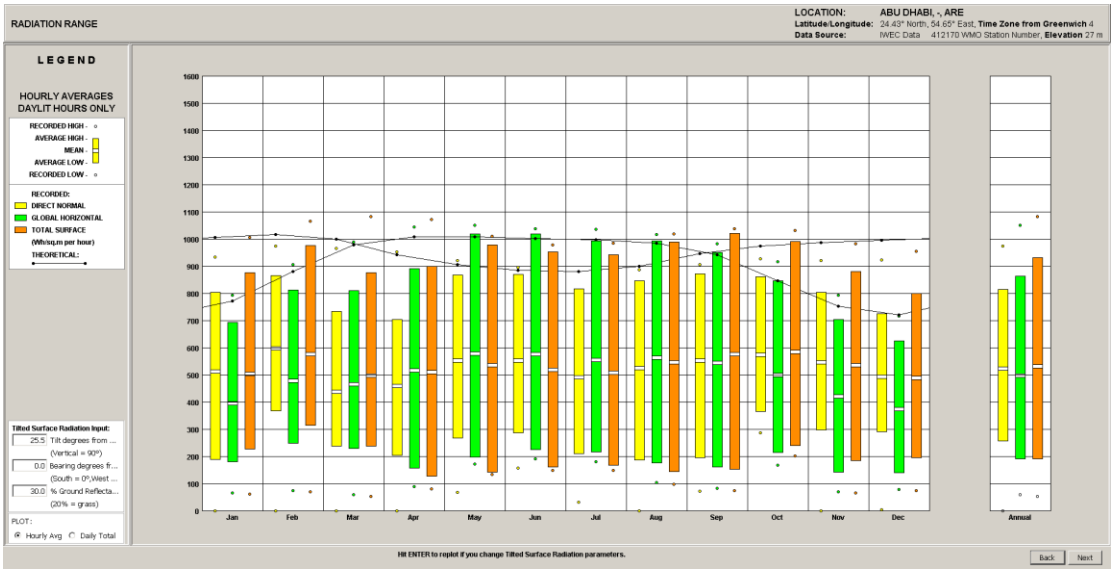

Figure 4.1 - Radiation analysis - Climate Consultant 6.0

The UAE is also very friendly to solar power due its relatively low sky cover that has an annual average of 18% and an average highest in the month of March at 70%. Though most months have an average high of less than 40%.

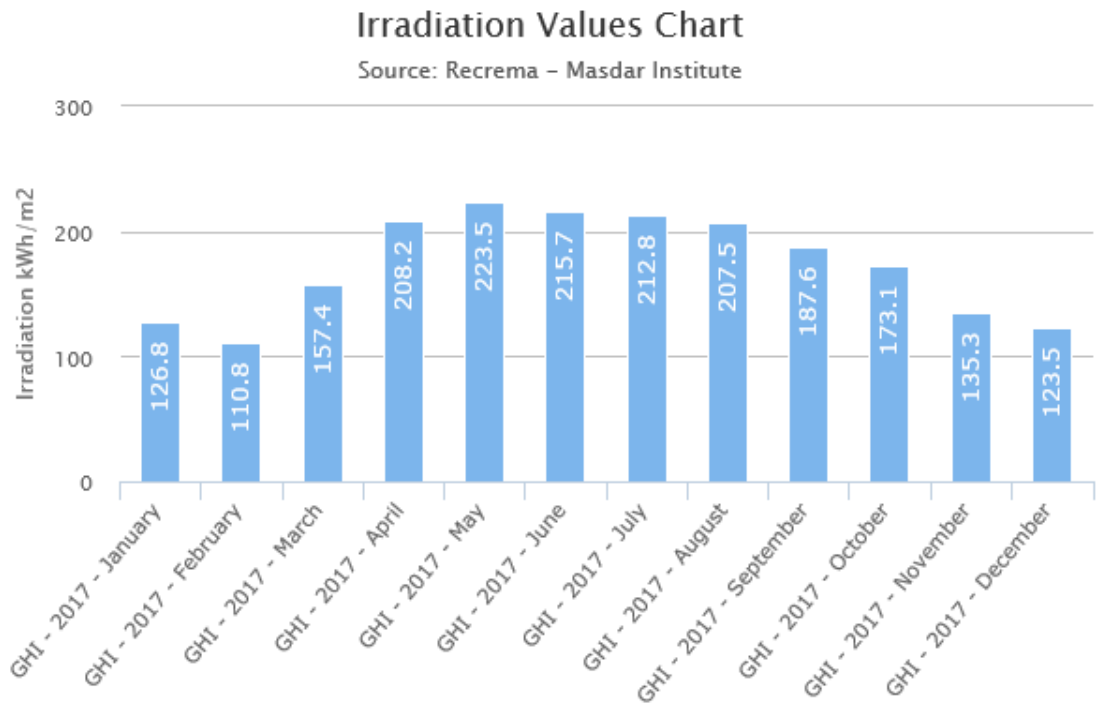

Figure 4.2 - Global horizontal irradiation at the American University of Sharjah [40].

Although the astronomical seasons have the aforementioned effect on the suns position in the sky, they don't however change the climate very much. The four common meteorological seasons are only experienced in latitudes higher than the Tropic of Cancer or lower than the Tropic of Capricorn. The region in between, including the UAE, is known as the tropics and does not experience seasons besides the hot summer and the colder winter.

Temperatures in the UAE range between an average year-round high of 43˚ C and an average low of 12˚ C with a mean temperature of 28 ˚C. The hottest month is July with an average record high exceeding 45 ˚C and a record low of 27 ˚C. The coldest month is January with a temperature range between 9 and 28 ˚C. Using Climate consultant and with accordance to the ASHRAE Standard 55 thermal comfort model, only three months of the year – namely March, April, and November – have a mean monthly temperature that falls within the comfort zone.

Furthermore, the long-term average temperatures of climate consultant were used to calculate the Cooling Degree Days (CDD) and the Heating Degree Days (HDD)

that may be used to compare the energy consumption potential in different places or to normalize consumption data with weather information. There are numerous sources in the literature to calculate the degree days, however it shall suffice to mention here that the degree days need to be calculated around a base temperature, the choice of which is generally left to the analyst and the purpose of the calculation. The base temperature may be chosen through a regression analysis of various base temperature degree days and consumption data, or, as is done here, may be chosen based on a theoretical analysis. Table 4.2 provides the monthly and yearly degree days around a base temperature of 20 ˚C, a base temperature commonly used by experts in the UAE.

Table 4.2 - Calculation of the degree days in UAE for a base temperature of 20 ˚C

Base 20 ˚C				
Month	**Month Name**	**Mean Temp. (˚C)**	**HDD**	**CDD**
1	January	18	65	3
2	February	20	27	26
3	March	22	11	81
4	April	27	0	196
5	May	31	0	335
6	June	33	0	384
7	July	34	0	448
8	August	35	0	459
9	September	33	0	377
10	October	29	0	266
11	November	24	0	131
12	December	20	20	23
	Total		123	2727

However, since the temperatures used to calculate the degree days are dry bulb temperatures, it seemed apt to lower the base temperature to 18 ˚C (table 4.3) to account for the latent cooling capacity required to remove moisture from the air. The HDD are generally ignored by experts in the UAE and hence not much attention is given to the base temperature they are calculated around.

Table 4.3 - Calculation of the degree days in UAE for a base temperature of 18 ˚C

Base 18 ˚C				
Month	**Month Name**	**Mean Temp. (˚C)**	**HDD**	**CDD**
1	January	18	18	18
2	February	20	4	59
3	March	22	2	133
4	April	27	0	256
5	May	31	0	397
6	June	33	0	444
7	July	34	0	510
8	August	35	0	521
9	September	33	0	437
10	October	29	0	328
11	November	24	0	191
12	December	20	0	65
	Total		24	3358

The degree days were also calculated around a base temperature of 10 ˚C to obtain a total CDD of 6254. This is required to obtain the climate zone of the UAE as per the ASHRAE Standard 90.1 which places the region in zone 1A, or 1B if the CDD10 > 5000 (for version 2004 to 2015) and climate zone 0B if the CDD10 >6000 (for version 2016). This is consistent with the Estidama code [41] that places the emirate of Abu Dhabi in zone 1B – "very hot and dry" – as per Standard 90.1 2007. Furthermore, according to the 2016 annual report by Dubai's RSB for Electricity and Water, there has been a general increase in the CDD's by 1.2% a year since 2000 [42].

The humidity in the UAE can get very high, however averages at a yearly mean of about 51%. Figure 4.3 shows the variation in average monthly humidity along the year and it can be observed that the humidity has an inverse relationship with the dry bulb temperature. This can be explained by the fact that at lower temperatures, air can hold less moisture than at higher temperatures, hence at a given absolute humidity, a given amount of cold air will have a higher relative humidity than the same amount of hot air.

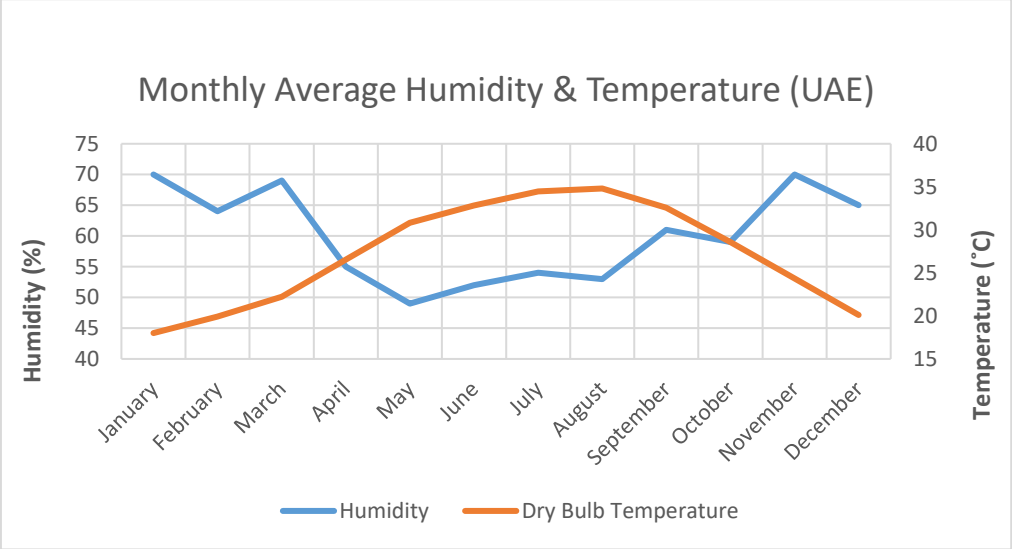

Figure 4.3 - Monthly average humidity and temperature (UAE).

To determine the variation of the effect of humidity on the latent cooling load and ultimately the energy consumption, the Absolute Humidity (AH) will be the metric of interest. Using the average monthly temperature and the relative humidity and assuming ideal gas behavior the average absolute humidity was plotted (figure 4.4) for each month of the year. It is evident that although the relative humidity decreases during the summer months, the absolute humidity or the amount of moisture in the air actually increases and it follows the dry bulb temperature trend.

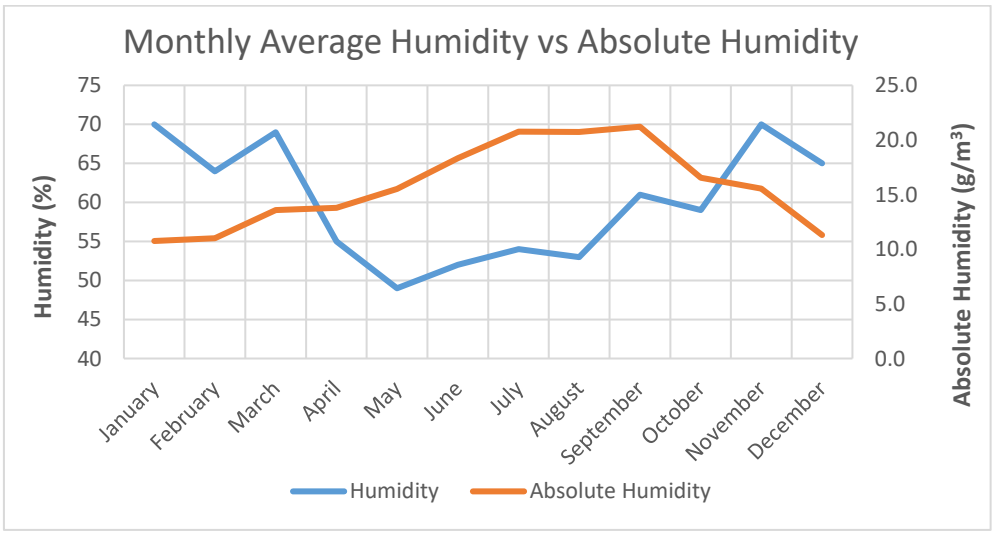

Figure 4.4 - Monthly avg. humidity vs absolute humidity (UAE)

Chapter 5. The Case Study Building

In this chapter the case study building used for this project is introduced, important information available about its envelope is presented, and its energy consumption is analyzed in detail.

5.1. General Area Breakdown

The case study building studied is the Campus Services Center (CSC) at the American University of Sharjah (figure 5.1), located at 25.312˚ N and 55.488˚ E. It consists of a ground + 2 floors office block and an adjoining warehouse. The warehouse is ignored for this study.

Figure 5.1 - The case study building - CSC building at AUS

The building has a gross floor area of 3,466.918 m^2 as determined from the as-built drawings and a perimeter of 59.3667 m (figure 5.2). The 3,466.918 m^2 gross area is divided between 1255.864 m^2 for the Lower Ground Floor (LGF), 1060.876 m^2 for the Upper Ground Floor (UGF), 1083.783 m^2 for the First Floor (FF), and 66.395 m^2 for the Top of the Roof (TOR) level. The LGF has about 515 m^2 of its space area (measured along the centerline of its walls) dedicated to workshops, about 45.7%; and 119.18 m^2 of its space area (10.6%) dedicated to a data center. The remainder of the building area is broken down as shown in table 5.1, where the space type “Shaft” includes any service shafts, elevator shafts, and staircase wells; the space type “Other”

consists of toilets, service rooms, and vestibules; the space type “Open office” includes offices, meeting rooms, reception, corridors and such; and the space type “Store” includes stores and cabinets. It can also be determined from this breakdown that about 65.5% of the total building area is used for office space (moderate energy demand), 20.1% is used for high energy demand workshops and data center, with the remaining 14.4% distributed between low energy demand areas. This is illustrated in figure 5.3.

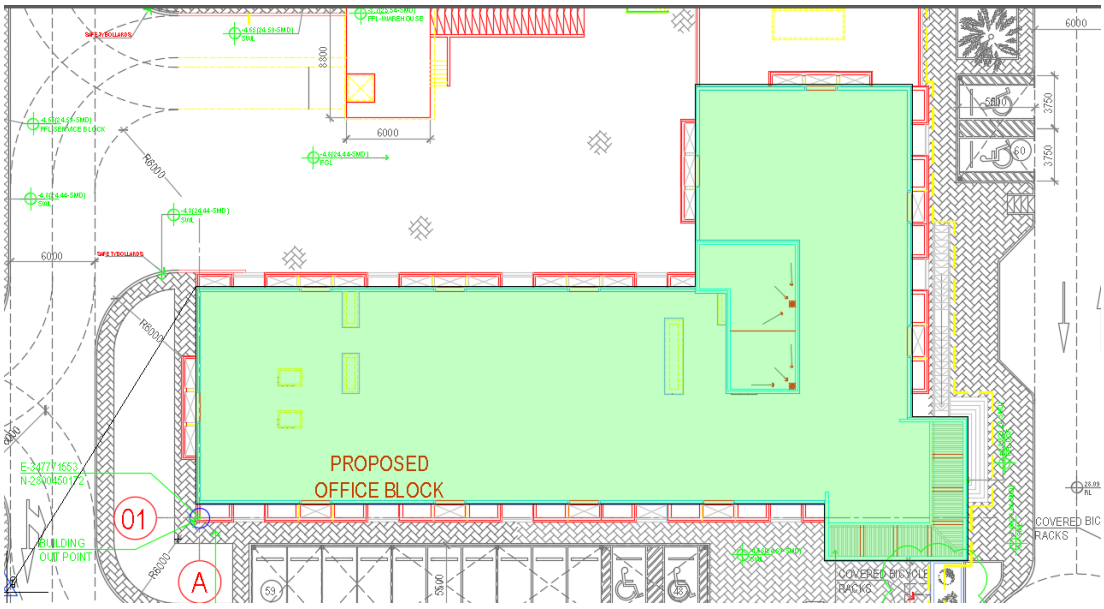

Figure 5.2 - The general footprint of the building determined from the as-built drawings

Table 5.1 - Area breakdown of the CSC building by floor

Level:	**LGF**	**UGF**	**FF**	**TOR**
Space Type		**Area (m^2)**		
Shaft	40.72 (3.6%)	44.04 (4.5%)	41.25 (4.2%)	19.59 (38.5%)
Other	83.18 (7.4%)	62.64 (6.3%)	58.14 (5.9%)	31.25 (61.5%)
Open Office	321.14 (28.5%)	869.09 (87.8%)	876.4 (88.6%)	
Store	46.97 (4.2%)	13.57 (1.4%)	13.57 (1.4%)	
Workshop	514.83 (45.7%)			
Data Center	119.18 (10.6%)			

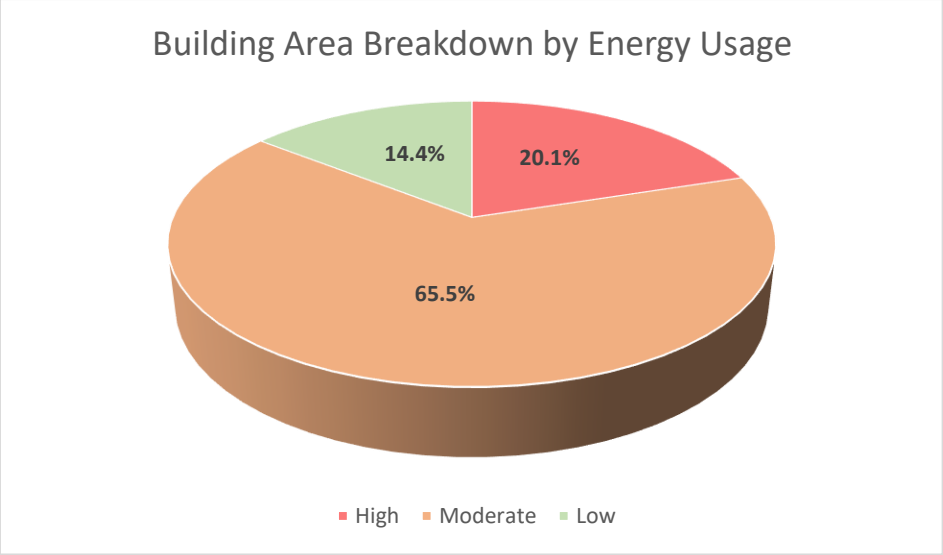

Figure 5.3 - Building area breakdown by energy usage

5.2. Building Envelope

The information available about the building envelope mainly includes:

- The exterior walls: which includes the exterior finish, a minimum of 100 mm extruded polystyrene (with U-values of 0.27 W/m^{2}K or less), the backup wall (concrete, block, column, etc. – determined from the as-built drawings), and the interior plaster and finish.
- The exterior windows: which are double glazed with a thickness of 6 + 16 + 6 mm and with Cardinal C240 glass for the northern façade and Cardinal C366 for the south, east, and west façade. As determined from Estidama's Villa Product Database [43], the C240 glass is sputter coated with a double layer of silver to obtain low-emissivity, while C366 is sputter coated with a triple layer of silver. Also, from Estidama's database, the U-value and solar heat gain coefficients of the northern façade glass are 1.66 W/m^{2}K (glass only) and 0.25, respectively; and for the East, West, and South façade glass they are 1.57 W/m^{2}K (glass only) and 0.28 respectively. Both glass conform to Estidama's RE-R1 Minimum Energy Performance requirement.
- The roof: which consists of a layer of stone ballast, filter fabric, minimum of 100 mm extruded polystyrene (with U-values of 0.3 W/m^{2}K or less), 2 ply modified bituminous roofing membrane, concrete screed, and the concrete structural slab.

5.3. Energy Consumption

The energy consumption of the building was obtained from the building's main grid meter for the months from March 2013 up to February 2018 and the average consumption of the building during this period was 540.3 MWh per year. Figure 5.4 shows the variation of monthly consumption for all months over that period while figure 5.5 shows the average consumption over the year using the same data.

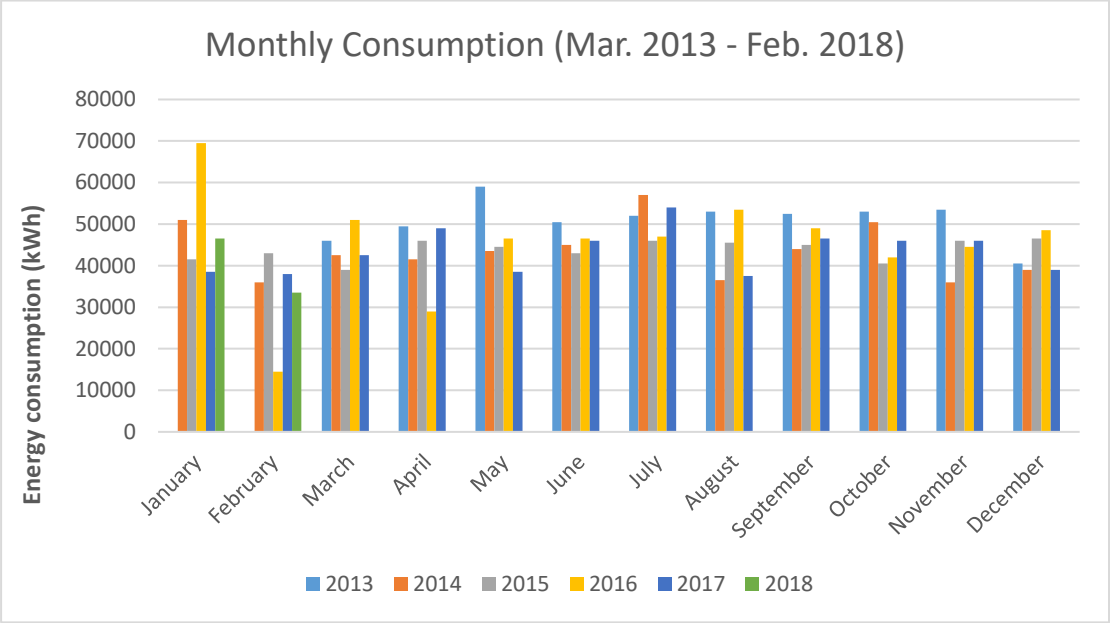

Figure 5.4 - Monthly consumption (Mar. 2013 - Feb. 2018)

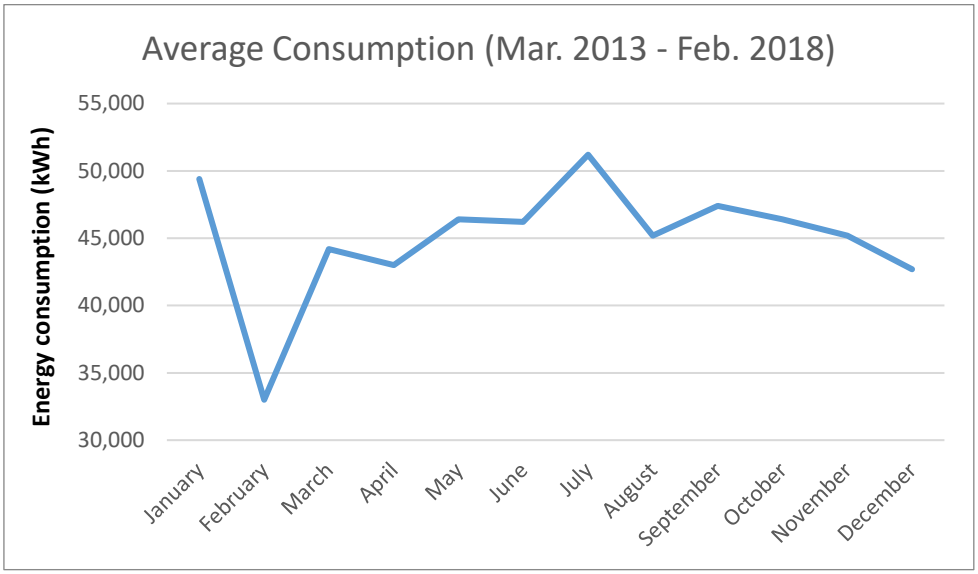

Figure 5.5 - Average monthly consumption for the CSC bldg.

It can be observed that the lowest consumption does occur during the coldest period of the year (January to February), the highest consumption does occur during the hottest month of the year, and there is a general decline of consumption during the colder months and an increase in the consumption during the hotter months. However, it can also be seen that the data is fairly irregular and is clearly not heavily influenced by the weather. To better understand the dependence of the consumption on the weather one can make use of the concept of degree days discussed earlier. For the United Arab Emirates, it is common for buildings to not use any heating all year round and only depend on cooling during the hotter months, hence only the cooling degree days (CDD) are needed. If the average monthly CDDs are plotted along with the average monthly consumption on the same graph (figure 5.6) the influence of the weather can be better assessed. Again, one can see that the consumption somewhat follows the CDD curve in shape, but significantly deviates in some areas. Instead of the monthly consumption figure 5.6 uses the monthly consumption over the baseline, which in this case is the consumption minus the lowest consumption of the year. The relationship will not change but it will allow both graphs to bottom at the same point on the y-axis (the zero mark) and hence allow for better comparison. It is also important to mention that the CDDs used here are around a base temperature of 25 ˚C.

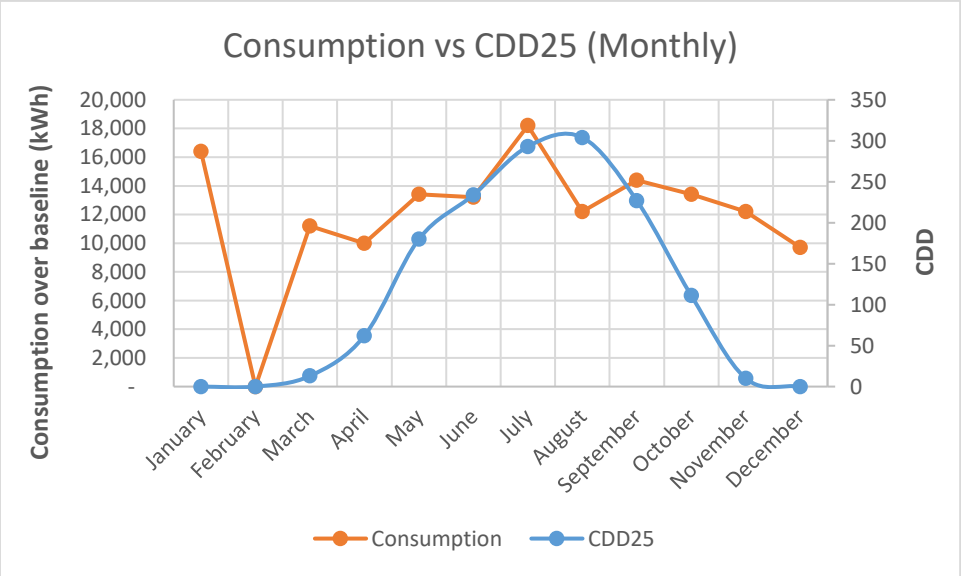

Figure 5.6 - Monthly consumption with monthly CDD25 (CSC building)

To quantify this result regression analysis was used and the consumption plotted against the CDDs on a scatter graph, and a linear trend line drawn to determine the coefficient of determination (R^2) value. That value for the CSC building is just about 0.24, which indicates a correlation between the variables, although a rather weak one. Furthermore, to obtain a more accurate analysis, the consumption per day can be plotted against the CDDs per day to account for the influence of the unequal periods of time, i.e the variation of the number of days in a month. However, as expected the variation is minimal and as can be seen in figure 5.8 the R^2 has increased to 0.27. The major advantage however is where the trend line crosses the y-axis, also called the baseline consumption – where figure 5.7 gives an average monthly baseline, figure 5.8 gives a per day baseline that can be multiplied by the number of days in a month to give a more accurate consumption figure. The equation of the line will also be more accurate and can be used to determine future consumption given the forecasted CDD25.

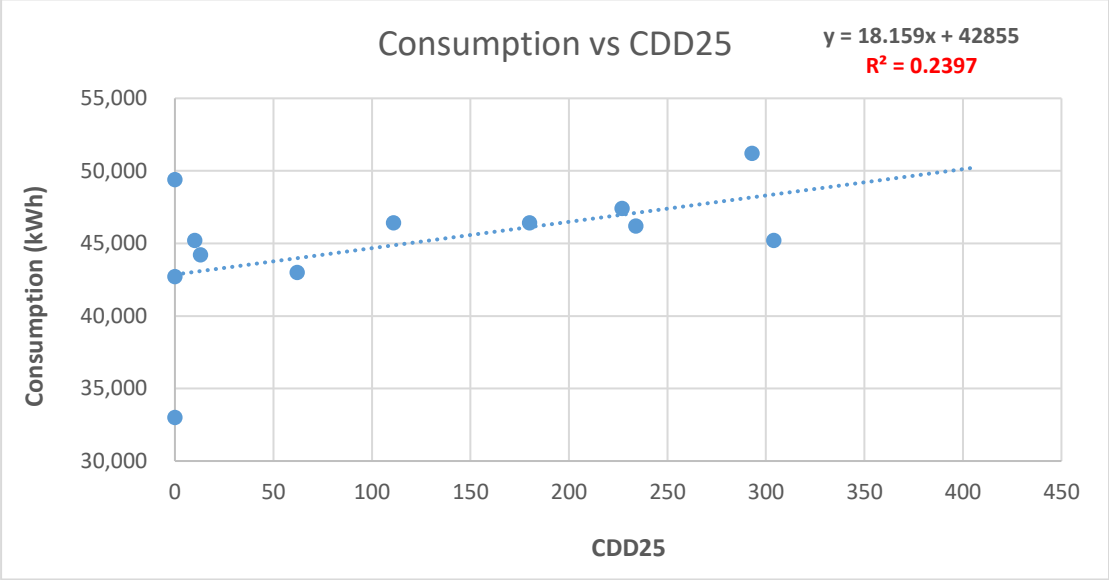

Figure 5.7 - Determining the coefficient of determination for the CSC bldg. (R^2 value)

The results above are expected, since the CSC building uses district cooling, where chilled water is served to it by a separate chiller building. The correlation is hence mainly due to the running of the mechanical equipment (the AHU's and FCU's) that form the part of the air conditioning within the building; with the major influence on the consumption coming from the occupational schedule.

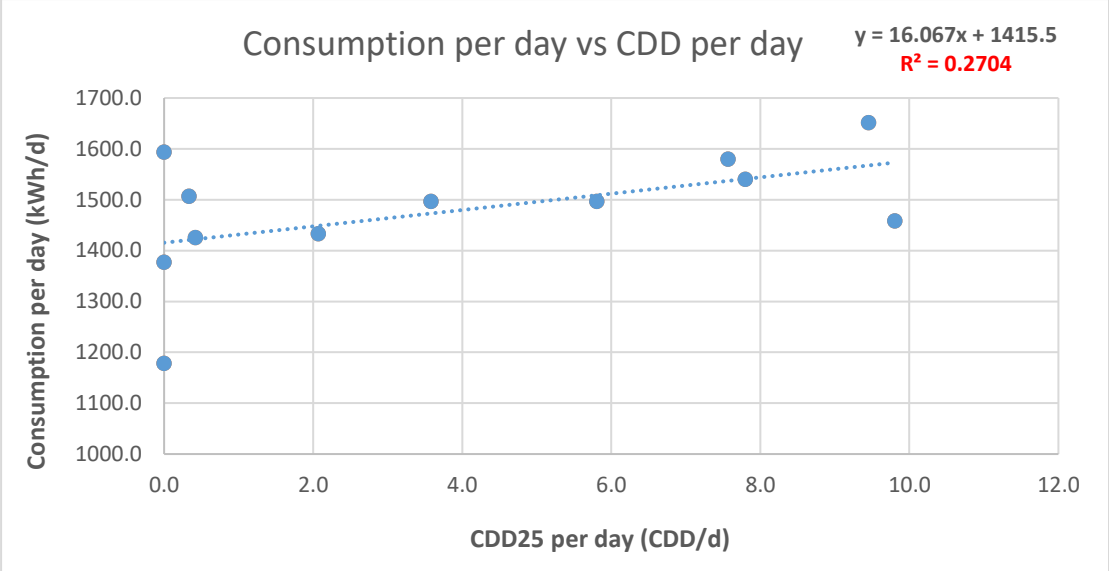

Figure 5.8 - Consumption per day against CDD per day (CSC building)

The impact of this correlation can be illustrated by performing the same procedure for the chiller building, which has the sole job of cooling water as per the seasonal requirement. From figure 5.9, it is clear that the consumption curve very closely matches the CDD25 curve and that is quantified in figure 5.10 where the R^2 value was determined as 0.916, hence showing a very high correlation between the weather and the consumption.

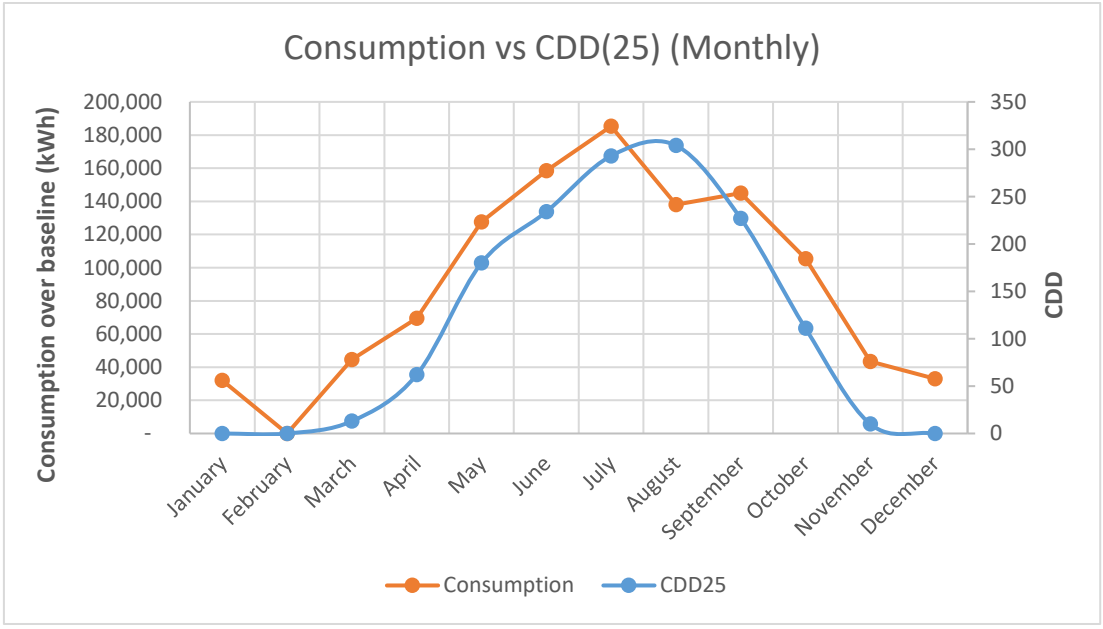

Figure 5.9 - Monthly consumption with monthly CDD25 (chiller building)

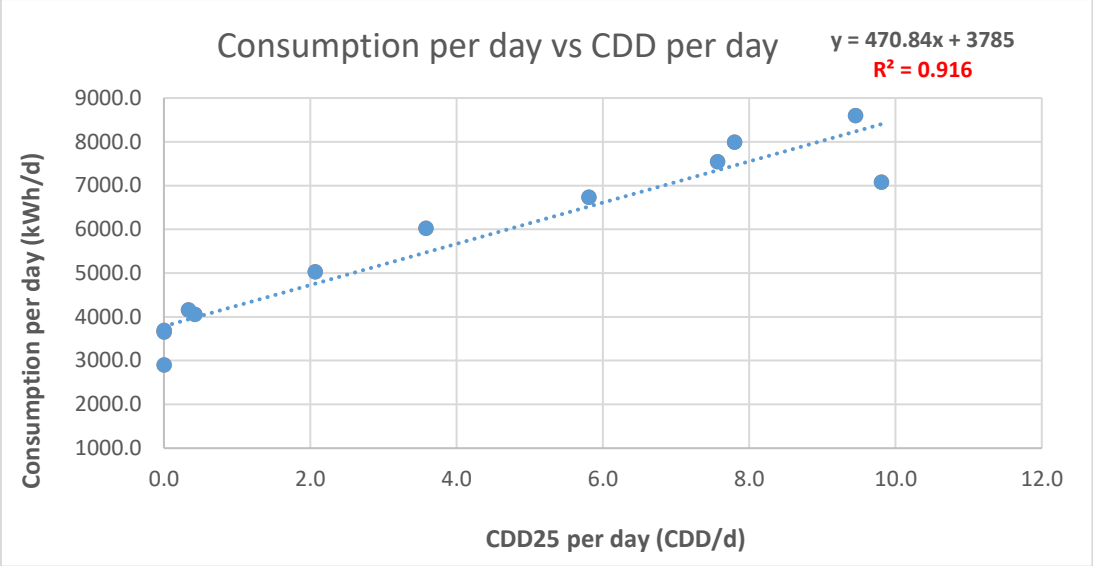

Figure 5.10 - Consumption per day against CDD per day (chiller building)

For a building that uses conventional cooling as well as serve other functions such as educational classes that have a distinct occupational schedule, the correlation will obviously be expected to be somewhere in the middle of the R squared values of 0.27 and 0.916. One such building is the Engineering Building at the American University of Sharjah and can be used to prove that the influence on the consumption of such a building would majorly come from cooling, since cooling generally consumes about 70% of a building's energy, as well as from the occupational schedule. Figure 5.11 proves that the R^2 value is indeed 0.83.

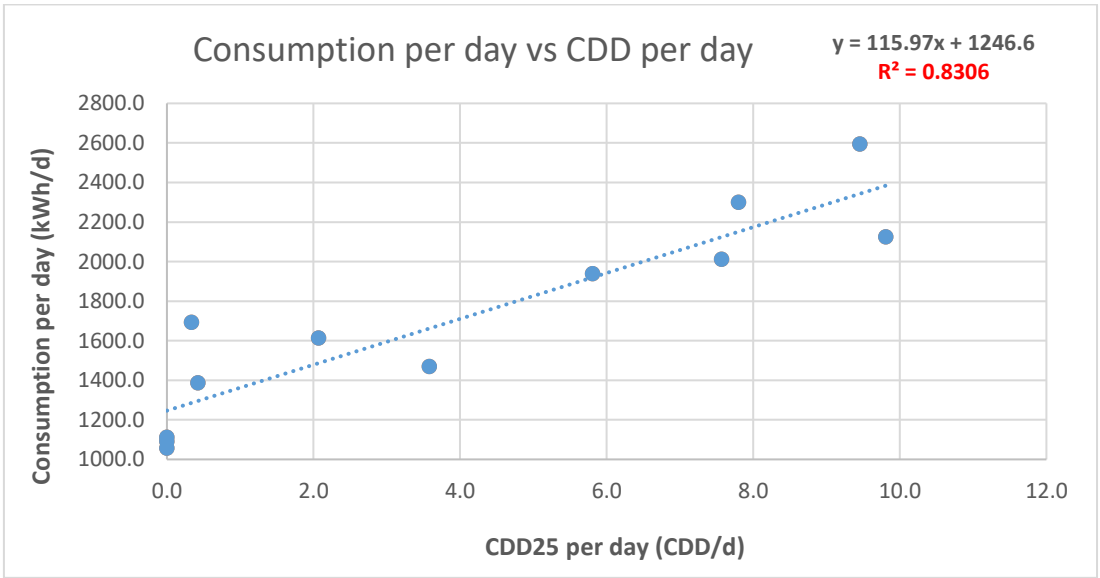

Figure 5.11 - Consumption per day against CDD per day (engineering building)

Furthermore, to be able to compare the consumption of the building from one period to the other in order to track the building's performance, it may be inaccurate to just compare the metered consumption since the weather might be different even for the same months from year to year. Hence to obtain a more accurate comparison the consumption can be normalized for the weather by dividing the consumption by the total CDDs for that period and then multiplying by the long-term average CDDs for the same period. Table 5.2 illustrates how the magnitude of the improvements is significantly underestimated without the normalization for the CSC building. Table 5.3 illustrates how the normalized consumption of the engineering building can detect improvements that the metered consumption cannot.

Table 5.2 - Normalizing the consumption of the CSC building

Year	Consumption (MWh)	Improvement	CDD25	MWh/CDD	Normalized Consumption (MWh)	Improvement
2014	522.5		1883	0.277	398	
2015	526.5	▼ -0.77%	1860	0.283	406	▼ -2.01%
2016	541.5	▼ -2.85%	1721	0.315	451	▼ -11.08%
2017	521.5	▲ 3.69%	1855	0.281	403	▲ 10.64%

Table 5.3 - Normalizing the consumption of the engineering building

Year	Consumption (MWh)	Improvement	CDD25	MWh/CDD	Normalized Consumption (MWh)	Improvement
2014	243.5		1883	0.129	185	
2015	847.5	▼ -248.05%	1860	0.456	653	▼ -252.97%
2016	902.5	▼ -6.49%	1721	0.524	752	▼ -15.16%
2017	950	▼ -5.26%	1855	0.512	734	▲ 2.39%

Chapter 6. Modelling and Simulation

In this chapter the modelling of the case study building in Autodesk Revit is outlined and the results of various thermal simulations run using IES VE are presented. Furthermore, the issues faced with interoperability specially through the transfer of data using the gbXML schema are discussed, the IES VE model is validated, and different design options are investigated. Finally, the modelled building is compared to Dubai Municipality's Green Building Regulations and Specifications Code as well as ASHRAE 90.1's building envelope requirements and the difference in performance is analyzed.

6.1. Revit for Geometric Modelling

The case study building was first modelled in as much detail as possible in Autodesk Revit (figure 6.1). The model was built by linking the as-built AutoCAD drawings to the project – in this case the floor plans for each floor were linked – and then the floor features such as the walls, columns, slabs, and windows were traced over the drawings. The project location was set in the Manage tab > Project Location Panel > Location and the project was rotated to align the project north with the true north through an angle of 55˚ 27' 44" East (55.46222˚). Figure 6.2 shows the orientation of the building. The origin of the drawing was set to the point on the grid A01 that coincides with the coordinates 25.312859 N, 55.487694 E.

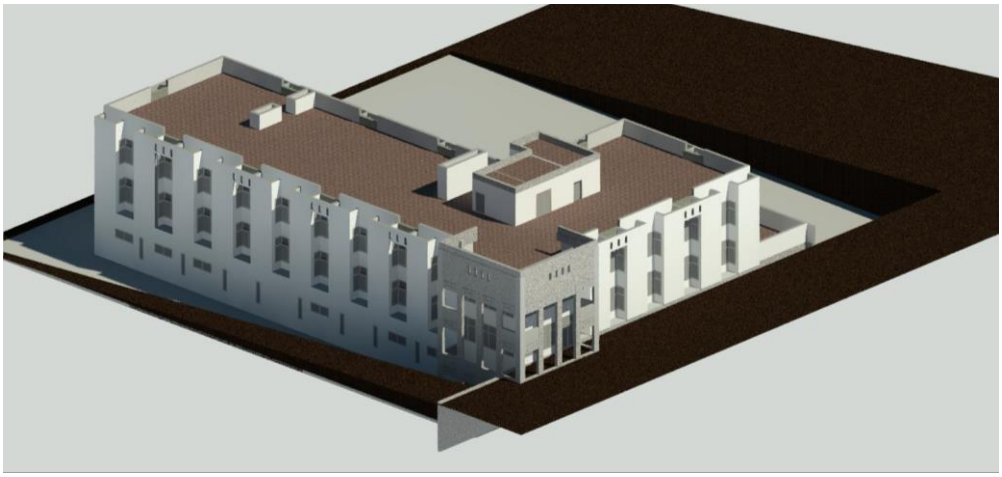

Figure 6.1 - The Revit model of the CSC building

The model was built starting with the structural elements such as the columns and core walls using Revit Structure. A total of 39 columns were modelled from 6 types – 3 rectangular columns and 3 L-shaped columns. It may be worthy to note that while the rectangular columns were included as default families in Revit Structure, the L-shaped columns had to be custom created as new families. Particular care must also be taken in aligning the top of the column to the level and locking it in place while creating the column family, in order for the column to be height-adjustable when used in the model. The columns were initially assumed necessary to include since they shall contribute with their thermal mass to the thermal simulation, however after several trials, it was evident that the columns cause complications in the building geometry with little effect on the building's energy consumption and were hence removed.

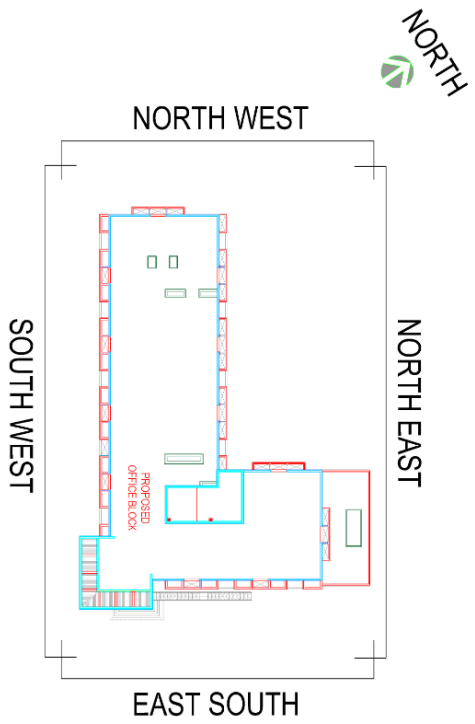

Figure 6.2 - The orientation of the CSC building

Revit allows for great flexibility in applying changes to a project by structuring all components, called elements, of the project such as columns, walls, and doors in a systematic manner. All categories of elements such as all round columns and all double doors form a "family", whilst all double doors of a particular size form a "type" in that door family, and each door in a particular location and placed at a particular height on a wall forms an individual "instance" of that type. This allows the user to change the

properties of an instance if only an individual element is required to be changed. Similarly, the user can change the type properties to administer a change to all instances of that type, such as all doors of a particular size.

Revit also allows the user to set the materials used for each component in the model and the layers that make up the walls of the building. Since the model was to be used for a thermal simulation it was also crucial to set the thermal properties for each material in the project. The materials used were default materials, however Revit does allow the user to change a material's property in most cases. The only exception encountered was the thermal and transmission properties of the windows. Revit provides a list of window panes to choose from, each with their own properties, but to add a custom set-up the "constructions.xml" file must be manually edited, and the custom window properties added.

Furthermore, to set up the model for thermal simulation Revit MEP was used to create "spaces" that cover the entire volume of the building. Each space is an enclosed volume that is thermally simulated and may be attributed certain thermal properties such as internal gains and cooling loads. A total of 82 spaces were created including the stair way wells, elevator shaft, and all other shafts. Appendix A provides details for all the spaces. The spaces are important to create since that is how all thermal simulation software will primarily determine if a wall is an exterior or an interior wall. Interior walls will have spaces on both sides of it while exterior walls will have a space on only one side. Walls with no spaces on either side are considered as shades.

The model was also checked for clashes between elements using the "Interference Check" tool and all intersecting and overlapping walls, floors, and roofs were properly joined. This is a crucial step since Revit will only consider one of the elements that are clashing and ignore the rest, causing gaps in the model and hence space leaks.

6.2. Interoperability and gbXML

The transfer of data between the geometric modelling software and the energy simulation software, or more generally between any software in the Building Information Modelling (BIM) framework, is known as interoperability and is perhaps the most important hurdle of the BIM framework. For this case study, the gbXML

(green building XML) schema was used for its suitability in energy projects and its applicability in both Revit and IES VE.

The Revit model was exported in the gbXML format using the Space Volumes option rather than the Energy Settings option. The energy settings option would create the energy analytical model (figure 6.3) within Revit based on certain resolution settings and then export those analytical surfaces and volumes. This leaves Revit to decide the number and sizes of the analytical surfaces and their function as Internal, External, or Shade. Although the analytical model looks well defined when inspected in Revit, the export to IES VE doesn't complete without errors and several surfaces and shades do not transfer (figure 6.4). The analytical model would also have a much larger number of surfaces making it more difficult to troubleshoot and inspect manually for errors. The Space Volumes option on the other hand provides manual control to the user to define the spaces that will be exported through Revit MEP and consequently the surfaces that are adjoining to them.

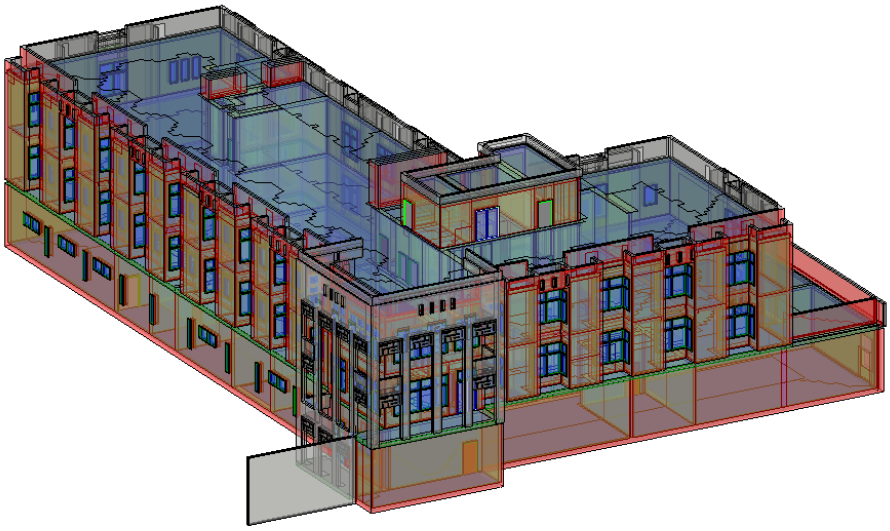

Figure 6.3 - The CSC energy analytical model in Revit

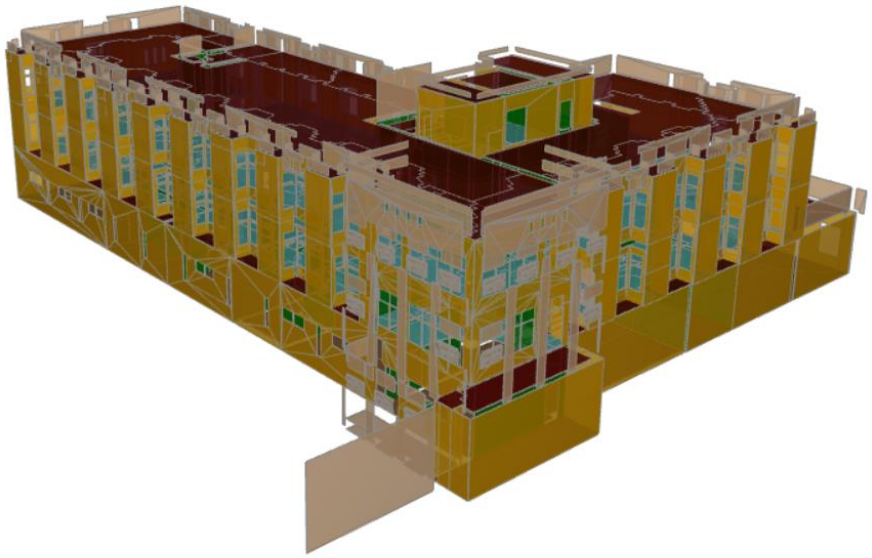

Figure 6.4 - gbXML export using the energy settings option

The gbXML format stores information according to a certain hierarchy beginning with the campus tag that contains information in the following order: the location, building type, spaces, surfaces, and openings. Then the file has tags that contain the constructions used, the layers in the construction, the materials for the layers, the operating schedules, and finally the space zones. It is also helpful to realize that the elements from Revit are exported as 2D objects and are thus exported to the centerline. Making walls uniform and simplifying the geometry would hence greatly help reduce the errors on export. Finally, the gbXML format does not export all the information related to the model and is hence wise to leave the data input to the thermal simulation software wherever possible.

As with the export of data to the gbXML format, it is crucial to be aware of what is input to the energy simulation software from the gbXML file. For this case study it was realized that the IES VE software does not import the constructions and materials from the gbXML file and hence all the elements had to be re-assigned a thermal construction within the IES VE program.

6.3. IES VE for Thermal Simulation

The import of the gbXML file although successful was still not free of errors and the model had to be inspected closely to ensure that all spaces were enclosed and had the correct adjacencies. In some cases, spaces were intersecting and in some critical cases some surfaces were warped. It was also realized that exporting the model from Revit with the model rotated caused problems with the geometry. The model was therefore returned to normal and then re-rotated within IES VE after the import. It may be worthy to note here that in IES the model is rotated counter clockwise and the input is in decimal, hence a 55˚ 27’ 44” East (55.46222˚) rotation in Revit would correspond to a 304.53778˚ rotation in IES VE. Part A of the model report provides geometry consistency checks and can be used to check for errors. Though some errors are critical such as non-planar surfaces and external holes, other errors such as intersections can be checked by the user and ignored if found to be negligible. Figures 6.5 and 6.6 show the CSC model in IES VE.

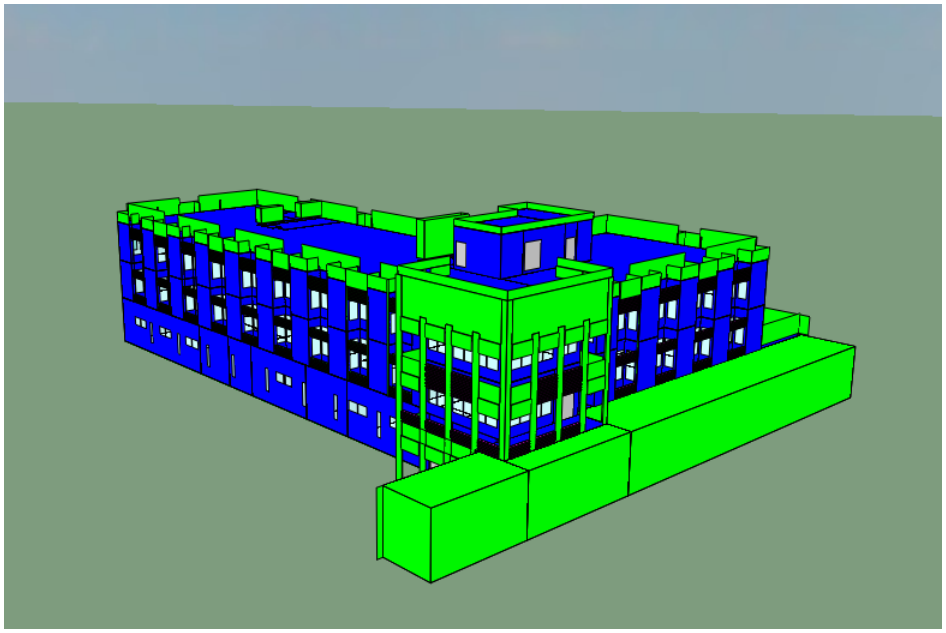

Figure 6.5 - The CSC model in IES VE Model Viewer

Once the imported geometry was successfully inspected and ensured, the window shades were drawn at this stage and topographic shades were modelled to form adjacencies to those walls that are going to be in contact with the ground, namely the East South wall of the lower ground floor (LGF).

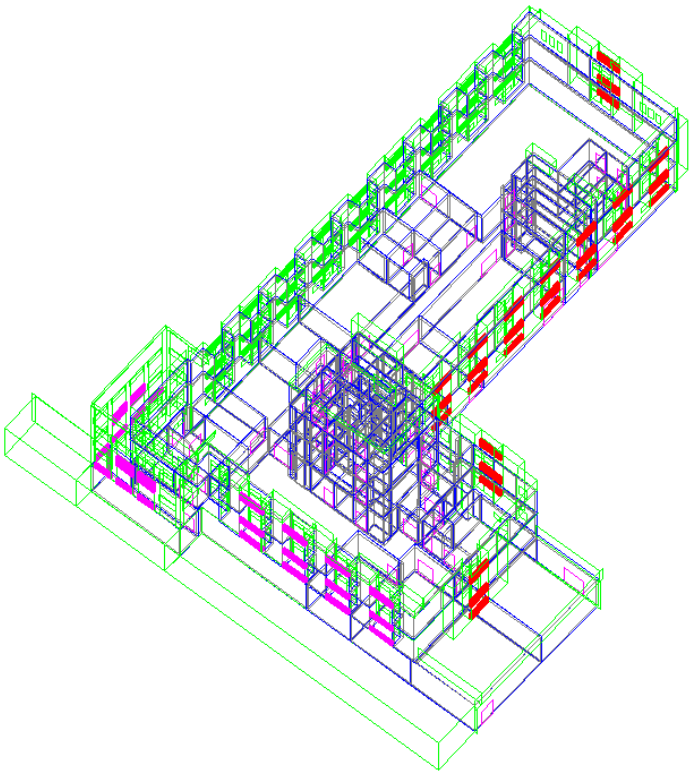

Figure 6.6 - The model in IES VE Workspace View

After the model geometry was deemed satisfactory, the element constructions were defined in the construction database and assigned to the walls, floors, and ceilings. Appendix A provides some details of the constructions and materials used in the project. Also, upon inspection of the geometric model, it was noticed that certain surfaces were assigned to the wrong categories, such as an interior floor being assigned the category of roof. If the area involved is negligible, then the error may be ignored and as done in this project a roof construction similar to that of the interior floor was created and assigned to those areas. Furthermore, it was also observed that parts of the exposed interior floor which although correctly assigned to the category of interior floor would rather have an insulated construction similar to that of the roof, hence the construction “Exposed Floor” was created. Finally, surfaces that connect spaces but do not actually have any physical partition in real life were assigned the construction named “2013 Internal Partition” as seen in Appendix A, where the thickness is 0.1 mm and the resistance is nil.

The thermal templates were then created and assigned to the spaces. To create the thermal templates, the operating schedules (profiles) were first created in the profile manager. A 7:00 am to 9:00 pm workday was first created and that was then applied to a 6-day work week – with Friday being an off-day. This profile was then used for the templates. Four templates (table 6.1) were then created according to the function of each space and then assigned accordingly. The heating was turned off continuously for all templates, the cooling was turned off for spaces with the "Not Occupied" Thermal Template, and the three other templates had its cooling follow the work week profile created. The cooling set point was set at 23.9 ˚C. Each thermal template had internal gains assigned to it as shown in table 6.1 and Appendix A provides details on each internal gain. The number of people, computers, and equipment in the building was approximated by an estimate after visiting the building. Furthermore, the weather file used for the simulation was set to Abu Dhabi in IES VE as that was the closest location.

Table 6.1 - Thermal template internal gains

Internal Gains for Each Thermal Template			
OfficeOpenPlan	**Workshop**	**Stores/Corridors**	**Not occupied**
Lighting Miscellaneous People (Office) Computers	Lighting People (Workshop) Machinery	Lighting People (store/Corridor)	Lighting

To properly configure the energy model such that it replicates the real building, the HVAC system needs to be modelled in ApacheHVAC. However, since that would be out of the scope of this project and would not affect our results provided the HVAC parameters were to be kept constant, the simpler method of using ApacheSys was used to configure the air conditioning. Furthermore, the UK NCM wizard was used in ApacheSys to provide default values based on the type of equipment used, which in this case are Fan Coil Systems. Appendix A provides details of the input parameters.

6.3.1. Base run and shading. The simulation was then run using the ApacheSim method twice – once without the SunCast Link which provides shading information into the simulation and once with the Link enabled. The result is a comparison in the energy consumption of the building with and without all the shades.

The total yearly consumption for the building without the shades was about 1261 MWh, compared to about 1240 MWh when enabling the shades. This is a difference of about 21 MWh or 1.67%. This might seem as a small percentage, but to put it into perspective that is the amount of energy saved if all lights in the building were turned off for over 2 months. Table 6.2 provides the monthly variation of the building's consumption while figure 6.7 provides the breakdown of the energy usage for the shaded building. While the lights energy is self-explanatory, the equipment energy is that used by all equipment defined in the internal gains, and the systems energy is that used by all heating and cooling systems in the building. Clearly the cooling of building consumes the most energy at 57%, while the equipment consumes about 34% of the total energy. Furthermore, figure 6.8 shows that while the lighting and equipment energy consumption remains fairly constant all year round, the systems energy varies considerably according to the weather. Appendix A contains the detailed monthly breakdown of the energy consumption as well as the carbon emissions that amount to 635,949 Kg of CO_2 a year.

Table 6.2 - Energy consumption for the CSC model with and without shading

	Total energy (MWh)	**Total energy (MWh)**
Date	**No Shading**	**Shading**
Jan 01-31	85.0172	83.0905
Feb 01-28	81.1234	79.0117
Mar 01-31	97.2632	95.5483
Apr 01-30	100.7336	99.2733
May 01-31	110.3277	108.8679
Jun 01-30	116.8498	115.4877
Jul 01-31	126.5797	125.2912
Aug 01-31	123.2257	121.7603
Sep 01-30	119.6039	117.8395
Oct 01-31	109.0322	106.9113
Nov 01-30	99.5302	97.2783
Dec 01-31	91.7937	89.7192
Summed total	1261.0802	1240.0791

Finally, the energy consumption of the building can be expressed as the Energy Use Intensity (EUI) by dividing the total consumption by the gross area of the building (3466 m^2) to obtain an EUI of 357.8 $kWh/m^2/yr$.

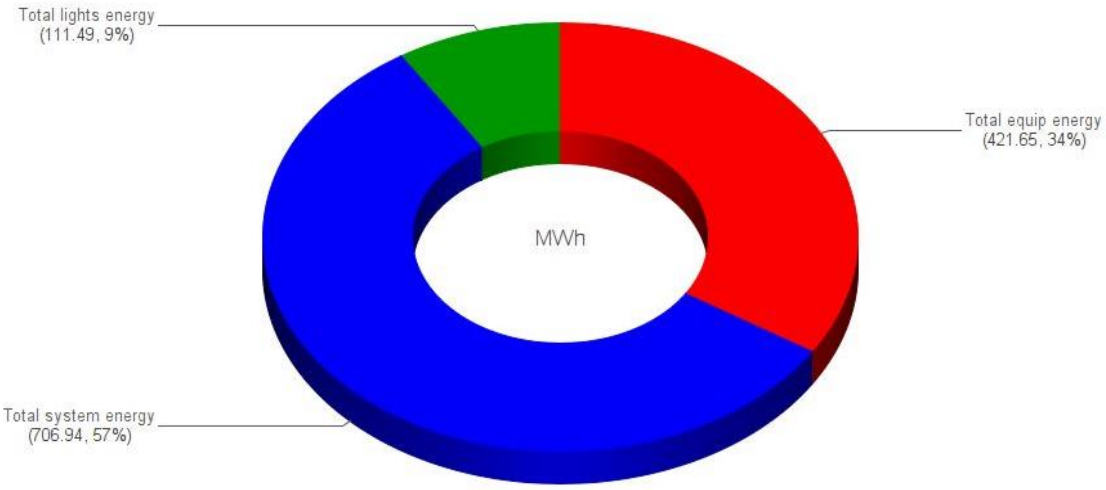

Figure 6.7 - Breakdown of the energy usage

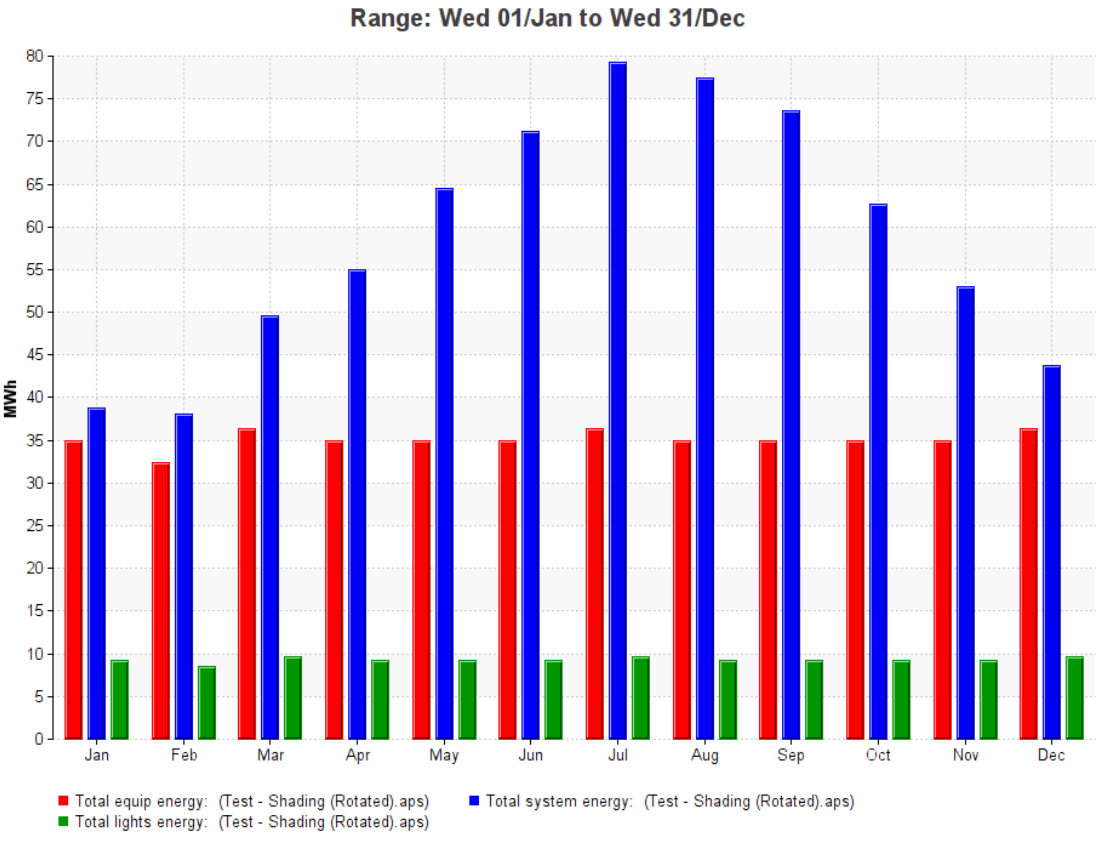

Figure 6.8 - Monthly variation of the model's consumption

6.3.2. Validation of the model. To ensure that the model constructed is a valid representation of the existing building, the energy consumption from the model was compared to that metered from the building. This however was not a direct procedure since the CSC building, as discussed earlier, uses district cooling where chilled water is served to it by an independent chiller building that has separate metering. The consumption from the model however includes the conditioning energy as well. To further complicate the problem, the chiller building serves another building besides the CSC building, namely the sports complex.

To solve the problem the proportion of the chilled water (CHW) flow from the chiller to the two buildings was used to proportion the energy consumption of the chiller building. Further, to ensure that this ratio is representative of the energy proportioning, the chilled water consumption and chilled water-cooling loads were also used. Table 6.3 shows these values for the two buildings and the proportioning can be worked out to be a ratio of CSC to Sports complex of 0.75 or a 43% split to the CSC building.

Table 6.3 - Chilled water proportioning

	CSC Building	Sports Complex	Total
CHW Flow (L/s)	18.2	24.4	42.6
CHW Consumption (L/s)	4.0	5.3	9.3
CHW Cooling Load (kW)	399.7	532.4	932.1

Hence by adding 43% of the chiller yard's energy consumption to the CSC building's metered consumption it is possible to obtain an accurate estimate of the total consumption the CSC building demands. Figure 6.9 plots this estimated actual consumption along with the model's monthly consumption. It is clear however that the model is quite accurate and very closely represents the actual building when comparing the colder months (about a 2% difference) although it does begin to deviate from the actual consumption as the weather gets hotter. This is expected as the problem with the model was indeed the lack of detailed HVAC modelling. The model's total yearly consumption as discussed earlier was about 1240 MWh which is about 87% of the average yearly total consumption of the actual estimate which was determined to be 1,425.3 MWh. This is quite accurate considering the model itself is a simplification. Finally, it can also be seen from table 6.2 that the highest consumption happens in the

month of July and the lowest consumption in the month of February, corresponding to the actual estimate.

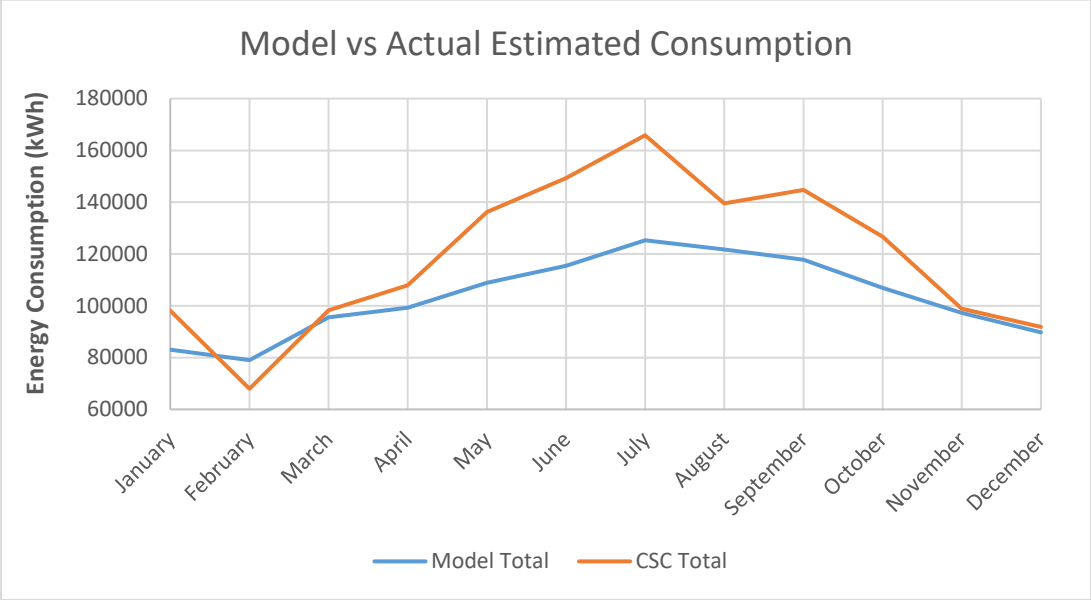

Figure 6.9 - Model vs actual estimated consumption

6.3.3. Effect of orientation. Several simulations were run with the model rotated through an angle (ϕ) of 45˚ each time to determine the effect of the building orientation on the energy consumption. Figure 6.10 illustrates the building's as-built position from north and the clockwise rotation of the building through the angle ϕ, incremented at 45˚ steps.

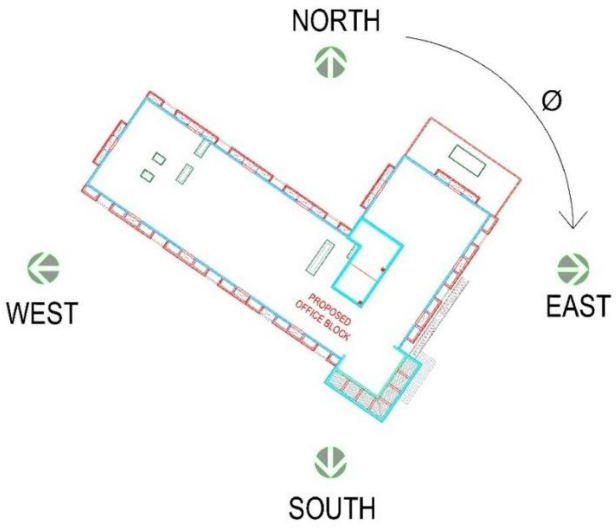

Figure 6.10 - Rotation of the building through an angle φ

The maximum savings were achieved when the building was rotated a whole 180˚ where almost 4 MWh and about 2000 Kg of CO_2 emissions were saved yearly (table 6.4). It can also clearly be seen from figure 6.11 that the worst building orientation is a rotation of 315˚ and more importantly, that the current building orientation (0˚) is the second to the worst.

Table 6.4 - Energy and carbon savings from the building orientation

Angle (φ)	Energy Consumption (MWh)	Energy Savings (MWh)	Change (%)	Carbon Emissions (Kg)	Carbon Savings (Kg)
0	1240.0791	-	-	635,949	-
45	1239.4733	0.6058	0.05%	635,635	314
90	1239.8365	0.2426	0.02%	635,824	125
135	1238.4628	1.6163	0.13%	635,111	838
180	1236.1678	3.9113	0.32%	633,920	2029
225	1236.7184	3.3607	0.27%	634,205	1744
270	1239.3815	0.6976	0.06%	635,587	362
315	1241.127	-1.0479	-0.08%	636,493	-544

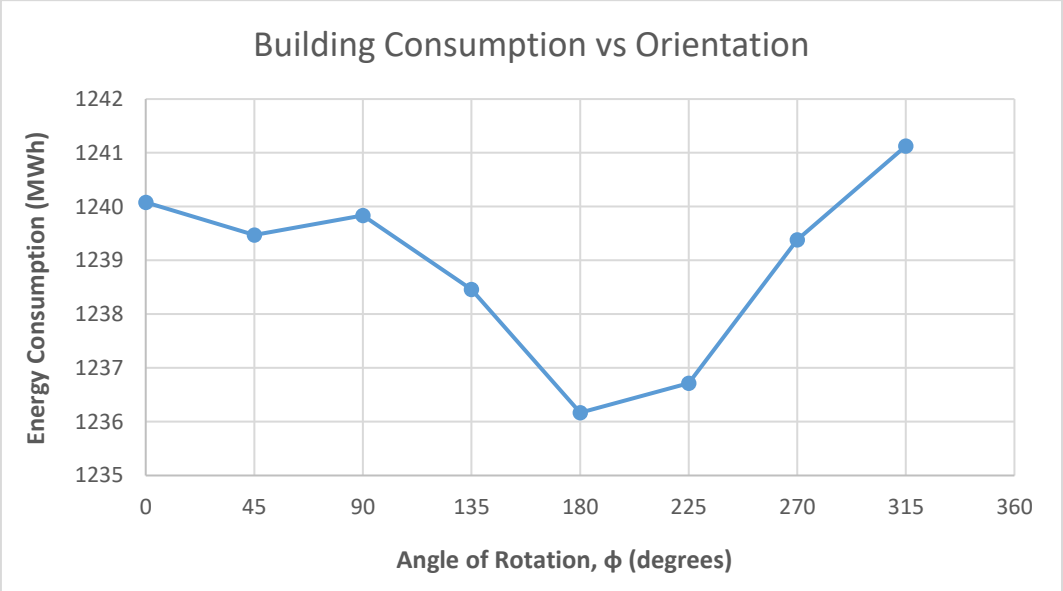

Figure 6.11 - Building consumption vs orientation

6.3.4. Effect of wall insulation. The effect of the wall insulation was also investigated by running several simulations where the exterior wall insulation was increased from 100 mm to 190 mm in increments of 15 mm. It is evident from table 6.5 and figure 6.12 that the energy consumption keeps reducing as the insulation is increased and a 90 mm increase in insulation saves up to 5.4 MWh of energy and 2,778 Kg of CO_2 yearly.

Table 6.5 - Energy and carbon savings from insulation increments

Insulation (mm)	Energy Consumption (MWh)	Energy Savings (MWh)	Change (%)	Marginal Savings (MWh)	Carbon Emissions (Kg)	Carbon Savings (Kg)
100	1240.0791	-	-	-	635,949	-
115	1238.5757	1.5034	0.121%	1.5034	635,169	780
130	1237.4451	2.634	0.212%	1.1306	634,582	1,367
145	1236.5618	3.5173	0.284%	0.8833	634,124	1,825
160	1235.8196	4.2595	0.343%	0.7422	633,739	2,210
175	1235.24	4.8391	0.390%	0.5796	633,438	2,511
190	1234.7269	5.3522	0.432%	0.5131	633,171	2,778

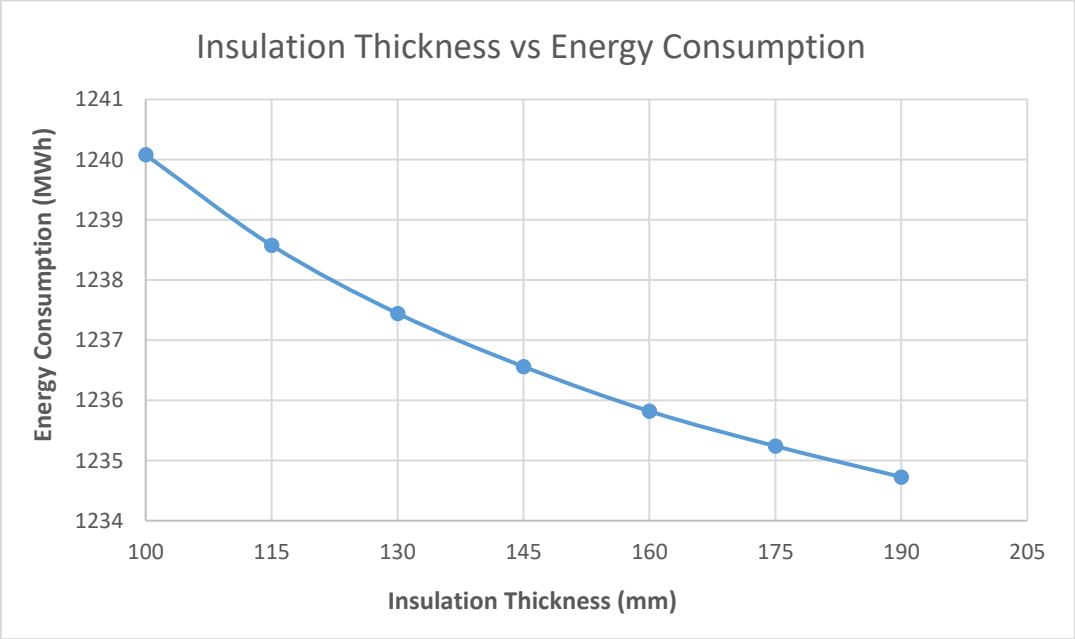

Figure 6.12 - Insulation vs energy consumption

However, it is also evident from the marginal savings in table 6.5 and figure 6.13 that the effectiveness of the increased insulation reduces with every increment.

The first 15 mm increment that brings the insulation to 115 mm in the external walls achieves a 1.5 MWh saving whereas the last 15 mm increment that brings the insulation to 190 mm added only 0.5 MWh to the savings. It is also important to realize that the insulation will have a larger effect on the building as the envelope increases in area, hence higher ratios of envelope to internal areas should pay considerable attention to the insulation.

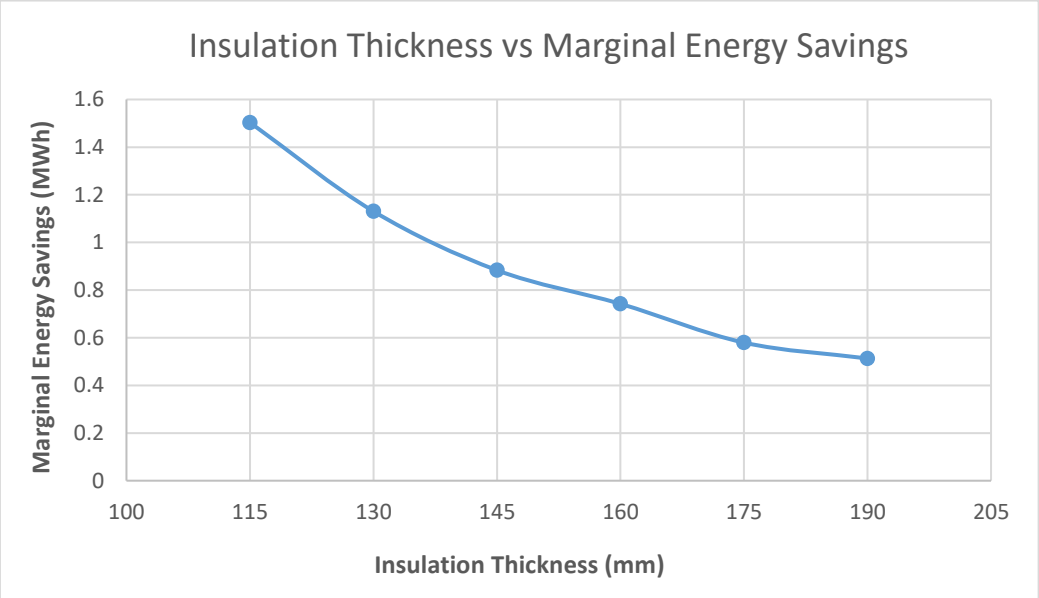

Figure 6.13 - Insulation vs marginal energy savings

6.3.5. Effect of windows. To investigate the effect of the windows on the energy consumption of the building, all windows were replaced with double and triple glazed glass of varying Solar Heat Gain coefficient (SHGC). The replacement double glazed glass had a glass U-value of 1.4 W/m^{2}K while the triple glazed had a glass U-value of 0.6 W/m^{2}K. Table 6.6 provides further details on the window options and the simulation results.

It can also be observed from table 6.6 that although the glass u-value was lower than the default in option 2, the marginally higher SHGC on just the north faces of the building caused an actual net increase in the energy consumption of about 0.6 MWh. This clearly proves the importance of the SHGC on the window's performance. This is further evident by calculating the marginal savings when changing the SHGC and the U-value. Changing the SHGC from 0.55 to 0.28 for the same U-value provides an

energy saving of about 27 MWh, while a change from 0.55 to 0.09 achieves a saving of about 44 MWh.

Table 6.6 - Energy and carbon savings from the window variations

Option	U-Value (W/m^2K)	SHGC	Energy Consumption (MWh)	Savings (MWh)	Change (%)	Carbon (Kg)	Savings (Kg)
default	1.57/1.66	0.25/0.28	1240.0791	-	-	635,949	-
1	1.4	0.55	1267.5819	-27.5028	-2.22%	650,223	-14274
2	1.4	0.28	1240.6666	-0.5875	-0.05%	636,254	-305
3	1.4	0.09	1223.8633	16.2158	1.31%	627,533	8416
4	0.6	0.55	1265.0691	-24.99	-2.02%	648,919	-12970
5	0.6	0.28	1237.9487	2.1304	0.17%	634,844	1105
6	0.6	0.09	1220.1902	19.8889	1.60%	625,627	10322

However, changing the U-value from 1.4 to 0.6 adds a saving of between 2.5 to 3.5 MWh depending on the SHGC. Even when attempting a fairer comparison, one can consider that from 0.55 to 0.28, provides a change in SHGC of about 50% while a change from 1.4 to 0.6 provides a change in U-value of about 57%. However, the savings from the SHGC (27 MWh) still far outweigh the best of that from the U-value (3.5 MWh). Furthermore, as mentioned above, the savings from the U-value depend on the SHGC as can be seen from figure 6.14.

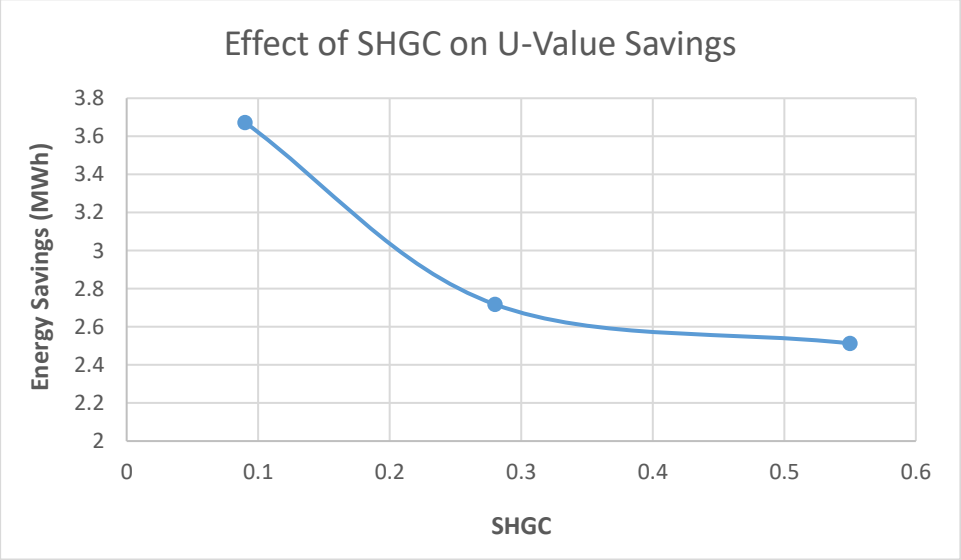

Figure 6.14 - Effect of the SHGC on the U-value savings

With a SHGC of 0.55, a change in glass U-value from 1.4 to 0.6, saves about 2.5 MWh, whereas at a SHGC of 0.09, the same change in U-value saves about 3.5 MWh. Further, from table 6.6 the maximum savings achieved were about 20 MWh and 10,300 Kg of Carbon, achieved with a triple glazed window having a glass U-value of 0.6 W/m^2K and a SHGC of 0.09. Finally, it may be worthy to note that windows of options 3 and 4 are products from very popular brands in the UAE. Option 3 also proves that a double-glazed window with a low SHGC can achieve substantial savings and effectively compete with triple glazed windows.

6.3.6. Effect of ground insulation. The default construction of the building did not have the ground slab insulated, and the effect of insulating the ground slab on the energy consumption was investigated by adding first a 50 mm layer of insulation and then a 100 mm layer of insulation. Just a 50 mm layer of extruded polystyrene insulation saved about 5 MWh of energy and 2700 Kg of carbon as shown in table 6.7. Increasing the insulation to 100 mm saved about 7 MWh of energy and about 3600 Kg of carbon.

Table 6.7 - Energy and carbon savings from adding ground insulation

Slab Insulation (mm)	Energy Consumption (MWh)	Energy Savings (MWh)	Energy Change (%)	Carbon (Kg)	Carbon Savings (Kg)
0	1240.0791	-	-	635,949	-
50	1234.8469	5.2322	0.42%	633,234	2715
100	1233.1776	6.9015	0.56%	632,367	3582

6.3.7. Cumulative effect of the saving strategies. If the energy and carbon savings from the best design options investigated above are added together that would give us a saving of about 36 MWh of energy and 18,700 Kg of carbon; or 2.9%. However, it is evident from table 6.8 that the sum of the individual savings does not equal the cumulative effect of running the simulation with all the strategies together. The efficiency of the strategies collectively reduces by 0.14% such that the savings are about 34 MWh instead of 36 MWh and 17800 Kg of carbon instead of 18700 Kg.

Table 6.8 –Simulated cumulative vs totaled savings

Option	Energy Consumption (MWh)	Energy Savings (MWh)	Energy Change (%)	Carbon (Kg)	Carbon Savings (Kg)
Default	1240.0791	-	-	635,949	-
100mm Slab Insulation	1233.1776	6.9015	0.56%	632,367	3582
Option 6 Window	1220.1902	19.8889	1.60%	625,627	10322
Insulation +190	1234.7269	5.3522	0.43%	633,171	2778
Orientation 180	1236.1678	3.9113	0.32%	633,920	2029
Total	-	36.0539	2.91%	-	18711
Cumulative Simulation	1205.7515	34.3276	2.77%	618,133	17816

6.4. The Modelled Building Envelope and Ashrae 90.1

To ensure that a building meets certain energy performance requirements, codes like the Ashrae 90.1 and the Dubai Green Building Regulations and Specifications provide certain prescriptive points for the building envelope to comply with.

The Dubai Green Building Regulations require for the sake of building energy performance the compliance with certain sections of the code including section “304.04 Orientation of the Glazed Facades” and section “501.01 Minimum Envelope Requirements”. These sections enforce that a minimum of 50% of the total glazing must have a northern orientation which includes an angle of 150˚from East to North West as well as envelope U-values as shown in table 6.9. The modelled building envelope although complies with all U-value requirements it does not comply with the orientation clause since only 4% of the total glazing is orientated within the stated angle.

ASHRAE 90.1 on the other hand makes its criteria more stringent as it evolves and table 6.9 includes the U-value requirements for the year 2004, one of its earlier versions, as well as for its latest 2016 version. The 2004 version mandates the total glazing to be less than 50% of the total above grade wall area, whereas in 2016 that was brought down to 40%. The CSC modelled building however complies swiftly as its

total glazing to wall ratio is only at 13%. The modelled building also complies with all except the interior floor U-value for the 2004 version and exceeds the minimum requirements for the roof, interior floors, doors, and windows in the 2016 version.

Table 6.9 - Envelope comparisons: modelled, ASHRAE 90.1, DM GBRS

Category	Element	Parameter	Parameter Value	ASHRAE 2004	ASHRAE 2016	DM GBRS
Above Grade Wall	WT1	U-Value	0.2354	3.293	3.293	0.57
Roof	R2 Roof	U-Value	0.249	0.36	0.22152	0.3
Roof	Exposed Floor	U-Value	0.249	0.36	0.22152	0.3
Below Grade Wall	Core 300	C-Value	0.23	6.473	6.473	-
Floors	Interior 275	U-Value	2.9709	1.825	1.825	-
Slab on Grade	Slab on Grade	F-Factor	1.26	1.264	1.264	-
Swinging Doors	Door	U-Value	2.3025	3.975	2.1	-
Window	GL1-b	U-value SHGC	1.9204 0.2457	6.93 0.25	1.82 0.22	2.1 0.348
Window (North)	GL1-a	U-value SHGC	1.9896 0.271	6.93 0.61	1.82 0.22	2.1 0.349

Furthermore, another simulation was run to investigate whether the default model still performs better than a similar model with all 2016 ASHRAE 90.1 minimum requirements. Table 6.10 shows that it indeed does, performing about 9% better due to the better wall insulation. Another simulation also showed that if the default model was modified to comply with the 2016 ASHRAE code where it previously didn't, it would perform 0.58% better, saving around 7 MWh of energy and 3,700 Kg of CO_2.

Table 6.10 - Model performance comparison to ASHRAE 90.1

	Energy Consumption (MWh)	Energy Savings (MWh)	Energy Change (%)	Carbon Emissions (Kg)	Carbon Savings (Kg)
Default	1240.0791	-	-	635,949	-
ASHRAE '16	1351.8798	-111.8007	-9.02%	693,974	-58025
Default + ASHRAE '16	1232.8796	7.1995	0.58%	632,213	3736

Chapter 7. Thermal Bridge Investigation

Thermal bridges are a break in the external insulation of the building such that heat is transmitted between the interior and exterior of the building. This increases the load on the Air Conditioning system and it consumes more energy in its effort to maintain internal thermal comfort. Thermal bridges can be easily detected with a thermal camera and depending on where they are viewed from, they would show up as either hotter or colder parts of the wall.

In the United Arab Emirates and its region, buildings are predominantly made of a concrete structural frame and filled in with insulated or hollow block. Thermal bridges may hence form on the structural frame, the perimeter of the slabs, and at balconies. Solutions for the frame and slab perimeter would be to insulate the building from the outside with continuous insulation, while balconies would have to be thermally broken during construction using structural thermal breaks.

Thermal bridges are important to detect, especially for the sake of developing or comparing to an energy model. Energy models assume their walls are uniform and assign U-values calculated based on the typical wall layers in each construction. It is up to the modeler therefore to include the effects of thermal bridges either through separate wall areas or more likely through new U-values as calculated using ISO 6946 or ISO 10211.

7.1. Thermal Survey Equipment and Conditions

The thermal camera used for this study was the Flir E75 (figure 7.1) with a thermal IR resolution of 320 x 240, a thermal sensitivity of 0.03˚C at 30˚C, a 10 mm lens, a spectral range of 7.5 to 14 µm, and an IFOV of 1.31 mrad/pixel. The camera satisfies the minimum requirements of ISO 6781 – "Thermal insulation – Qualitative detection of thermal irregularities in building envelopes – Infrared Method" – that mainly requires an operating wavelength of greater than 2 µm, and a sensitivity of 0.5˚C.

The thermal survey for the case study building was conducted from outside the building and with the building being kept cooler on the inside, thermal bridges are to appear as colder areas on the IR images. The survey was conducted on the 2nd of September 2018 between 8:30 pm to 9:00 pm, about 2 hours after sunset to avoid the

effect of solar loading as much as possible, and just before the air conditioning is switched off in the building at 9:00 pm to maintain as much of a temperature difference between the inside and out as possible. Table 7.1 provides more details on the site conditions.

Figure 7.1- Flir E75, the thermal camera used for this study

Table 7.1 - Thermal survey site conditions

Date of Test	2nd September, 2018
Time of Test	8:30 pm to 9:00 pm
Outside Temperature	34˚C
Inside Temperature (CSC Building)	23˚C to 24˚C
Temperature Difference (CSC Building)	9˚C to 10˚C
Outside Humidity	47%
Sky Condition	Clear all day

7.2. Survey Results and Conclusions

The survey concluded that the CSC building is well insulated, and no thermal bridges were detected. Figures 7.2 and 7.6 show the difference in temperature between the concrete that is in contact with the interior (Sp1) and the concrete that is just used as a shade (Sp2). The mortar that is used to hold the GRC panels together is also clearly visible in the North West and North East walls. Figures 7.2 to 7.9 cover all faces of the CSC building and indicate the temperature of the façade is between 32˚C to 33˚C.

About a degree cooler than the outside air temperature. The shade concrete in figure 7.2 is at a temperature of 36.7˚C, about 2 degrees higher than the outside air temperature, and that is due to the effect of solar loading. Various windows and external doors were also checked as shown in figure 7.10 and no air leakages were detected. Furthermore, it was unclear if the East South LGF wall was insulated from the as-built drawings, and its corresponding construction in the energy model – "Core 300" – was assumed insulated. Figure 7.11 proves that it was indeed insulated, and the assumption was correct.

Finally, for illustration purposes, various buildings on campus were also scanned for thermal bridges. Figure 7.12 shows an uninsulated concrete column and beam visible as a thermal bridge in the IR image and is impossible to detect just from an optical image. Figure7.13 also shows an uninsulated slab perimeter visible in the IR image of one of the dormitories. Figure 7.14 shows an uninsulated structural member clearly visible in the IR image of the structural laboratory. In this case however, the image was taken from inside the building and hence the thermal bridge shows up as a hotter object. It can also be noticed that all thermal bridges detected are about 2˚C different from the insulated elements.

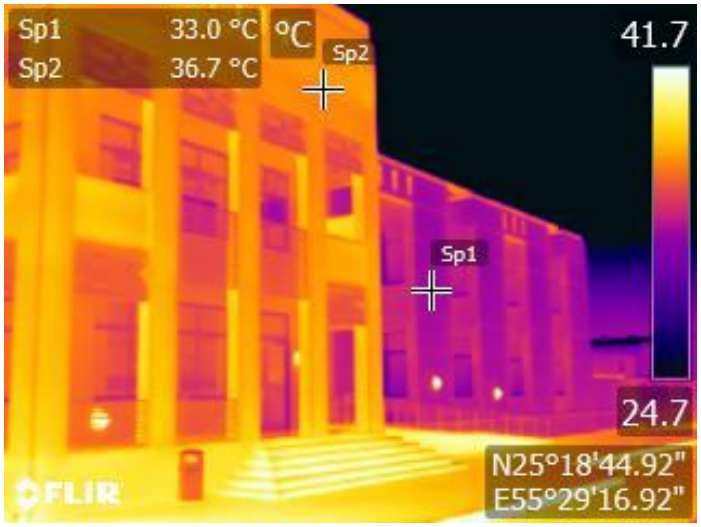

Figure 7.2 - Thermal image of the East South façade

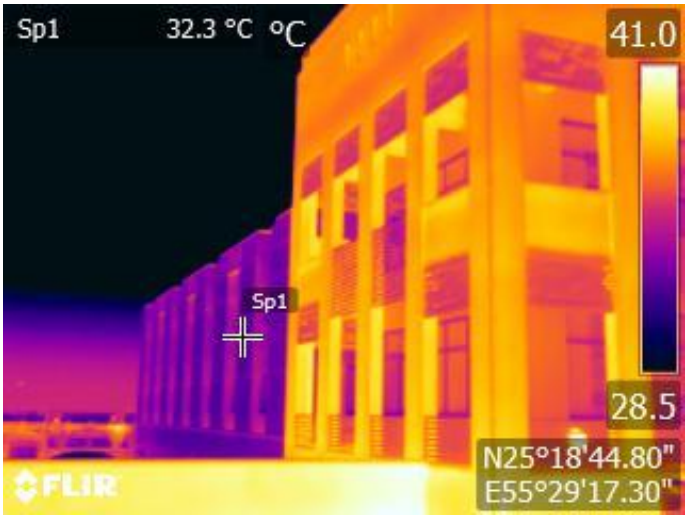

Figure 7.3 - Thermal image of the South West façade

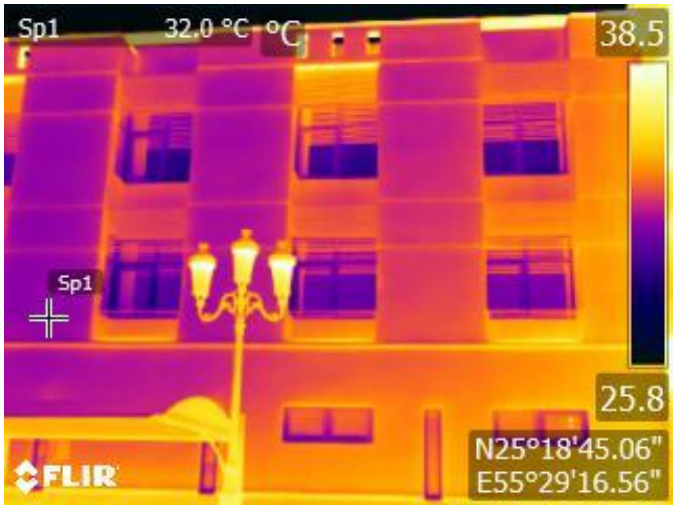

Figure 7.4 - Closer image of the South West façade

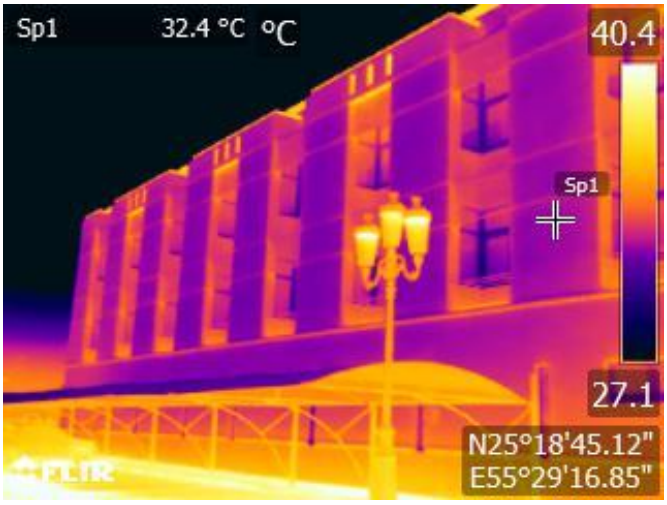

Figure 7.5 - Continuation of the South West facade close up

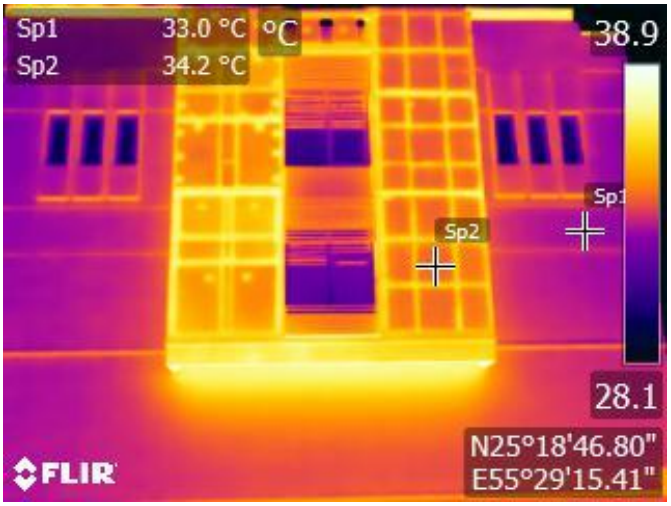

Figure 7.6 - Thermal image of the North West façade - the hotter part of the wall is GRC shade.

Figure 7.7 - Continuation of the North West façade

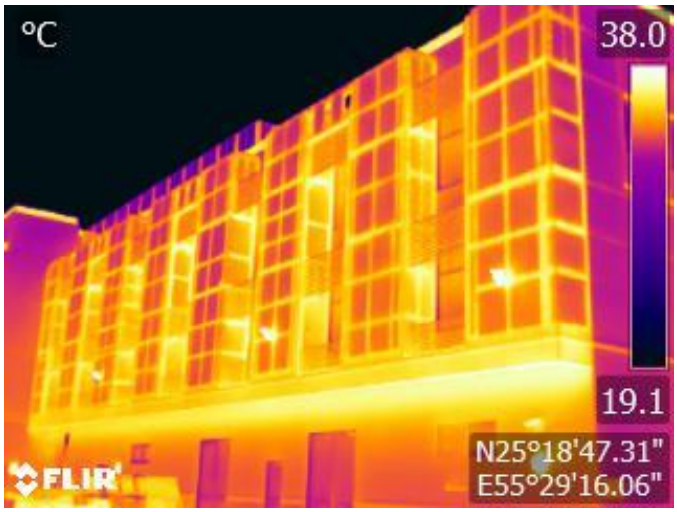

Figure 7.8 - Thermal image of the North East façade

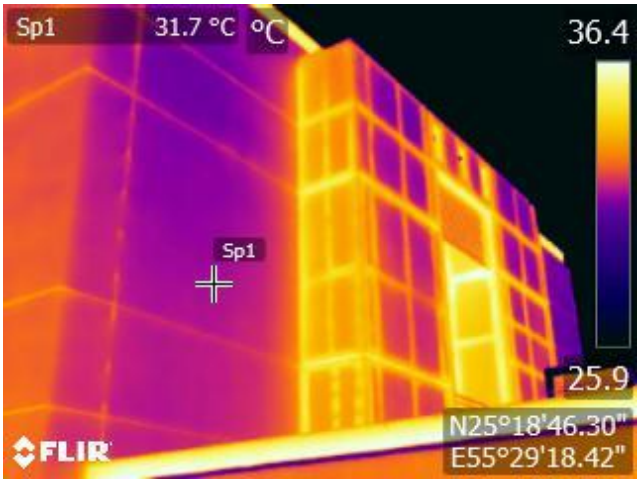

Figure 7.9 - Continuation of the North East façade

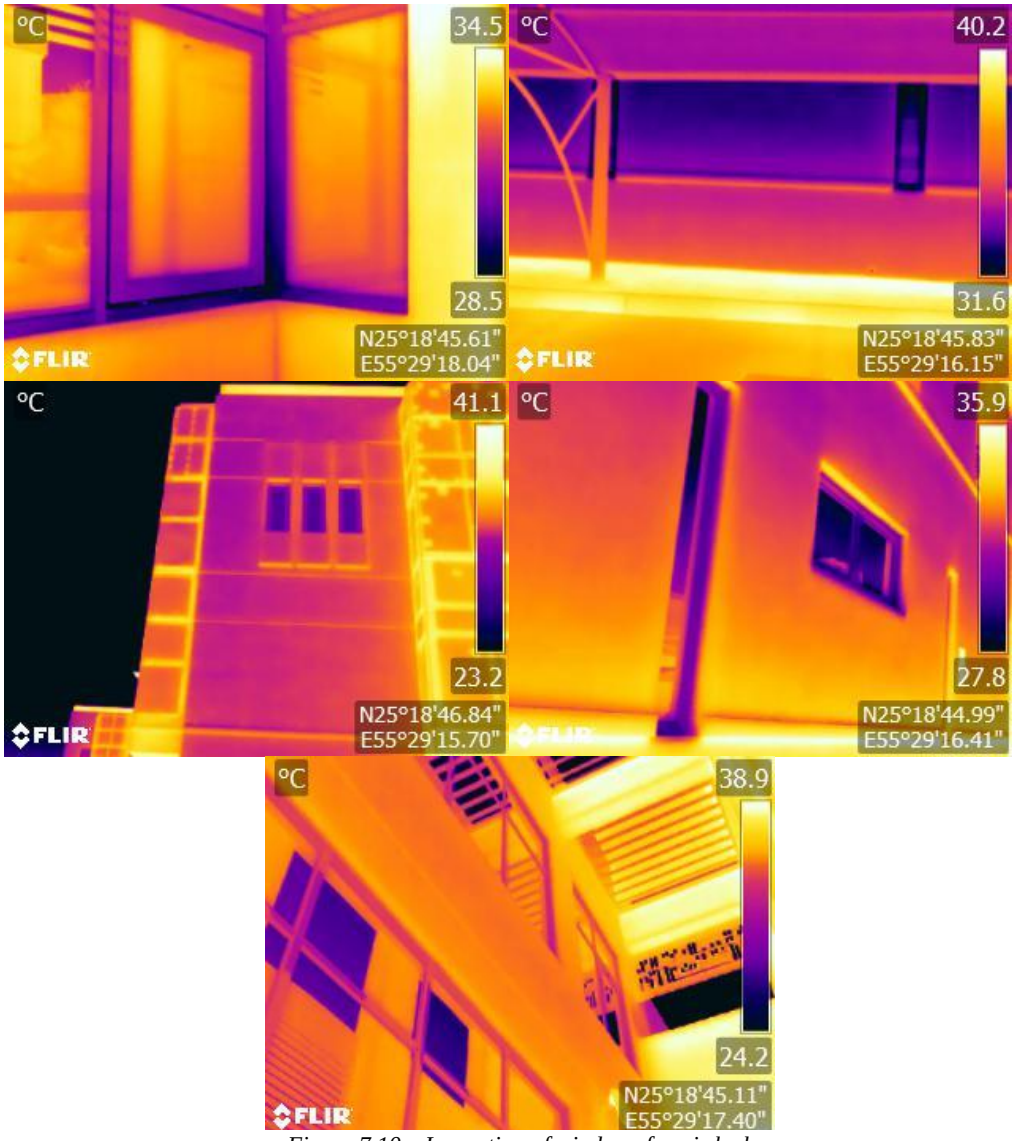

Figure 7.10 – Inspection of windows for air leakage

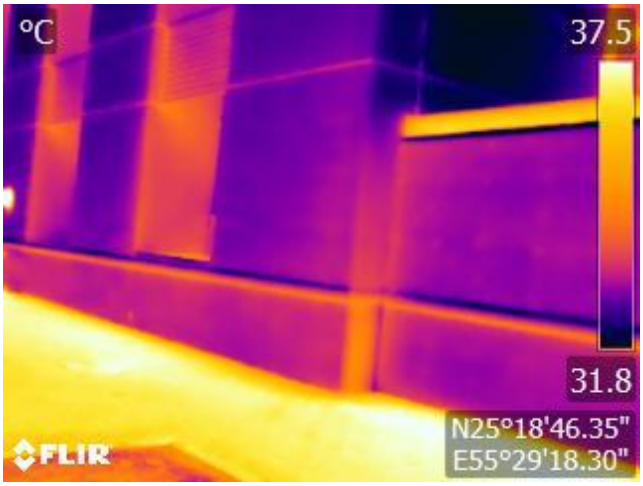

Figure 7.11 - Inspecting the "Core 300" wall for insulation.

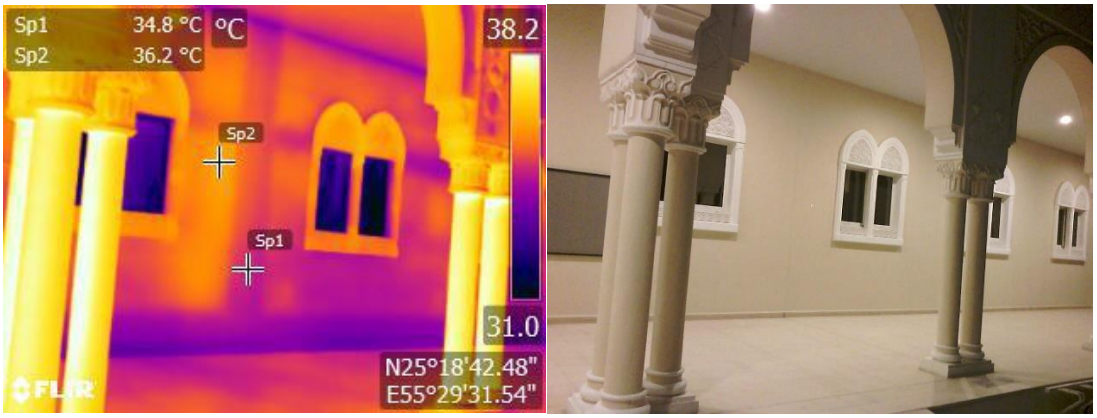

Figure 7.12 - Example of thermal bridges on engineering building 2

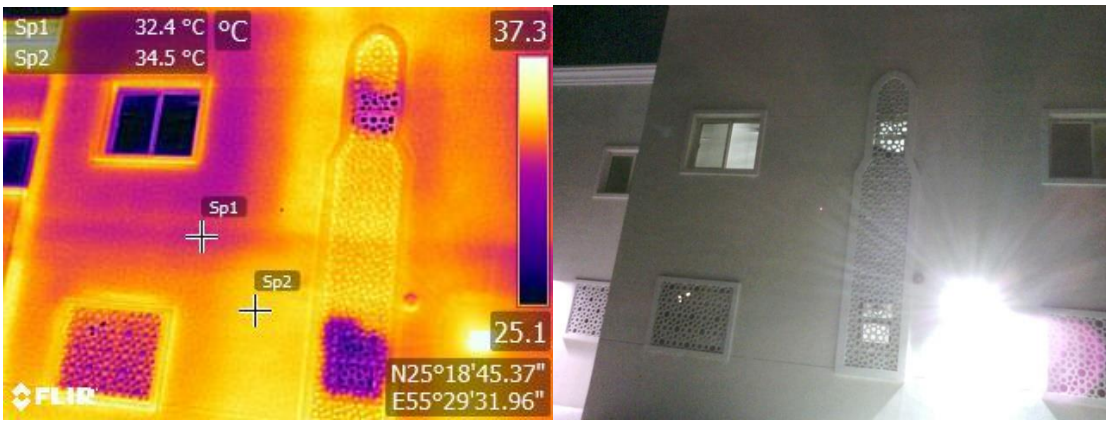

Figure 7.13 - Example of uninsulated slab perimeter in the dorms

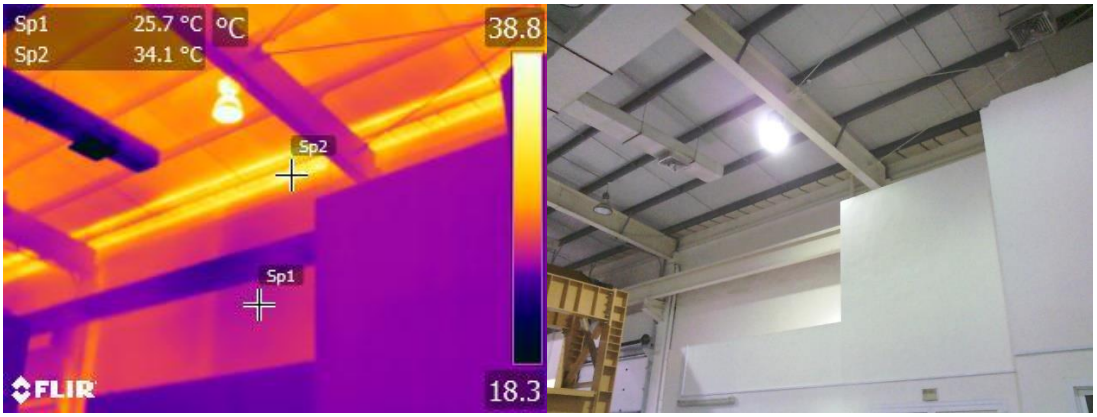

Figure 7.14 - Example of uninsulated structural member viewed from inside

Chapter 8. In-situ Measurements

To ensure that the energy model accurately represents the real case study building, it is helpful to compare the actual U-value of the building's envelope to the theoretical calculated one used by the model.

8.1. Calculated U-value

The theoretical value may be calculated according to ISO 6946 and the construction layers obtained from the as-built drawings. Since majority of the case study building's external wall is of the "WT1" construction, it would have the largest effect on the building's energy consumption and was hence chosen for this inspection. Details of this wall construction can be found in Appendix A, however some of its relevant layer properties are duplicated in table 8.1.

Table 8.1 - External wall "WT1" construction layers

Layer	Thickness (d)	Thermal Conductivity (λ)
Insulation	100 mm	0.027 W/mK
Concrete Block (Medium)	200 mm	0.51 W/mK
Plaster	1 mm	0.5 W/mK

According to ISO 6946, the thermal resistance (R) for each layer may be obtained from equation 1, while the total thermal resistance (R_T) is the summation of all layer resistances as well as the internal and external boundary layers, R_{si} and R_{se} respectively. The U-value would then be the reciprocal of the total thermal resistance, R_T, as shown in Equation 2.

$$R\ (m^2K/W) = \frac{d}{\lambda} \tag{1}$$

$$R_T\ (m^2K/W) = \frac{1}{U} = R_{si} + R_1 + R_2 + \cdots + R_N + R_{se} \tag{2}$$

Using the equations above and the layer information presented to calculate:

$$R_1 = \frac{100\ mm}{1000\ \frac{mm}{m} \times 0.027\ W/mK} = 3.7037\ m^2K/W$$

$$R_2 = \frac{200\ mm}{1000\ \frac{mm}{m} \times 0.51\ W/mK} = 0.3922\ m^2K/W$$

$$R_3 = \frac{1\ mm}{1000\ \frac{mm}{m} \times 0.5\ W/mK} = 0.002\ m^2K/W$$

R_{si} and R_{se} are found in ISO 6946 to be 0.13 m^2K/W and 0.04 m^2K/W, respectively. Hence the total thermal resistance may be obtained and consequently the U-value.

$$R_T = 0.13 + 3.7037 + 0.392156 + 0.002 + 0.04 = 4.2678\ m^2K/W$$

$$U = \frac{1}{R_T} = \frac{1}{4.2678} = 0.2343\ W/m^2K$$

Comparing these values to those calculated by the software it is evident that the thermal resistances are identical except for the total thermal resistance. This can be found to be due to differing boundary layer values. The final U-values as calculated by the IES VE software and as calculated by ISO 6946 are 0.2354 and 0.2343 W/m^2K respectively. This has a negligible difference of about 0.5%.

8.2. Actual U-value

The actual U-value for "WT1" was measured using ISO 9869 and the TRSYS01 (figure 8.1) in-situ thermal transmittance measurement apparatus by Hukesflux. The apparatus has a data logger (MCU01), a thermocouple with a temperature sensitivity of < 0.02 ˚C, and the HFP01 (figure8.2) heat flux sensor with a sensitivity of < 0.02 W/m^2.

Figure 8.1 - The TRSYS01 apparatus by Hukesflux

Figure 8.2 - HFP01 heat flux sensor

On the case study building, the apparatus was set up at the only place with granted access: on the second floor of the south west façade as shown in figure 8.3. Figures 8.4 and 8.5 show the sensors installed on the inside and the outside respectively. A piece of cardboard was also used to shield the sensors from direct sunlight and limit the effect of wind.

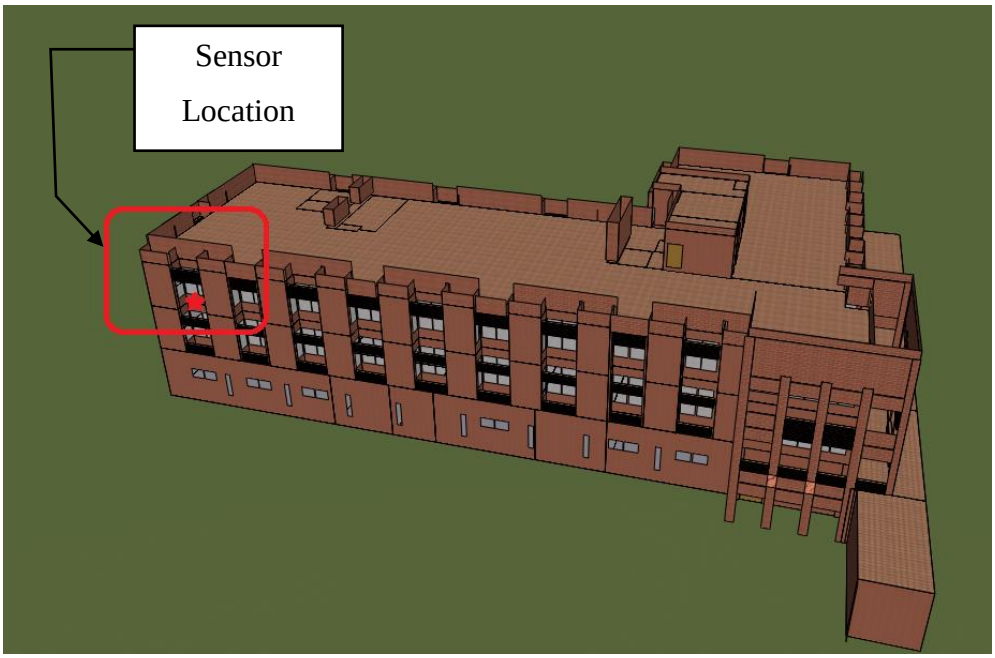

Figure 8.3 - Location of the sensor on the building.

Figure 8.4 - Set up of the inside sensors

Figure 8.5 – Set up of the outside sensors

Furthermore, the test was conducted for three days in accordance with ISO 9869 that stipulates a minimum of 72 hours. This is to obtain a measurement as close as possible to that of a steady state. In accordance with best practices, measurements were also recorded in averaged 10 min intervals and the temperature difference between the inside and out was at an average of 10˚C. Figure 8.6 and table 8.2 show the measured U-value for each day of the test and the percentage change that does not exceed 5%, hence indicating a stable measurement.

Table 8.2 - The daily U-value and the percentage change with each day

	Day 1	**Day 2**	**Day 3**
U-Value (W/m^2K)	0.332	0.349	0.336
Change (%)		5.006	-3.528

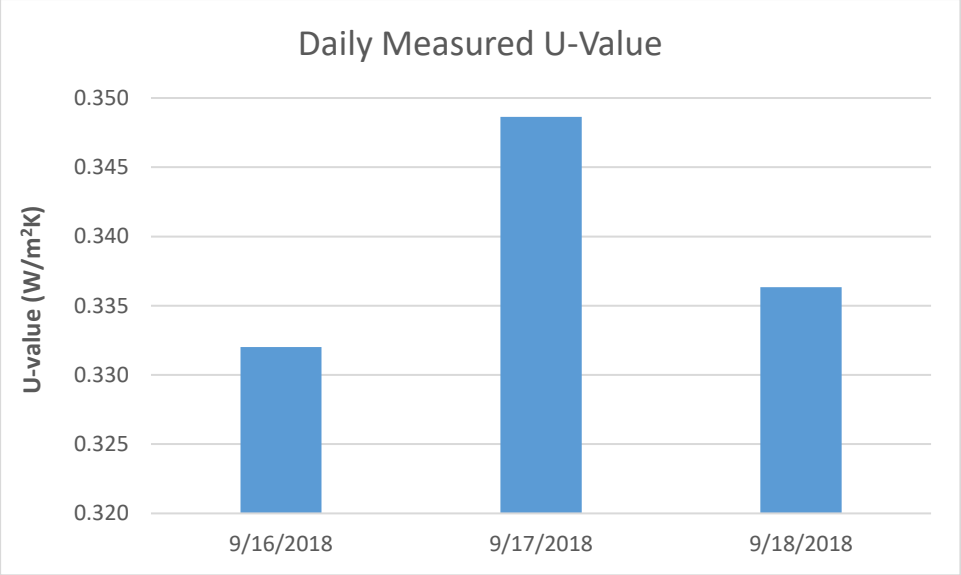

Figure 8.6 - The U-value for each day of the test period

The U-value was calculated according to equation 3 obtained from the average method in ISO 9869. At the end of the

$$U = \frac{\sum_{j=1}^{n} q_j}{\sum_{j=1}^{n} (T_{ij} - T_{ej})} \quad (3)$$

where,

q = density of heat flow rate or heat flux (W/m^2)

T_i = interior environmental (ambient) temperature (˚C or K)

T_e = exterior environmental (ambient) temperature (˚C or K)

j = number of the individual measurement

Furthermore, according to ISO 9869, the test may be terminated if the following conditions are met:

1. The duration of the test exceeds 72 hours;
2. The R-value obtained at the end of the test does not deviate by more than ± 5 % from the value obtained 24 hours before;
3. The R-value obtained by analyzing the data from the first time period during INT(2 x D_T/3) d does not deviate by more than ± 5 % from the values obtained from the data of the last time period of the same duration. D_T being the test duration in days and INT being the integer part.

The test was run for more than 72 hours, hence meeting the first condition, and the R-values can be obtained by re-arranging equation 2 to obtain equation 4 and then computing the difference required for condition 2.

$$R = \frac{1}{U} - R_{si} - R_{se} \tag{4}$$

The U-value at the end of the test was calculated to be 0.339 W/m^{2}K, while that for the last 24 h period was computed to be 0.336 W/m^{2}K. Using equation 4 the R-values are then computed as follows:

$$R_{end} = \frac{1}{0.339} - 0.13 - 0.04 = 2.782\ m^2K/W$$

$$R_{last} = \frac{1}{0.336} - 0.13 - 0.04 = 2.803\ m^2K/W$$

The difference would be 0.8%, which is less than the ± 5 % required by the code, hence satisfying condition 2. Finally, to satisfy condition 3, the integer part of the expression in equation 5 when the duration of the test in days is substituted for D_T as required, provides the duration of the period the condition needs to be tested for. For this case, the duration of the test was 3 days, hence the integer part is 2.

$$INT\left(2 \times \frac{3}{3}\right) = 2 \tag{5}$$

The R-value for the first 2 days was then computed using equation 4 to be 0.2772 m^{2}K/W and the R-value for the last 2 days of the test was computed to be 2.751 m^{2}K/W. This make a difference of 0.7%, which is below the ± 5 % required by the code, hence satisfying condition 3.

The final measured U-value of 0.339 W/m^{2}K differs by about 31% from the software calculated value of 0.2354 W/m^{2}K. This creates an increase of 0.34% in the total energy consumption of the building as shown in table 8.3, however this change is too small to affect the validity of the model and the change is negligible and barely noticeable as seen in figure 8.7. Appendix B provides the detailed consumption for the new model along with the differences between the actual and model consumptions, and also detailed graphs of the measured U-value parameters.

Table 8.3 - Energy consumption for actual WT1 wall U-value

WT1 U-value (W/m^2K)	Energy Consumption (MWh)	Energy Savings (MWh)	Energy Change (%)	Carbon Emissions (Kg)	Carbon Savings (Kg)
0.2354	1240.079	-	-	635,949	-
0.339	1244.305	-4.2263	-0.34%	638,143	-638139

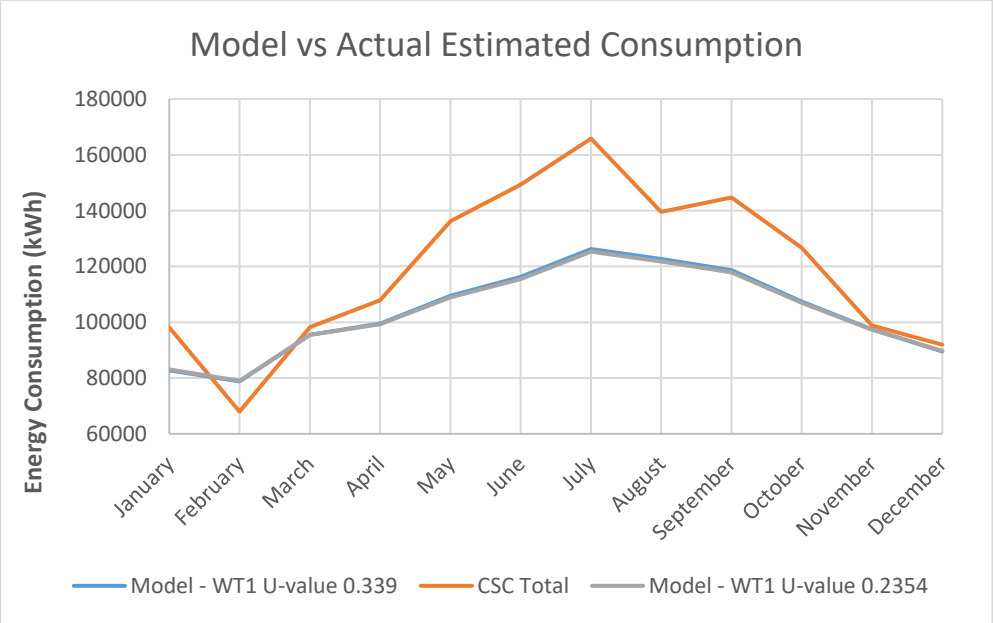

Figure 8.7 - Consumption of models with different WT1 U-value compared to actual

Chapter 9. Conclusion and Recommendations

9.1. Conclusion

In conclusion, this study shows that it is possible to accurately model an existing building to within a 3% deviation from the actual consumption without much knowledge about the specific HVAC details of the building by considering only the colder months. Furthermore, when using different software for modeling and energy simulation and transferring the data using gbXML, special attention must be given to the data that is exported by the modelling software and the data accepted by the simulation software. The gbXML format itself stores limited fields and that must be taken into consideration as well to avoid any work delays or data losses. The study also demonstrated the possibility of estimating the total consumption of a building that uses district cooling and with a cooling plant that serves multiple buildings. Hence making it possible to compare the model to the actual building.

The case study building was found to have an EUI of 357.8 kWh/m^2/yr according to the model's consumption, this is relatively lower than the actual EUI of the building of 411.2 kWh/m^2/yr obtained using the building's total estimated consumption. However, if these values are to be compared to a typical US office building from Energy Star's Portfolio Manager, they would be considerably higher than their US counterpart of 253 kWh/m^2/yr. The building is also far from reaching the nearly zero energy building (nZEB) mark set in the UAE by an EUI of less than 90 kWh/m^2/yr [44]. Though, the EUI may be easily lowered with the use of solar panels that would be quite efficient in the building's location.

The model was also verified by ensuring that the building was indeed free from thermal bridges with the use of thermal imagery. The thermal analysis was proven to be an easy and efficient method to detect thermal bridges. In-situ measurements of the building's U-value further verified the model's inputs. The in-situ measurements of the building's external wall were conducted according to ISO 9869 and a difference of 31% was detected between the actual U-value and that calculated by the software. However, as shown through the various runs of simulating the building with different insulation levels, the effectiveness of the insulation decreases with increasing insulation levels. Since the building had high levels of insulation achieving theoretical values of 0.23 W/m^2K, a slight increase in the U-value would not affect the energy consumption

considerably. Both thermal imaging and the in-situ measurement of U-values would still be highly recommended to include in the process of energy modelling.

As a fact, without changing the form or the glazing percentage, it was found that changing the envelope of the building would have a small effect on the total energy consumption of the building. The maximum energy savings achieved for any one variation in the building envelope was 1.6% from fitting high-performance triple glazed glass. The total savings achieved by increasing the insulation levels of the external wall, adding 100 mm of insulation to the slab on grade, fitting high performance windows, and optimizing the orientation of the building, was 2.77%. Furthermore, it was found that the marginal savings achieved by increasing the performance of the insulation and windows decreased as the performance increased. Finally, the difference between the best and worst orientations amounted to 4.9592 MWh/annum.

9.2. Recommendations

Energy modelling is a very powerful tool that can be used to simulate the effects of various energy efficiency measures. This study investigated strategies that minimize heat gain and further research can investigate strategies that maximize natural ventilation. Research could also be done to optimize the HVAC systems and comparisons may be drawn between the active and passive measures.

Energy simulation software may be improved to provide greater control over the category of the construction elements such as which walls are considered internal or external. They may also be improved to allow manufacturers of energy efficiency measures such as Internet of Things (IoT) devices to integrate their products with the software making it easier for the industry to investigate their efficiency.

In terms of insulation materials, studies may be conducted on Styrofoam concrete as a replacement to normal concrete block, or the use of transparent aerogels to further insulate windows.

A cost analysis of all efficiency measures may be performed to develop a framework for choosing efficiency measures based on their up-front costs and pay-back periods. Finally, the effect of the wind on the in-situ U-value measurement may be investigated.

References

[1] P. Huedo, E. Mulet, and B. López-Mesa, "A model for the sustainable selection of building envelope assemblies," *Environ. Impact Assess. Rev.*, vol. 57, pp. 63–77, 2016.

[2] J. K. W. Wong and J. Zhou, "Enhancing environmental sustainability over building life cycles through green BIM: A review," *Autom. Constr.*, vol. 57, pp. 156–165, 2015.

[3] A. Jafari and V. Valentin, "An optimization framework for building energy retrofits decision-making," *Build. Environ.*, vol. 115, pp. 118–129, 2017.

[4] M. V. Shoubi, M. V. Shoubi, A. Bagchi, and A. S. Barough, "Reducing the operational energy demand in buildings using building information modeling tools and sustainability approaches," *Ain Shams Eng. J.*, vol. 6, no. 1, pp. 41–55, 2014.

[5] M. H. Anbouhi, N. Farahza, S. Mohammad, and H. Ayatollahi, "Analysis of Thermal Behavior of Materials in the Building Envelope Using Building Information Modeling (BIM) — A Case Study Approach," *Open J. Energy Effic.*, vol. 5, no. 3, pp. 88–106, 2016.

[6] R. Ruparathna, K. Hewage, and R. Sadiq, "Economic evaluation of building energy retrofits: A fuzzy based approach," *Energy Build.*, vol. 139, pp. 395–406, 2017.

[7] Ministry of Energy and Industry UAE, "Vice President unveils UAE energy strategy for next three decades" 2017. [Online]. Available: https://www.moei.gov.ae/en/media-centre/news/10/1/2017/%D9%85%D8%AD%D9%85%D8%AF-%D8%A8%D9%86-%D8%B1%D8%A7%D8%B4%D8%AF-%D9%8A%D8%B9%D9%84%D9%86-%D8%A7%D8%B3%D8%AA%D8%B1%D8%A7%D8%AA%D9%8A%D8%AC%D9%8A%D8%A9-%D8%AF%D9%88%D9%84%D8%A9-%D8%A7%D9%84%D8%A5%D9%85%D8%A7%D8%B1%D8%A7%D8%AA-%D9%84%D9%84%D8%B7%D8%A7%D9%82%D8%A9-%D9%84%D9%84%D8%B9%D9%82%D9%88%D8%AF-%D8%A7%D9%84%D8%AB%D9%84%D8%A7%D8%AB%D8%A9-%D8%A7%D9%84%D9%85%D9%82%D8%A8%D9%84%D8%A9.aspx#page=1. [Accessed: 14-Mar-2017].

[8] EAD, "Abu Dhabi - Environment Vision 2030," 2012.

[9] A. Menon, "Dubai energy services firm Etihad ESCO to launch $44mln of new projects this year -CEO - Zawya Projects," 2017. [Online]. Available: https://projects.zawya.com/Dubai_energy_services_firm_Etihad_ESCO_to_launch_44mln_of_new_projects_this_year_CEO/story/ZAWYA20170223061001/. [Accessed: 13-Mar-2017].

[10] "Dubai Municipality-Circular No.198." Dubai Municipality, 2014.

[11] Dubai Municipality, "Green Building in Dubai." [Online]. Available:

https://www.dm.gov.ae/en/Business/PlanningAndConstruction/GreenBuildings/Pages/Green-Buildings-Publications.aspx. [Accessed: 14-Mar-2017].

[12] F. D. K. Ching and I. M. Shapiro, *Green Building Illustrated*. Hoboken, New Jersey: John Wiley & Sons, Inc., 2014.

[13] F. H. Abanda and L. Byers, "An investigation of the impact of building orientation on energy consumption in a domestic building using emerging BIM (Building Information Modelling)," *Energy*, vol. 97, pp. 517–527, 2016.

[14] L. Pérez-Lombard, J. Ortiz, and C. Pout, "A review on buildings energy consumption information," *Energy Build.*, vol. 40, no. 3, pp. 394–398, 2008.

[15] L. Pérez-Lombard, J. Ortiz, J. F. Coronel, and I. R. Maestre, "A review of HVAC systems requirements in building energy regulations," *Energy Build.*, vol. 43, no. 2–3, pp. 255–268, 2011.

[16] A. Afshari, C. Nikolopoulou, and M. Martin, "Life-Cycle Analysis of Building Retrofits at the Urban Scale—A Case Study in United Arab Emirates," *Sustainability*, vol. 6, pp. 453–473, 2014.

[17] N. Mostafavi, M. Farzinmoghadam, and S. Hoque, "Envelope retrofit analysis using eQUEST, IESVE Revit Plug-in and Green Building Studio: a university dormitory case study," *Int. J. Sustain. Energy*, vol. 34, no. 9, pp. 594–613, 2015.

[18] W. A. Friess and K. Rakhshan, "A review of passive envelope measures for improved building energy e ffi ciency in the UAE," *Renew. Sustain. Energy Rev.*, vol. 72, no. 5, pp. 485–496, 2017.

[19] Government of Dubai, *Green Building Regulations & Specifications*. 2011, p. 77.

[20] Y. L. Langston and C. A. Langston, "Reliability of building embodied energy modelling: an analysis of 30 Melbourne case studies," *Constr. Manag. Econ.*, vol. 26, no. 2, pp. 147–160, 2008.

[21] S. Copiello, "Building energy efficiency: A research branch made of paradoxes," *Renew. Sustain. Energy Rev.*, vol. 69, no. 3, pp. 1064–1076, 2017.

[22] S. Liu, X. Meng, and C. Tam, "Building information modeling based building design optimization for sustainability," *Energy Build.*, vol. 105, pp. 139–153, 2015.

[23] F. H. Abanda, C. Vidalakis, A. H. Oti, and J. H. M. Tah, "A critical analysis of Building Information Modelling systems used in construction projects," *Adv. Eng. Softw.*, vol. 90, no. 12, pp. 183–201, 2015.

[24] A. Lee *et al.*, "nD modelling - a driver or enabler for construction improvement ? RICS Research paper series," *RICS Res.*, vol. 5, no. 6, p. 16, 2005.

[25] A. GhaffarianHoseini *et al.*, "Application of nD BIM Integrated Knowledge-based Building Management System (BIM-IKBMS) for inspecting post-construction energy efficiency," *Renew. Sustain. Energy Rev.*, vol. 72, no. 5, pp. 935–949, 2017.

[26] buildingSMART, "All Applications by Category — Welcome to

buildingSMART-Tech.org." [Online]. Available: http://www.buildingsmart-tech.org/implementation/implementations/allplominoform.application/?widget=BASIC. [Accessed: 04-Apr-2017].

[27] W. A. Friess, K. Rakhshan, T. A. Hendawi, and S. Tajerzadeh, "Wall insulation measures for residential villas in Dubai: A case study in energy efficiency," *Energy Build.*, vol. 44, no. 1, pp. 26–32, 2012.

[28] C. A. Balaras and A. A. Argiriou, "Infrared thermography for building diagnostics," *Energy Build.*, vol. 34, no. 2, pp. 171–183, 2002.

[29] A. Taileb and H. Dekkiche, "Infrared Imaging as a Means of Analyzing and Improving Energy Efficiency of Building Envelopes: The case of a LEED Gold Building," *Procedia Eng.*, vol. 118, pp. 639–646, 2015.

[30] M. Fox, S. Goodhew, and P. De Wilde, "Building defect detection: External versus internal thermography," *Build. Environ.*, vol. 105, no. 8, pp. 317–331, 2016.

[31] *Thermal insulation — Building elements — In-situ measurement of thermal resistance and thermal transmittance — Part 1: Heat flow meter method*, ISO Standard 9869, 2014.

[32] F. Asdrubali, F. D'Alessandro, G. Baldinelli, and F. Bianchi, "Evaluating in situ thermal transmittance of green buildings masonries—A case study," *Case Stud. Constr. Mater.*, vol. 1, pp. 53–59, Jan. 2014.

[33] T. Samardzioska and R. Apostolska, "Measurement of heat-flux of new type façade walls," *Sustainability*, vol. 8, no. 10, pp. 1031–1042, 2016.

[34] K. Gaspar, M. Casals, and M. Gangolells, "In situ measurement of façades with a low U-value: Avoiding deviations," *Energy Build.*, vol. 170, pp. 61–73, 2018.

[35] B. P. Jelle, "Traditional, state-of-the-art and future thermal building insulation materials and solutions - Properties, requirements and possibilities," *Energy Build.*, vol. 43, no. 10, pp. 2549–2563, 2011.

[36] A. M. Papadopoulos, "State of the art in thermal insulation materials and aims for future developments," *Energy Build.*, vol. 37, no. 1, pp. 77–86, 2005.

[37] *Thermal Insulation - Qualitative detection of thermal irregularities in building envelopes - Infrared method*, ISO Standard 6781, 2017.

[38] *Building components and building elements -- Thermal resistance and thermal transmittance -- Calculation method*, ISO Standard 6946, 2007.

[39] M. Ahmed and S. Shaikh, "Solar Radiation Studies for Dubai and Sharjah, UAE," *Int. J. Phys. Math. Sci.*, vol. 7, no. 1, pp. 130–137, 2013.

[40] Research Center for Renewable Energy Mapping and Assessment, "UAE Solar Atlas." [Online]. Available: https://atlas.masdar.ac.ae/. [Accessed: 27-Jun-2018].

[41] Estidama, "Estidama Pearl Rating System : Information Bulletin # 8 RE-R1 : Minimum Energy Performance," pp. 1–4, 2011.

[42] Regulatory & Supervisory Bureau and For Electricity & Water, "Annual Report

2016," Dubai, 2016.

[43] Estidama, "Windows and Glazing Products : Centre Pane Only.",Oct. 2011. [Online]. Available: https://www.upc.gov.ae/-/media/Files/Estidama/Media/111025%20evpd%20-%20windows%20and%20glazing.pdf [Accessed: 24-Jun-2017].

[44] M. Fayyad and J. John, "Defining Nearly Zero Energy Buildings in the UAE," Dubai, 2017. [Online]. Available: https://emiratesgbc.org/wp-content/uploads/2017/03/Defining-nZEBs-in-the-UAE-2017.pdf [Accessed: 10-Sep-2018]

Appendix A: The Energy Model

Table A-1 – Schedule of spaces from Revit and IES VE

Space ID	Space No.	Space Name	Floor	Story No.	Thermal template	Floor Area (m^2)	Volume (m^3)	Ext. Window Area (m^2)	Ext. Wall Area (m^2)	No. of Windows	Vertical Glazing Area (%)	Glazing Orientation
AIM27020	19	L-1 LGF-Vestibule 01	LGF	0	Stores/Corridors	4.542	19.39	1.029	14.301	2	7%	SW
AIM27820	20	L-2a LGF-Store 01	LGF	0	Stores/Corridors	21.048	88.825	0	77.485	0	0%	
AIM28500	21	L-3 LGF-Staff Hall - Breakout Area	LGF	0	OfficeOpenPlan	178.776	769.42	3.964	75.155	1	5%	SW
AIM31650	22	L-4 LGF-MeetingRoom	LGF	0	OfficeOpenPlan	30.36	129.03	0	21.6	0	0%	
AIM32180	23	L-8 LGF-Data Center	LGF	0	Workshop	119.184	506.747	0	102.656	0	0%	
AIM33200	24	L-9 LGF-Appliances	LGF	0	Workshop	68.375	290.773	0	77.193	0	0%	
AIM34060	25	L-10 LGF-office	LGF	0	OfficeOpenPlan	14.673	62.36	1.154	14.4	2	8%	NW
AIM34590	26	L-11 LGF-Janitor	LGF	0	Stores/Corridors	2.4	10.198	0	0	0		
AIM35070	27	L-12 LGF-Store02	LGF	0	Stores/Corridors	6.213	27.961	0	20.437	0	0%	
AIM35800	28	L-14 LGF-Vestibule02	LGF	0	Stores/Corridors	6.369	27.067	0	11.7	0	0%	
AIM36330	29	L-16 LGF-FHC 01	LGF	0	Not Occupied	1.24	5.27	0	0	0		
AIM36810	30	L-17 LGF - Staircase 2	LGF	0	Stores/Corridors	18.626	83.384	0	25.162	0	0%	
AIM37790	31	L-18 LGF-HC Toilet	LGF	0	Stores/Corridors	4.439	18.865	0	0	0		
AIM38270	32	L-19 LGF-Handwash	LGF	0	Stores/Corridors	6	25.452	0	0.754	0	0%	
AIM41100	33	L-21 LGF-Elect 01	LGF	0	Not Occupied	5.28	22.197	0	1.395	0	0%	
AIM41830	34	L-23 LGF-Corridor 02	LGF	0	Stores/Corridors	79.863	339.415	0	0.757	0	0%	
AIM43690	35	L-24 LGF-ElectricalWorkshop	LGF	0	Workshop	54.116	229.991	4.014	40.435	5	10%	SW

Table A-1 – Schedule of spaces from Revit and IES VE (Cont'd)

Space ID	Space No.	Space Name	Floor	Story No.	Thermal template	Floor Area (m^2)	Volume (m^3)	Ext. Window Area (m^2)	Ext. Wall Area (m^2)	No. of Windows	Vertical Glazing Area (%)	Glazing Orientation
AIM44320	36	L-25 LGF ElectronicKey/CCTV	LGF	0	Workshop	23.905	101.596	0.764	23.625	1	3%	SW
AIM44960	37	L-26 LGF-TelRoom	LGF	0	Not Occupied	6.1	25.925	0	0	0		
AIM45440	38	L-27a LGF-Corridor 03	LGF	0	Stores/Corridors	9.016	38.319	0	0	0		
AIM45920	39	L-28 LGF-Vestibule03	LGF	0	Stores/Corridors	2.702	11.483	0	9.04	0	0%	
AIM46450	40	L-29 LGF Garbage	LGF	0	Stores/Corridors	20.719	93.234	0	17.319	0	0%	
AIM47080	41	L-30 LGF-Plumbing/pump	LGF	0	Workshop	32.058	136.248	0	21.811	0	0%	
AIM47560	42	L-31 LGF-AC Workshop	LGF	0	Workshop	46.429	197.322	3.153	34.875	4	9%	SW
AIM48190	43	L-32 LGF - Alum-Welding	LGF	0	Workshop	73.474	312.266	1.625	49.05	2	3%	NE
AIM48720	44	L-33 LGF-Printroom	LGF	0	Stores/Corridors	8.455	35.81	0	0	0		
AIM49410	45	L-33a LGF-SerCabinet	LGF	0	Not Occupied	0.51	2.167	0	0	0		
AIM49890	46	L-34 LGF-Keyshop	LGF	0	Workshop	10.228	43.347	0.764	15.75	1	5%	SW
AIM50420	47	L-35 LGF-PaintShop	LGF	0	Workshop	14.258	60.595	0.764	21.6	1	4%	SW
AIM50900	48	L-35a LGF-Store 3	LGF	0	Stores/Corridors	13.11	55.717	0	0	0		
AIM51380	49	L-36 LGF-FHC 02	LGF	0	Not Occupied	1.2	5.1	0	0	0		

Table A-1 – Schedule of spaces from Revit and IES VE (Cont'd)

Space ID	Space No.	Space Name	Floor	Story No.	Thermal template	Floor Area (m^2)	Volume (m^3)	Ext. Window Area (m^2)	Ext. Wall Area (m^2)	No. of Windows	Vertical Glazing Area (%)	Glazing Orientation
AIM51910	50	L-37 LGF - Staircase 03	LGF	0	Stores/Corridors	18.27	81.842	0	14.85	0	0%	
AIM52690	51	L-38 LGF-Cabinet 2	LGF	0	Not Occupied	4.15	17.636	0	3.832	0	0%	
AIM53220	52	L-39 LGF woodworkshop	LGF	0	Workshop	191.988	815.947	8.028	186.426	10	4%	SW
AIM54010	53	L - Lift LGF - Lift	LGF	0	Not Occupied	3.825	16.922	0	0	0		
RM00000D	81	L-20 LGF - Toilets 01	UGF	0	Stores/Corridors	24.12	122.918	0	3.488	0	0%	
AIM57250	58	Shaft 01 Shaft 01	UGF	1	Not Occupied	2.79	21.204	0	0	0		
AIM57780	59	U-2 UGF-Vestibule 01	UGF	1	Stores/Corridors	3.73	13.255	0.945	15.67	1	6%	SE
AIM58420	60	U-3 UGF-Reception	UGF	1	Stores/Corridors	58.32	207.037	20.959	59.175	20	35%	SW
AIM59380	61	U-4 UGF-Open Office	UGF	1	OfficeOpenPlan	787.15	2798.511	124.123	621.477	117	20%	SE
AIM67680	62	U-5 UGF-Hand Wash Area01	UGF	1	Stores/Corridors	8.21	28.991	1.137	15.2	1	7%	NW
AIM68580	63	U-5a UGF-Printer Room	UGF	1	OfficeOpenPlan	17.53	62.236	0	0	0		
AIM69110	64	U-6 UGF-FHC 01	UGF	1	Not Occupied	1.24	4.402	0	0	0		
AIM69590	65	U-8 UGF-Corridor 02	UGF	1	Stores/Corridors	6.09	21.619	0	0	0		
AIM70320	66	U-10 UGF-Ladies Toilet	UGF	1	Stores/Corridors	12.55	44.452	0	0	0		
AIM71650	67	U-11 UGF-Janitor	UGF	1	Stores/Corridors	0.765	2.716	0	0	0		

Table A-1 – Schedule of spaces from Revit and IES VE (Cont'd)

Space ID	Space No.	Space Name	Floor	Story No.	Thermal template	Floor Area (m^2)	Volume (m^3)	Ext. Window Area (m^2)	Ext. Wall Area (m^2)	No. of Windows	Vertical Glazing Area (%)	Glazing Orientation
AIM72130	68	U-12 UGF-G/Toi Vestibule	UGF	1	Not Occupied	3.298	11.656	0	0	0		
AIM72810	69	U-13 UGF-Gents Toilet	UGF	1	Stores/Corridors	11.55	40.788	0	7.636	0	0%	
AIM74300	70	U-14 UGF-HC Toilet	UGF	1	Stores/Corridors	5.23	18.558	0	0	0		
AIM74830	71	U-15 UGF-Tel Room	UGF	1	Stores/Corridors	4.51	15.843	0	0	0		
AIM75460	72	U-16 UGF-Elect Room	UGF	1	Stores/Corridors	4.19	14.883	0	0	0		
AIM75940	73	U-17 UGF-FHC 02	UGF	1	Not Occupied	1.2	4.26	0	0	0		
AIM76470	74	U-17s UGF - Staircase 2	UGF	1	Stores/Corridors	18.63	70.385	0	12.542	0	0%	
AIM77550	75	U-19 UGF-Cabinet 01	UGF	1	Not Occupied	4.14	14.695	0	3.23	0	0%	
AIM78180	76	U-20 UGF-Store 01	UGF	1	Stores/Corridors	6.99	24.812	0	0	0		
AIM78660	77	U-21 UGF- Hand Wash Area 02	UGF	1	Stores/Corridors	8.61	30.562	4.275	15.808	4	27%	NE
AIM79240	78	U-37s UGF - Staircase 03	UGF	1	Stores/Corridors	18.21	69.198	0	12.54	0	0%	
AIM79980	79	U-Lift UGF - Lift	UGF	1	Not Occupied	3.82	14.282	0	0	0		
AIM80780	80	U - Shaft 02 UGF - Shaft 02	UGF	1	Not Occupied	0.585	2.198	0	0	0		
AIM02900	0	F-1 FF-Open Office	First	2	OfficeOpenPlan	245.524	932.851	38.012	213.411	35	18%	SE

Table A-1 - Schedule of spaces from Revit and IES VE (Cont'd)

Space ID	Space No.	Space Name	Floor	Story No.	Thermal template	Floor Area (m^2)	Volume (m^3)	Ext. Window Area (m^2)	Ext. Wall Area (m^2)	No. of Windows	Vertical Glazing Area (%)	Glazing Orientation
AIM06550	1	F-2 FF-Hand Wash Area 01	First	2	Stores/Corridors	8.212	31.027	1.137	15.2	1	7%	NW
AIM07450	2	F-3 FF-FHR 01	First	2	Not Occupied	1.24	4.453	0	0	0		
AIM08070	3	F-6 FF-Corridor 02	First	2	Stores/Corridors	6.94	24.759	0	0	0		
AIM09050	4	F-7 FF-Ladies Toilet	First	2	Stores/Corridors	12.553	44.749	0	0	0		
AIM10800	5	F-9 FF-G/Toi Vestibule	First	2	Not Occupied	3.298	12.19	0	0	0		
AIM11570	6	F-10 FF-Gents Toilets	First	2	Stores/Corridors	11.537	43.661	0	8.776	0	0%	
AIM13060	7	F-11 FF-HC Toilet	First	2	Stores/Corridors	5.228	19.865	0	0.38	0	0%	
AIM13590	8	F-12 FF-TelRM	First	2	Stores/Corridors	4.507	16.766	0	0	0		
AIM14430	9	F-13 FF-Elect Room	First	2	Stores/Corridors	4.192	15.057	0	0	0		
AIM15050	10	F-14 FF-FHC 02	First	2	Not Occupied	1.2	4.56	0	0	0		
AIM15580	11	F-16 FF-Cabinet 01	First	2	Not Occupied	4.139	15.73	0	3.23	0	0%	
AIM16210	12	F-17 FF-Hand Wash Area 02	First	2	Stores/Corridors	8.609	32.714	4.275	15.808	4	27%	NE
AIM16790	13	F-17s FF - Staircase 2	First	2	Stores/Corridors	18.626	70.484	0	12.542	0	0%	
AIM18010	14	F-18 FF-Store 01	First	2	Stores/Corridors	6.989	26.56	0	0	0		
AIM18490	15	F-23 FF-Office11	First	2	OfficeOpenPlan	623.933	2375.749	115.772	486.018	112	24%	SW
AIM24810	16	F-37s FF - Staircase 03	First	2	Stores/Corridors	18.21	69.198	0	12.54	0	0%	

Table A-1 - Schedule of spaces from Revit and IES VE (Cont'd)

Space ID	Space No.	Space Name	Floor	Story No.	Thermal template	Floor Area (m^2)	Volume (m^3)	Ext. Window Area (m^2)	Ext. Wall Area (m^2)	No. of Windows	Vertical Glazing Area (%)	Glazing Orientation
AIM25550	17	F - Lift FF - Lift	First	2	Not Occupied	3.825	13.571	0	0	0		
AIM26490	18	F - Shaft 02 FF - Shaft 02	First	2	Not Occupied	0.585	2.222	0	0	0		
AIM54860	54	R-2 R-Services Room	Roof	3	Workshop	21.15	66.097	0	32.541	0	0%	
AIM55500	55	R-3 R-Central Battery Room	Roof	3	Workshop	10.1	31.55	0	33.215	0	0%	
AIM55980	56	R-4 R-4	Roof	3	Not Occupied	1.09	3.391	0	9.388	0	0%	
AIM56460	57	R-17s R - Staircase 2	Roof	3	Stores/Corridors	18.5	57.579	0	44.344	0	0%	
Total	82					3155.546	12282.065	335.894	2535.767	324	13%	

Table A-2 – Constructions used in IES VE and their thermal properties.

Category	**Description**	**U Value ($W/m^2 \cdot K$)**	**Thickness (mm)**	**R Value (m^2K/W)**	**Thermal Capacity ($kJ/(m^2 \cdot K)$)**	**Density (kg/m^3)**
External Wall	SharedWall	0.793	527	1.1114	140	1261.86
External Wall	WT1	0.2354	301	4.0979	139.9	946.179
External Wall	Core 300	0.251	400	3.8341	230	1733.75
Internal Partition	Hollow CMU 200	1.5831	200	0.3922	140	1400
Internal Partition	Hollow CMU 300	1.2081	300	0.5882	140	1400
Internal Partition	2013 Internal Partition	4.1752	0.1	0	0.1755	7800
Ground/Exposed Floor	SlabOnGrade	0.6092	375.508	0.1393	230	1985.388
Internal Ceiling/Floor	Interior 275	2.9709	275	0.1217	230	2290.909
Ground/Exposed Floor	Exposed Floor	0.2491	375	3.8233	230	1696
Roof	Interior Floor	3.8594	275	0.1217	230	2290.909
Roof	R2 Roof	0.2494	380	3.8311	230	1664.737
Door		2.3025	37	0.2846	13.875	500
External Window	GL1-b	1.9204	28	0.4858		
External Window	GL1-a	1.9896	28	0.4527		

Table A-3 - Material layers for each construction.

Construction	Material	Material ID	Thickness (mm)	Conductivity (W/m·K)	Density (kg/m³)	Specific Heat Capacity (J/Kg·K)	Resistance (m^2K/W)	Vapor Resistivity (GN·s/Kg·m)
Shared Wall	Concrete Block (Medium)	CBM1	300	0.51	1400	1000	0.5882	120
	Cavity		52	-	-	-	0.18	-
	Concrete Block (Medium)	CBM1	175	0.51	1400	1000	0.3431	120
WT1	Insulation	STD_PHF1	100	0.027	35	1470	3.7037	-
	Concrete Block (Medium)	CBM1	200	0.51	1400	1000	0.3922	120
	Plaster (Dense)	PLD	1	0.5	1300	1000	0.002	50
Core 300	Insulation	STD_PHF1	100	0.027	35	1470	3.7037	-
	Reinforced Concrete	STD_CC2	300	2.3	2300	1000	0.1304	-
Hollow CMU 200	Concrete Block (Medium)	CBM1	200	0.51	1400	1000	0.3922	120
Hollow CMU 300	Concrete Block (Medium)	CBM1	200	0.51	1400	1000	0.5882	120
2013 Internal Partition	Rainscreen	STD_SM1	0.1	50	7800	450	0	-

Table A-3 - Material layers for each construction (Cont'd).

Construction	Material	Material ID	Thickness (mm)	Conductivity (W/m·K)	Density (kg/m³)	Specific Heat Capacity (J/Kg·K)	Resistance (m^2K/W)	Vapor Resistivity (GN·s/Kg·m)
SlabOnGrade	U-Value Correction Layer	VLCR0000	65.5	0.05	550	1000	1.3102	0
	Reinforced Concrete	STD_CC2	300	2.3	2300	1000	0.1304	-
	Screed	STD_SC1	5	1.15	1800	1000	0.0043	-
	Concrete Tiles	CT	5	1.1	2100	837	0.0045	500
Interior 275	Reinforced Concrete	STD_CC2	270	2.3	2300	1000	0.1174	-
	Screed	STD_SC1	5	1.15	1800	1000	0.0043	-
Exposed Floor	Insulation	STD_PHF1	100	0.027	35	1470	3.7037	-
	Reinforced Concrete	STD_CC2	275	2.3	2300	1000	0.1196	-
Interior Floor	Reinforced Concrete	STD_CC2	270	2.3	2300	1000	0.1174	-
	Screed	STD_SC1	5	1.15	1800	1000	0.0043	-

Table A-3 - Material layers for each construction (Cont'd).

Construction	Material	Material ID	Thickness (mm)	Conductivity (W/m·K)	Density (kg/m³)	Specific Heat Capacity (J/Kg·K)	Resistance (m^2K/W)	Vapor Resistivity (GN·s/Kg·m)
R2 Roof	Gravel	GRVL	15	0.36	1840	840	0.0417	250
	Insulation	STD_PHF1	100	0.027	35	1470	3.7037	-
	Asphalt	ASP	5	0.5	1700	1000	0.01	5000
	Screed	STD_SC1	10	1.15	18000	1000	0.0087	-
	Reinforced Concrete	STD_CC2	250	2.3	2300	1000	0.1087	-

Table A-4 - Model's window thermal properties.

Window Type	U-Value (with frame) ($W/m^2·K$)	U-Value (glass only) ($W/m^2·K$)	SHGC (center-pane)
GL1-a	1.9896	1.66	0.2457
GL1-b	1.9204	1.5735	0.271

Table A-5 -Internal gains used in the energy model.

Gain Reference	Maximum Sensible Gain	Maximum Latent Gain	Occupancy	Maximum Power Consumption	Radiant Fraction
Machinery	1000 Watts	1000 Watts	-	7000 Watts	0.22
People (Workshop)	80.594 W/person	139.208 W/person	4 people	-	-
People (Office)	73.268 W/person	58.614 W/person	11.613 m^2/people	-	-
People (Store/Corridor)	73.268 W/person	58.614 W/person	2 people	-	-
Computers	65 Watts	-	-	65 Watts	0.22
Miscellaneous	10.764 W/m^2	0 W/m^2	-	10.764 W/m^2	0.22
Fluorescent Lighting	11.840 W/m^2	-	-	11.840 W/m^2	0.45

Table A-6 - Usage of the internal gains.

Internal Gains for Each Thermal Template			
OfficeOpenPlan	**Workshop**	**Stores/Corridors**	**Not occupied**
Lighting	Lighting	Lighting	Lighting
Miscellaneous	People (Workshop)	People (store/Corridor)	
People (Office)	Machinery		
Computers			

Table A-7 - HVAC input parameters

HVAC Input Parameters	
UK NCM Type	Fan Coil Systems
Heating	
Seasonal Efficiency	0.65
SCoP kW/kW	0.5991
Cooling	
Cooling/Ventilation mechanism	Air conditioning
Nominal EER kW/kW	2.5
Seasonal EER kW/kW	2
SSEER kW/kW	1.3539
Heat Rejection	10%
Hot Water	
DHW Delivery Efficiency	0.95
Cold Water Inlet Temp. (°C)	10
Hot Water Supply Temp. (°C)	60
Auxiliary Energy	
Method	Use AEV
Air Supply Mechanism	Centralized balanced AC or mech vent system
Auxiliary Energy Value W/m^2	13.574
Auxiliary Energy Fan Fraction	0.5

Table A-8 - Detailed monthly energy consumption of the model

Date	Total lights energy (MWh)	Total equip energy (MWh)	Boilers energy (MWh)	Ap Sys chillers energy (MWh)	Ap Sys aux + DHW/solar pumps energy (MWh)	Ap Sys heat rej fans/pumps energy (MWh)	Total energy (MWh)	Total Carbon emissions (Kg)
Jan 01-31	9.2608	35.0251	2.0971	11.8364	21.3201	3.5509	83.0905	42488
Feb 01-28	8.5485	32.3308	1.9358	13.0306	19.2569	3.9092	79.0117	40420
Mar 01-31	9.617	36.3722	2.1778	20.0471	21.3201	6.0141	95.5483	48930
Apr 01-30	9.2608	35.0251	2.0971	24.8137	20.6324	7.4441	99.2733	50887
May 01-31	9.2608	35.0251	2.0971	31.6652	21.3201	9.4996	108.8679	55867
Jun 01-30	9.2608	35.0251	2.0971	37.2864	20.6324	11.1859	115.4877	59302
Jul 01-31	9.617	36.3722	2.1778	42.9262	21.3201	12.8779	125.2912	64366
Aug 01-31	9.2608	35.0251	2.0971	41.5824	21.3201	12.4747	121.7603	62558
Sep 01-30	9.2608	35.0251	2.0971	39.0955	20.6324	11.7286	117.8395	60523
Oct 01-31	9.2608	35.0251	2.0971	30.1601	21.3201	9.048	106.9113	54851
Nov 01-30	9.2608	35.0251	2.0971	23.2791	20.6324	6.9837	97.2783	49852
Dec 01-31	9.617	36.3722	2.1778	15.5631	21.3201	4.6689	89.7192	45904
Summed total	111.486	421.6477	25.2458	331.286	251.0274	99.3858	1240.0791	635949

Appendix B: U-Value Measurement

Table B-1 - Deviation of model consumption from the actual

	CSC Actual Consumption (kWh)	Model Consumption, U-0.2354 (kWh)	Error	Model Consumption, U-0.339 (kWh)	Error
January	98144.8	82771.2	15.3%	82771.2	15.7%
February	67967.6	78794.6	-16.2%	78794.6	-15.9%
March	98302.6	95504	2.8%	95504	2.8%
April	107869.8	99557.8	8.0%	99557.8	7.7%
May	136201.2	109463.3	20.1%	109463.3	19.6%
June	149305.4	116282.1	22.7%	116282.1	22.1%
July	165838	126240	24.4%	126240	23.9%
August	139524.8	122733.9	12.7%	122733.9	12.0%
September	144700.4	118639.9	18.6%	118639.9	18.0%
October	126698.2	107391.7	15.6%	107391.7	15.2%
November	98855.4	97415.1	1.6%	97415.1	1.5%
December	91892	89511.7	2.4%	89511.7	2.6%

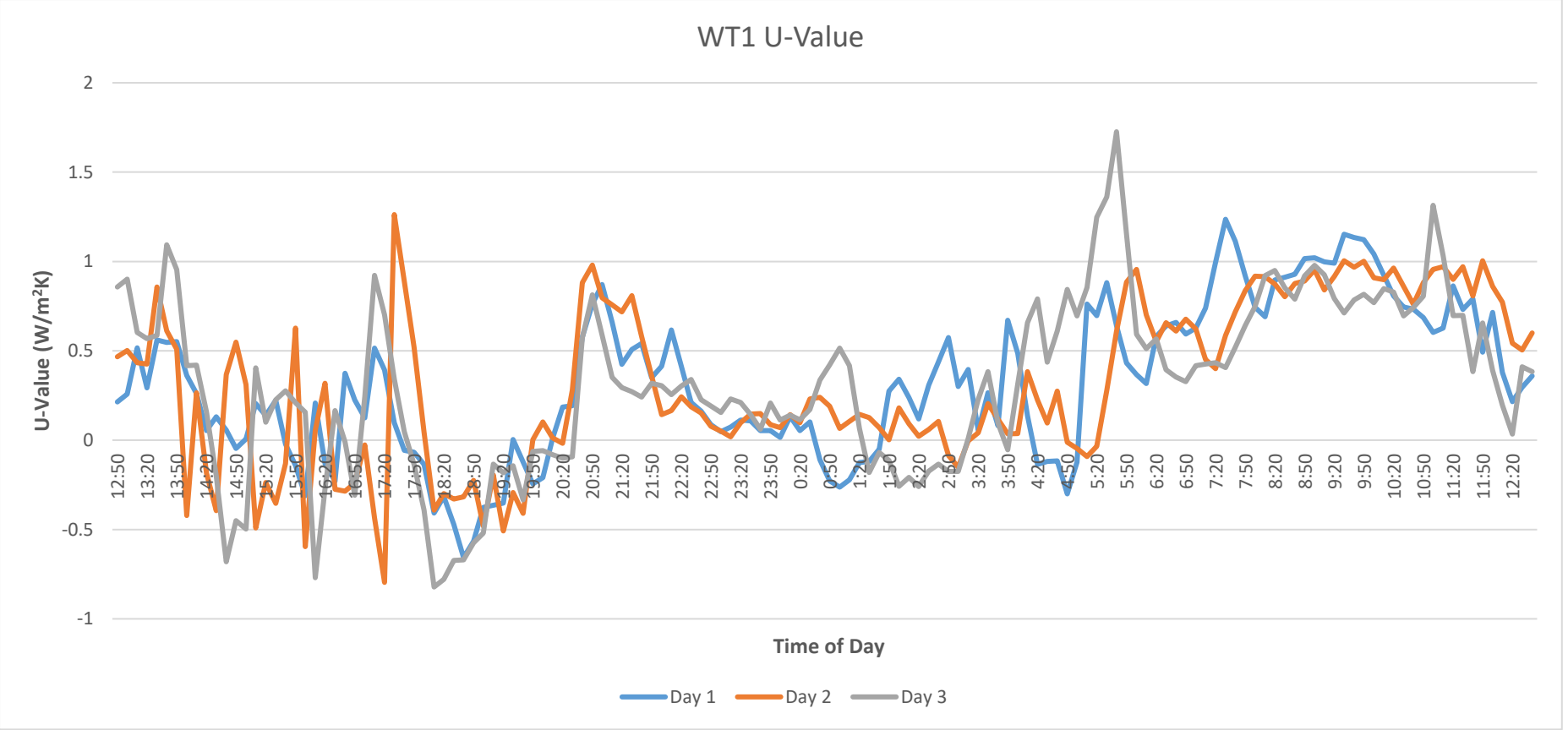

Figure B-1 - Continuous WT1 U-value for each day

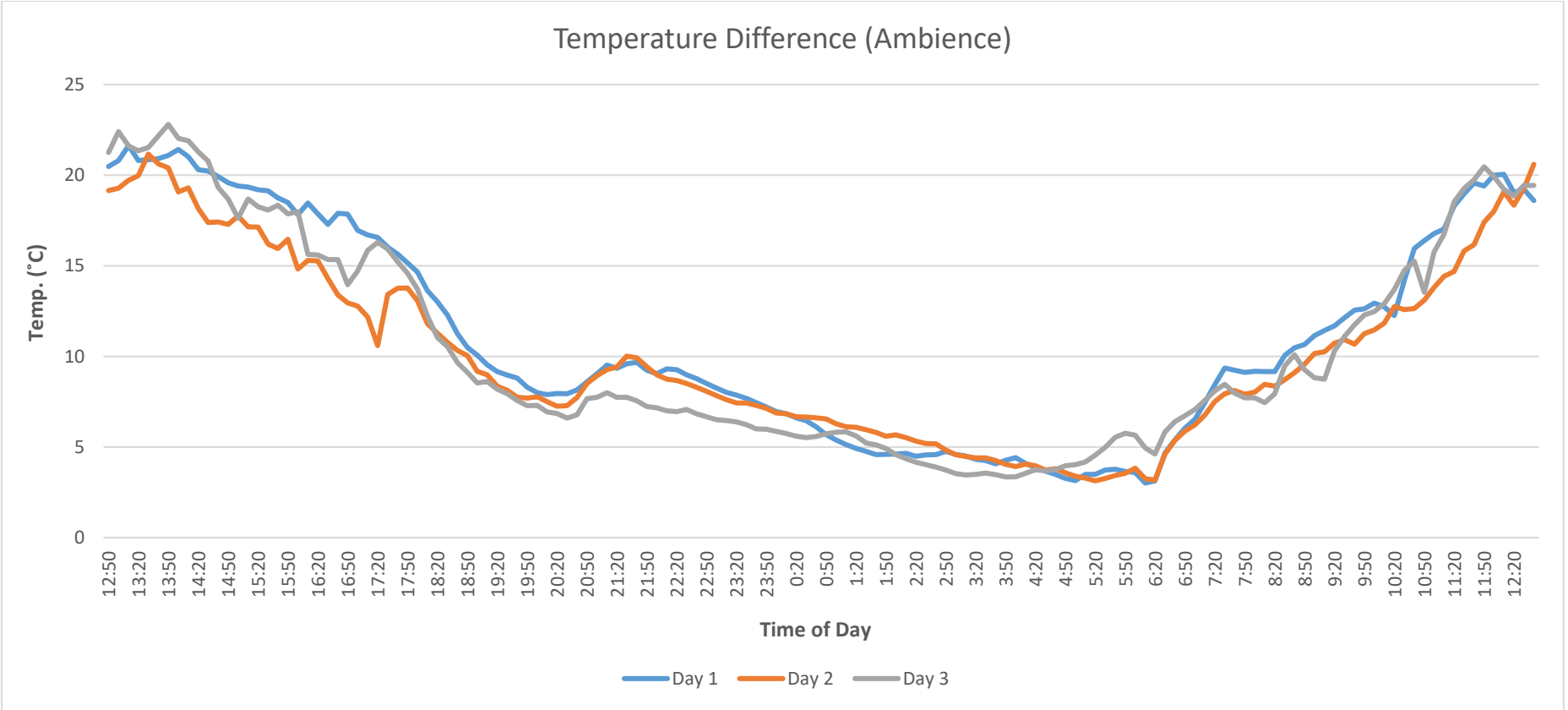

Figure B-2 - Variation of the temperature difference for each day

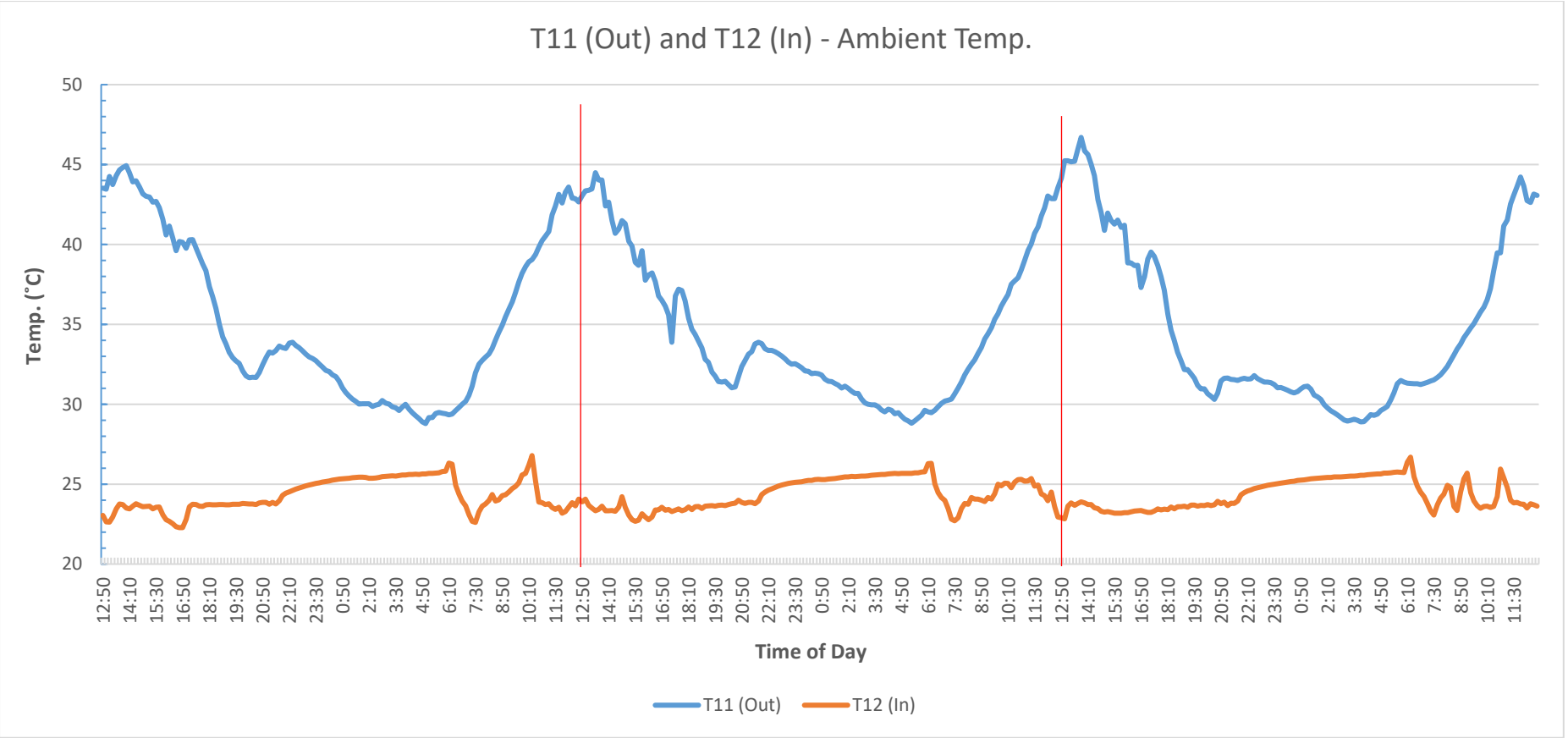

Figure B-3 - Variation of the outside and inside temperature with the time of the test

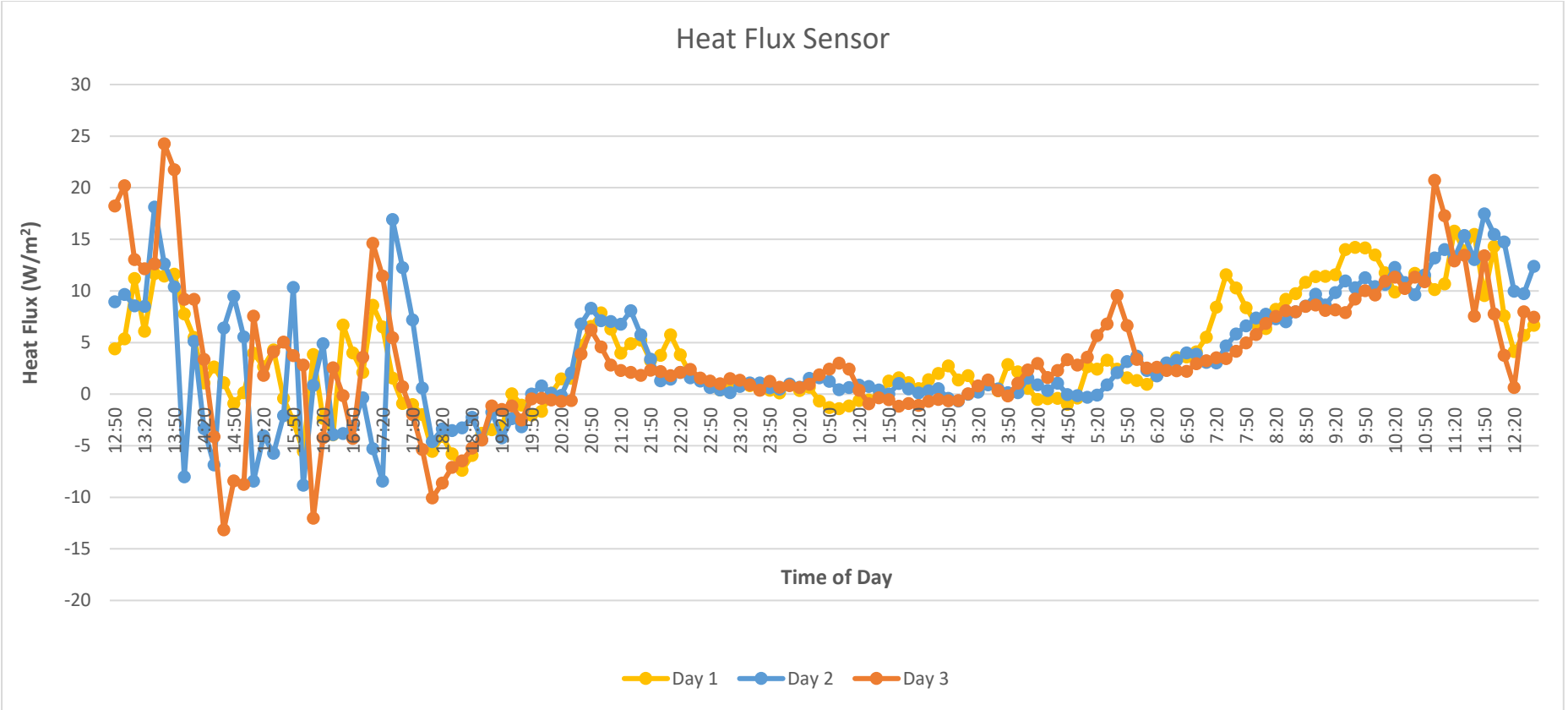

Figure B-4 - Variation of the heat flux for each day

Vita

Haidar Emad Alhaidary was born in 1989, in Sharjah, United Arab Emirates. He received his primary and secondary education in Sharjah and in 2016 he graduated with a Bachelor of Science, and within the top three of his batch, from the University of Sharjah, Department of Civil and Environmental Engineering. He then joined the Civil Engineering master's program at the American University of Sharjah with a Graduate Assistantship where he worked as both a teaching and research assistant. His research activities during this period included nanotechnology in concrete, corrosion of steel, wastewater in concrete, waste plastic in concrete, and post-installed anchor strength. He was the Vice President of the Graduate Student Association for the year 2017/18 and also received the 2017/18 AUS Graduate Student Academic and Leadership Excellence Award in recognition for his overall performance as indicated by academic accomplishment and leadership as demonstrated through contributions to the program, university, community and profession.